DoR INSIGHT

Vol. 32 July 2025

Department of Roads (DoR)

E-mail: mis@dor.gov.np | Website: www.dor.gov.np

Table of Contents

1.0 Appointment of new Director General (DG)

Dr Bijaya Jaishi has been appointed as the new Director General (DG) of the Department of Roads on 2082-02-11. The department's employees warmly welcomed the new DG. He did Msc in Structural Engineering-TU, Pulchowk: PhD in Structural Engineering, China; Post Doc. in Bridge Engineering, Sheffield University, UK; Post Doc in Structural Engineering Yonsei University, S. Korea (Visiting Scholar: Northen Illinois University, USA). He received the Young Scientist Award from the Nepal Academy of Science and Technology (NAST) in 2006/2007 (B.S. 2063/2064) for developing a technology to detect potential damage in any part of a bridge. He has published more than 10 articles in the American Society of Civil Engineers (ASCE) and other reputed international journals.

He Presented research papers at several prestigious universities and conferences around the world, including: Sheffield University (UK), Washington University in St. Louis (USA), EPFL (Switzerland), INRIA (France), and IRIS in Zell am See (Austria). He contributed to solving issues related to several national highway bridges that had remained incomplete or problematic for years during construction. Working as part of the **Department of Roads team**, helped resolve these problems by applying **new technologies and design modifications**. He played a key role in developing BID documents and norms for the construction of bridges using the Design and Build technology in the Department of Roads. He played a key role in preparing the Standard Bid Document (SBD), Tunnel Norms, and Specifications for the construction of roads, bridges, and tunnels under the globally successful Engineering Procurement and Construction (EPC) modality. For the first time in the Department of Roads, this SBD and Tunnel Norms were used for contract management of the Siddha Baba Tunnel and Gwarko Flyover, both of which are currently under construction now. He played a leading role within the Department's team in internalizing and implementing the design and construction of long-span bridges (such as the Mugling Arch Bridge and Jayaramghat Suspension Bridge), signature bridges (such as the Dhobikhola Network Bridge), prestress technologies (including Box Girder, T-Girder, and I-Girder), as well as tunnel design and construction in Nepal. He checked RCC T-Girder and designed various spans of prestressed concrete bridges, and prepared standard drawings. Under the leadership of International Bridge Expert Dr. V.K. Raina, formed various groups and standardized superstructure drawings for spans ranging from 6m to 40m. He played a key role in reviving the DOR NEWS working as Chief editor, which had been discontinued for several years.

After taking the leadership of the Department, the new Director General has prioritized following activities within the department. He divided his actions as Immediate actions (from 1 to 3 months) and Medium-term/Long-term tasks (more than 3 months). His immediate actions are not limited to:

- Improvement of the Department of Roads office; Regular Senior Management Team (SMT) meeting, establish library, Zero hour meeting, gate control etc.
- Assess the status of various application tools under the Department of Roads (including around 13 tools such as the Contract Management Software (CMS)) and make them operational.
- Ensure smooth operation of transportation along the BP highway, Dhulikhel–Khawa road and other critical roads during this monsoon season.
- Repair the guide bund damaged by last year's flood and ensure safe transportation over the Mahakali Bridge during this monsoon season through joint efforts of the Nepal Army and the Department of Roads.
- Install appropriate road information boards on roads; for example, many users are unaware of the Madan Bhandari Road.
- Finalize the design of the Signature Bridge over the Narayani River and immediately commence construction work.
- Identify potential locations in Kathmandu and other major cities to remove waterlogged areas causing traffic difficulties during the upcoming monsoon season by using water jet cleaning.
- Keep all roads under one's jurisdiction pothole-free.
- Use the press and social media to highlight good works,| Immediately refute false news.
- Each technician will carry a bag with a toolkit when going to the field, and line level checks will be conducted in every division.
- Implement concrete casting technology to achieve a smooth finish like that done abroad
- Immediately implement the amendment to the Standard Specification for Roads and Bridges.
- Have the bridge designs checked by jury members before finalizing.
- Make it mandatory to get road designs approved by the Director General.

- Have the training database maintained by QRDC, database maintained of employees going for training abroad.
- Establish and implement some minimum standards for employee transfers.
- Since it takes years to get VO approval for projects funded by EXIM Bank loans under the Road Improvement Project, discuss with EXIM Bank to find a solution.
- Sign MOUs with various universities/ engineering colleges within the country to conduct research on topics useful to the Department of Roads (DOR).
- Establish an innovation committee to introduce new practices in roads and bridges. Form a team to facilitate technology transfer on the ongoing Fast Track project.
- Play a role in getting approval for the Master Plan for Road Connectivity being prepared by the ADB Project Directorate

His medium term and long term actions are not limited to:

- Complete the construction of the Nagdhunga Tunnel, select a service provider, and commence transportation operations as soon as possible.
- The Department of Roads will initiate efforts through the concerned authorities to ensure that, as per the Constitution, it is responsible only for national highways. Appropriate decisions will be made regarding the maintenance of LRN (Local Road Network) bridges. A work plan will be prepared to immediately hand over local road bridges constructed by the Department of Roads to the provincial and local governments.
- Carry out the necessary tasks to digitize all files related to the Department of Roads and all divisional projects.
- Immediately repair potholes as soon as they appear and develop an infrastructure ambulance system for road maintenance.
- Establish a museum dedicated to the construction of large bridges and tunnels.
- Take actions to strengthen the division laboratories, Strengthen the Heavy Equipment Divisions and construct new modern buildings.
- Work towards eliminating chronic contracts within the Department of Roads.
- Work on a policy to construct small tunnels to shorten road alignments.
- Work to register the land of the Department of Roads across the country in the name of the Department of Roads.
- Form a gang within the Department of Roads' Mechanical Branch capable of erecting Bailey Bridges.
- Work to implement development tax in accordance with the Public Roads Act.
- Carry forward bridge maintenance work in the Department of Roads as a campaign.
- Prepare landslide inventory | Monitor landslides | Maintain history of past landslides.

2.0 Major achievements during tenure of former DG Mr. Ram Hari Pokharel

- Coordinating with the ministry for disaster recovery and demonstrating participation and coordination in all tasks, including prioritization of plans and budget management.
- Identifying the distressed and problematic contracts under the department, and taking steps towards the management of these contracts, including formulation of a committee for proper management and resolution of these contracts.
- Participating in the negotiation of BMP III funded by the World Bank Group.
- Breakthrough of Siddababa Tunnel.
- Issuing of Guideline for Construction of Cement Treated Sub-base/Base and Guideline for Design and Construction of Surface Dressing.
- Preparation of a Priority Investment Plan (PIP) and submit for approval.
- Initation of extensive training programs to boost the technical and managerial skills of DoR staff.
- Starting of the work of measuring the International Roughness Index (IRI) on national highways across the country by the department's internal technical team.

3.0 Major achievements during tenure of former DG Mr. Sushil Babu Dhakal

- Improved laboratory facilities of department offices for enhanced quality control in construction works.
- Increased the effectiveness of internal technical audit/supervision by Federal Roads Supervision and Monitoring Offices.
- Issued guidelines and directives for Dispute/ Claim Handling and Contract Termination/ Post Termination Management
- Initiated the use of Government Integrated Office Management System (GIOMS) for office automation among all DoR offices.
- Timely amendment of known issues in Norms and Technical Specifications.
- Use of innovative technology in pavement maintenance.
- Blackspot identification for reduction of road crashes.
- Finalized Employee job description.
- Encouraged meetings on virtual platforms for monitoring and regular meetings.
- Discoursed road encroachment and removal of properties within the right of way built without permission.
- Initiated Training to Road Supervisors for axle load monitoring on National Highways.
- Continuation of Bio-engineering and promotion of nature-based solutions.
- Mitigation of landslide, based on rigorous investigations and historical evidence.

4.0 Influence of the Restricted Zone of Fine Aggregate on Marshall Design Parameters and Performance of the Wearing Course

-Late Binod Prasad Sapkota

Senior Divisional Engineer, Department of Roads

1. BACKGROUND

(1) General

The most common form of pavement worldwide is asphalt. Asphalt finds its application in a wide range of areas, including residential streets, expressways, parking lots, seaport facilities, bike lanes, and airport runways. There will be variations in the type of mix chosen and the mix design criteria according to factors including traffic, climate, materials available, and the location within the pavement structure.

The term "Hot Mix Asphalt" (HMA) refers to the process of heating both the aggregate and the asphalt binder before mixing to get appropriate mixing and workability.

In general, there are three types of HMA. These are Dense graded, Open graded, and gap graded or Stone Matrix Asphalt. This research focuses on the dense graded asphalt mixture. Dense graded asphalt mix has well-distributed aggregate gradation throughout the entire range of sieves used. It is the specified type of mix and can be used in the base, intermediate layers, and surface of the pavement structure[1)].

The Asphalt Institute's published asphalt mix design methods provide an overview of the development of asphalt concrete mix design procedures. Three different types of approaches are available. Marshall, Superpave, and Hveem techniques[1)].

a) Aggregate Gradation

An experimental program was created and implemented using standard asphalt paving mixtures with varying aggregate gradations and sources. Wheel track testing was used to quantify permanent deformation in samples that had been prepared at the optimum asphalt content, as determined by the Marshall Method. The study's findings demonstrated that the type of aggregate and mix gradation has an impact on an asphalt paving mix's resistance to rutting. For all aggregate types, coarser gradation had the strongest resistance to rutting, while open graded mixes exhibited the lowest resistance. The most resistant material across all gradations was dolomite. The Marshall flow demonstrated the strongest linear connection (coefficient of determination = 0.74), with rutting[4)].

Elliot et al.[5)] conducted a study to evaluate the relationship between different aggregate gradations and the properties of asphalt mixtures. Two improperly graded materials, ranging from coarser than JMF to finer than JMF (coarse-fine) and from finer than JMF to coarser than JMF (fine-coarse), along with coarse, fine, and mid-band (Job Mix Formula – JMF), were used to construct the various aggregate mixes. Elliot et al. reached the following conclusions considering this study:

- Variations in gradation have the greatest impact on mixture attributes when the gradation curve is reshaped from coarse to fine or fine to coarse.
- The Marshall stability is increased by fine gradation and decreased by fine-coarse poor gradation. All the gradations, however, had stability values that are evaluated to be more than sufficient.
- Marshall Air Void and VMA are increased by fine-coarse gradation, whereas they are decreased by coarse-fine gradation.
- The maximum Marshall flow is produced by coarse-fine gradation, whereas the lowest is produced by fine-coarse gradation[5)].
- As the combination gets closer to the Fuller curve (maximum density line), the mixture gradation reduces VMA and produces a mixture that is very susceptible to proportioning errors. It is advised to keep the mix away from the maximum density line[6)].

  A study also recommended the following actions to prevent any long-term deformation of HMA pavements[7)].
- Gradation close to the maximum density line should be avoided as it results in a well-packed mixture with comparatively few voids. Low void mixtures are extremely susceptible to

asphalt binder content and flushing danger.

- When compared to rounder particles, angular aggregate particles offer more interlock and internal friction, which increases the mechanical stability of the mixtures.
- Use of aggregate with a rough surface will create higher VMA in compacted mixtures and a good mechanical bond[7)].

Grading standards for the filler, fine, and coarse aggregate components of the mixture are usually provided, along with specifications for the paving mixture's overall composition. A variety of agencies have introduced various standard specifications. Among others, specifications of ASTM 3515[8)], Standard specification for Road and Bridge Work, Nepal Standard[9)], and Japan Standard[10)] for dense graded Nominal Aggregate Maximum Size 13 mm are shown in **Table 1**.

b) Fine Aggregate

In asphalt mixtures, aggregate particles usually comprise between 94 to 96 percent of the total mix, with approximately 40 percent being fine aggregate (passing 2.36 mm). The quality and quantity of fine and coarse aggregates play a very important role in the asphalt mixture. For instance, the geometric irregularity of both coarse and fine aggregate has a major effect on the volumetric properties and performance of asphalt mixtures, which include stiffness, stability, durability, permeability, resistance to moisture damage, resistance to rutting, and total air voids in the mixture[11)].

Table1. *Standards of Mineral Aggregate Gradation of Wearing Course*

Sieve Size	Japan Standard		Nepal Standard		ASDM 3515	
Mm	Lower Limit	Upper Limit	Lower Limits	Upper Limits	Lower Limits	Upper Limits
19	100	100	100	100	100	100
13.2	95	100	90	100	90	100
9.5	-	-	70	88	-	-
4.75	55	70	53	71	44	74
2.36	35	50	42	58	28	58
1.18	-	-	34	48	-	-

Asphalt fine aggregate matrix is a predominant component related to the field performance of HMA. Researches show that the rheological performance of asphalt fine aggregate is significantly affected by asphalt content, gradation, air void content, and testing frequency. Air void is concluded to be the decisive factor that influences the stability of HMA, playing a major role in enhancing the flow resistance of HMA, even though with the richest asphalt content[12)].

Fine Aggregate Angularity has been identified as one of the important aggregate properties contributing to the stability of Hot Mix Asphalt and its resistance against permanent deformation. The performance of dense graded asphalt mixture is significantly influenced by the shape, angularity, and surface texture of fine aggregates. From the Wheel Tracking Test, it was observed that the rut depth for specimens with crushed granite is lower compared to specimens with natural sand. Therefore, it can be concluded that fine aggregates with a more angular shape provide better stability and increase the rutting resistance[13)].

A significant aspect influencing an asphalt concrete mixture's tenderness is the quantity of particles that pass through the 4.75 mm sieve. Soft mixtures are also more likely to be made using spherical, uncrushed particles. The mixture increases the susceptibility to permanent deformation when there is more uncrushed material through a 4.75 mm screen[14)].

c) Filler

The performance of asphalt mastic and asphalt mixtures is significantly influenced by mineral fillers, which are fine-grained mineral particles that are artificial or naturally present in aggregates. Fillers such as diatomite, hydrated lime, and cement can enhance the performance of mastic and mixture at high temperatures and their durability. Fillers, however, such as bentonite, steel slag, and glass powder, negatively impact low-temperature performance. To enhance the performance of the asphalt mixture, it is important that the type and proportion of mineral filler be properly chosen[15)].

One of the main causes of physical distress in asphalt mixes is the loss of adhesion, which has a detrimental effect on the mix's durability. Analyzing the active and passive adhesions between the bitumen and aggregates that make up the asphalt mix allowed researchers to investigate how filler affects this mechanism. The findings of the statistical research demonstrated that both active and passive adhesion are highly impacted by the type and quantity of filler used in asphalt mixtures. The outcomes also showed that both adhesions significantly improved when calcium-based fillers were used[16].

The filler addresses the workability of the asphalt mixture. A low ratio of filler to binder often results in a tender mix, which lacks cohesion and is difficult to compact when applied in the field. Mixes tend to stiffen as the filler increases, but too much filler will also result in a tender mix. A high filler-to-binder ratio will often exhibit a multitude of small stress cracks during the compaction process, called Check cracking. This property is usually calculated for a dense graded mix only[1]. If an excessive amount of large-sized mineral filler is present in the asphalt mixture, the asphalt content may increase[17].

(2) Restricted Zone

SUPERPAVE, which stands for Superior Performing Asphalt Pavement, is a revolutionary mix design technology that was first proposed by the Strategic Highway Research Program back in 1993. Superpave offers bituminous mix field performance, and its gradation chart incorporates control points, a limited zone, and a 0.45 power line.

The restricted zone was first introduced by the Superpave system. It is known that if the gradation passes through the restricted zone between 2.36 mm and 0.3 mm, it is an indication that there is too much natural sand in the mix, resulting in mix tenderness and residing along the maximum density line. **Fig. 1** and **Table 2** show the Control Points, Maximum Density line, and Restricted zone for 13 mm Nominal Maximum Aggregate Size (NMAS)[1].

A study conducted to examine the impact of a restricted zone on HMA performance concluded with suggestions that finely graded mixtures could yield reliable performance, and the study showed that the Superpave Restricted Zone and HMA permanent deformation or fatigue performance are uncorrelated[18].

When compared to gradations that pass outside of the restricted zone, Superpave gradations that comply with the zone were thought to have reduced rut resistance. The bituminous mix's elastic properties under repeated load tests are defined by the resilient modulus, which is determined using an indirect tensile strength setup. A laboratory study was carried out to identify the gradation-affecting elements. Using Minitab-15 statistical software, a two-way factorial design was implemented. The findings showed that temperature and load duration, as well as the interplay of these parameters, had a substantial impact on the HMA's performance[19].

Table2. *Control Points, Maximum Density land, and Restricted Zone*

Sieve Size mm	Maximum Density Line	Control Points		Restricted Zone	
		LL	UL	LL	UL
19	100				
12.5	82.8	90	100		
9.5	73.2				
6.25	60.6				
4.75	53.6				
2.36	39.1	28	58	39.1	39.1
1.18	28.6			25.6	31.6
0.6	21.1			19.1	23.1
0.3	15.5			15.5	15.5
0.15	11.3				
0.075	8.3	2	10		

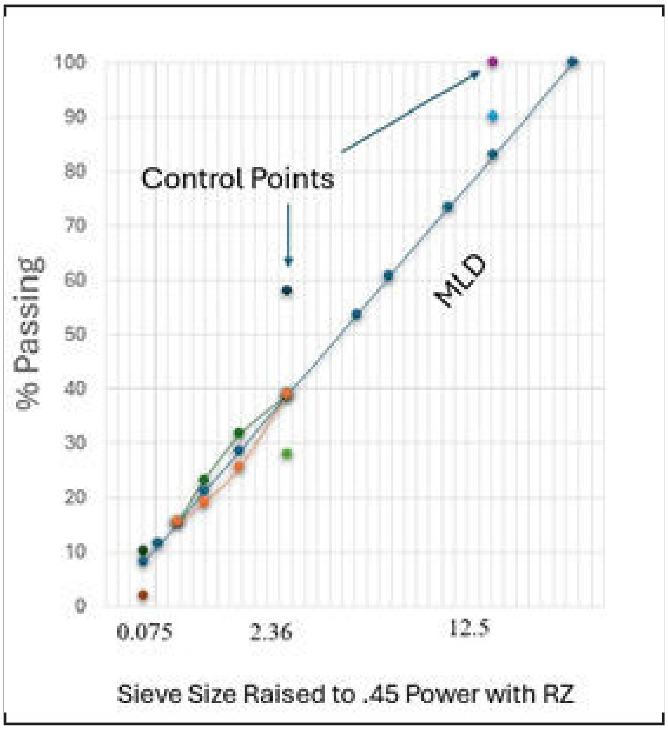

Fig.1 *Restricted zone with Control Points of 13 mm NMAS*

(3) Performance of Asphalt mixture

When it came to Superpave, gradations that passed through the restricted zone were thought to be more rut-resistant than those that did not. Three different gradations that passed through, above, and below the restricted zone were focused on and analyzed. The findings indicate that, in comparison to gradations that pass outside of the restricted zone, those that pass through it not only meet Superpave volumetric standards but also perform better against rutting.[19)]

In Japan, a Wheel Tracking (WT) test is widely used to evaluate the plastic deformation of asphalt mixtures. The WT test was introduced by the Traffic Road Research Laboratory (TRRL) of Britain. In this test, small rubber wheels with a load travel back and forth on a sample of a specified size at a specified speed for a specified duration at a specified temperature, and the dynamic stability (times/mm) is obtained from the degree of deformation per unit of time. However, since the test precision is affected when the value reaches 6,000 (times/mm), caution is necessary in the judgment and handling of the value. For the test, a roller compactor, a mixer with a capacity of 20 kg or more (a high mixing capacity for kneading the modifying material), and a mold are necessary in addition to a WT tester.

Number of times that wheels pass through (for 15 minutes between 45 minutes and 60 minutes after the start of the wheel tracking test) until the sample is deformed by 1 mm. This is referred to as Dynamic Stability (DS). Table 3 shows the test conditions for the Wheel Tracking Test[20)].

Table 3 Test condition for Wheel Tracking Test

Indoor/ Outdoor	Indoor (Contact line Pressure 29.4 KN/m, Room Temperature Curing 12 Hours)
Sample Size	300X300X50 mm
Load	686 N
Test Temperature	60°C
Test Duration	60 Minutes
Number of Run	42 times/minutes, Travel Distance=23 cm
Curing Time	5 hours at Test Temperature
Standard Density	2.434 g/cm3 (Measured)

The Ideal Cracking Test determines the cracking resistance of asphalt mixes through a fracture mechanics–based parameter, Cracking Tolerance Index (CT Index). The larger the CT Index, the better the cracking resistance. The Ideal Cracking Test is typically run with cylindrical specimens at room temperature and a loading rate of 50 mm/min. using the indirect tensile loading frame. Different from other cracking tests, the Ideal Cracking Test integrates all seven desirable features listed below:

- Simplicity: no instrumentation, cutting, gluing, drilling, or notching.
- Practicality: minimum training needed for routine operation.
- Efficiency: test completion within 1 min.
- Test equipment: existing or low-cost equipment.
- Repeatability: coefficient of variation (COV) less than 20 percent.
- Sensitivity: sensitive to asphalt mix characteristics.
- Good correlation with field cracking performance: validated with many field test sections[21)].

The Ideal CT was validated in a number of field test sections, such as FHWA ALF, MnRoad, and Texas, on service roads. The findings indicate that the ideal CT has positive relationships with field fatigue cracking, reflective cracking, and thermal cracking[22)]. Generally, CT index increases with Disk Shaped Compact Tension (DCT) fracture energy[23)].

2. RESEARCH PURPOSE & OBJECTIVE

In Nepal, the Standard Specification for Road and Bridge Work has specified Gradation limits and Standard Procedures. The specification specifies following the procedure in the manual published by the Asphalt Institute, US, for the design of asphalt mixture. In the manual, the Superpave gradation curve specifies a restricted zone that should be avoided while considering the design of the asphalt mix. Figure 1 shows the gradation of the Restricted zone of 13.2 NMAS. Hence, some government or private agencies in Nepal entirely reject any mixture passing through the restricted zone. For the asphalt mix designer restricted zone creates confusion about its effect on asphalt mix properties, as well as rutting and fatigue behavior of the asphalt mixture. Therefore, this study is focused on the effect of the restricted zone on the Marshall design and performance of the asphalt mixture. For researchers working in asphalt engineering worldwide, this paper is especially important.

The major objective of this study is to investigate the influence of the Superpave restricted zone of the fine aggregate on Marshall design properties and performance of the wearing course. This study focuses on evaluating the volumetric properties, stability, flow behavior, rutting, and cracking behavior of Hot Mix Asphalt.

3. MATERIALS AND METHODOLOGY

(1) Selection of binder

There are numerous kinds of binders available in Japan. The use of a typical binder that is compatible with both Nepal and Japan standards was selected for this study. Binder selection also relies on the country's climate; thus, for research purposes, a binder 80/100 penetration grade binder equivalent to Viscosity Grade 10 in Nepal standard was used.

(2) Selection of Course Aggregate, Fine aggregate, and filler

Aggregates are classified into natural, artificial, screening, and special types. Sandstone is a common type of sedimentary rock that is available locally in Nepal as well as Japan. So, sandstone was used as coarse aggregate and fine aggregate for research purposes. Natural fine aggregates were also used. Similarly, stone dust from limestone was used for research purposes, which is common in all countries. **Table 5** shows the gradation of different kinds of mineral aggregates, which were used for research purposes. The nominal maximum aggregate size of 13 mm was chosen for the wearing course because the thickness of the wearing course is about 40 mm only, as per the standard guideline published by the Department of Roads, Nepal. All materials meet the physical requirements for the asphalt pavement as per the Japan Standard as well as the Nepal standard.

(3) Gradation and Mixes

Three types of Gradation were prepared by Job mix, which were passed above the Restricted Zone (ARZ), through the Restricted Zone (TRZ), and below the Restricted Zone (BRZ). The gradation chart in **Fig. 2** shows the gradation lines of three mixes with Upper Limit of Restricted Zone (ULRZ) and Lower Limit of Restricted Zone (LLRZ). A dense graded asphalt mixture was prepared using the Marshall method. Dense graded asphalt mixture can be used for both the ordinary region and the cold region. So, the guideline of the Handbook for asphalt pavement by the Japan Road Association was used for the Marshall test.

(4) Determination of Optimum Asphalt Content

The Optimum Asphalt Content was found to meet the Marshall criteria that were taken into consideration. **Table 6** shows the limits and Marshall criteria that were applied in this study. The asphalt content was plotted against the Marshall Stability, Marshall Flow, Air Void, Voids Fill with Asphalt, and Void in Mineral Aggregate using the calculated data.

Table 5. *Gradation for different types of mineral aggregates*

Size mm	Grade 6 (13-10)	Grade 6 (10-5)	Grade 7	Crushed fine aggregate	Natural Fine Sand	Filler
19	100	100	100	100	100	100
13.2	86.3	100	100	100	100	100
9.5	3.7	94	100	100	100	100
4.75	0.8	2.6	89.5	100	100	100
2.36	0.8	1	3.9	91.2	99.7	100
1.18	0	1	0	67.16	97.5	100
0.6	0	1	0	43.1	83.8	100
0.3	0	0	0	23.2	25.5	99.6
0.15	0	0	0	8.8	2.7	95.6
0.075	0	0	0	3	1	84.1

Table 6. *Gradation of ARZ, TRZ and BRZ*

Sieve Size	Permissible Limits		Gradation of Mix		
(mm)	LL	UL	ARZ	TRZ	BRZ
19	100	100	100	100	100
13.2	95	100	97.3	97.3	97.1
9.5	95	100	79.7	79.8	79
4.75	55	70	62	62.4	62.5
2.36	35	50	41.7	37.2	33.9
1.18	-	-	32.4	28.5	25.2
0.6	18	30	24	21.1	18
0.3	10	21	15.5	14.7	12
0.15	6	16	9.8	9.9	7.4
0.075	4	8	6.9	7.2	5.1

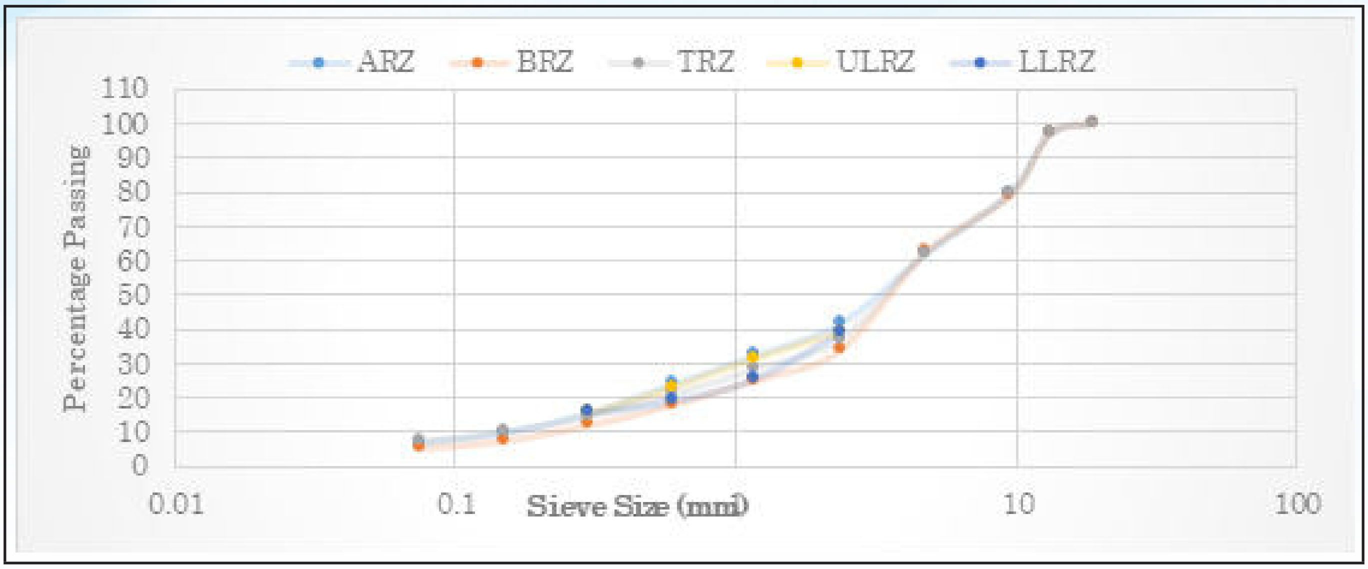

Fig.2 Gradation Chart for different mixes

The design asphalt content was determined by looking at the common range of asphalt content that meets all the Marshall design parameters. For a given mixture, the design Asphalt content is the median value of the common range as specified in the handbook[10].

Table.6 *Marshall Design Standard*

Design Criteria	Heavy Traffic
Number of Blows	75
Percentage of Air Voids (%)	3 – 6
Voids Filled with Asphalt (%)	70 - 85
Marshall Stability (KN)	7.35 or more
Flow Value 1/100 (cm)	20 - 40

(5) Performance Test of Asphalt

A performance test was conducted to predict the performance of the asphalt mixture to fatigue cracking and Rutting. The Tests that were conducted using the Wheel Tracking Test and the Ideal CT index Test.

Table 4. *Test condition for Ideal CT index Test*

Load	Vertical Monotonic Load at Constant Rate of 50 mm/min
Specimen Dimension	150 mm dia and 62 mm height
Height Tolerance	62±1 mm
Air Void of Specimen	7± 1%
Test Temperature	25°C
Curing of Sample	2 hours at 25°C
Specimen Fabrication	Gyratory Compactor

The Wheel Tracking Test was conducted by preparing a sample of three gradation ARZ, TRZ, and BRZ with a designed OAC. All together nine samples, three of each gradation, were prepared and tested as per the standards mentioned in the Japan Road Association pavement condition survey and testing handbook test number B003. The test condition is mentioned in **Table 3,** Dynamic Stability, Number of Cycles of wheel track per millimeter was calculated by using the following formula.

$$DS = 42 \times \frac{t_1 - t_2}{d_2 - d_1} \times C_1 \times C_2 \qquad (1)$$

Here,

DS: Dynamic Stability (Times/mm)

d_1: Deformation in mm at 45 minutes

d_2: Deformation in mm at 60 minutes

C_1: Correction Coefficient according to the type of testing machine, Variable speed drive by crank = 1.0, fixed speed drive by chain =1.5

C_2: Correction factor for specimen type

Indoor specimen (width 300 mm) =1.0, On site cut specimen (width 150 mm) = 0.8

Three gradations of Samples ARZ, TRZ, and BRZ were prepared at the designed OBC to conduct the Ideal CT index Test. Three samples from each zone, altogether nine samples, were tested on the CT index test machine. The standard method proposed by Zhou[21)] was used. The test condition is shown in **Table 4**. The formula for calculating the Ideal CT index Test is shown below: -

$$\text{CT}_{\text{ Index}} = \frac{t}{62} \times \frac{l_{75}}{D} \times \frac{G_f}{|m_{75}|} \quad (2)$$

Here,

$\text{CT}_{\text{ Index}}$ = Cracking Tolerance Index

G_f = Failure Energy (Joules/m^2)

$|m75|$ =absolute Value of the Post-Peak slope (N/m)

l_{75} =Displacement at 75% of the peak load after the Peak (mm)

$$G_f = \frac{W_f}{D \times t} \times 10^6 \quad (3)$$

Here,

W_f = Work of Failure (Joule)

D = Diameter of Sample Specimen in mm

t = Thickness of Sample Specimen in mm

Fig.3 shows a sample of the load versus load line displacement graph, which was used to calculate the CT Index value. Similarly, **Fig. 4** shows the equipment used for the Ideal CT Index Test. The equipment, similar to that used for the Tensile Strength Ratio Test, was equipped with software to generate load versus load line displacement graphs.

In **Equation 3,** W_f was calculated using the Load vs Displacement Curve. The whole area was calculated using the following formula: -

$$W_f = \sum_{i=1}^{n-1} (l_{i+1} - l_i) \times p_i + \frac{1}{2} \times ((l_{i+1} - l_i) \times (p_{i+1} - p_i)) \quad (4)$$

Here,

P_i = Applied load (kN) at the i load step application

P_{i+1} = applied load (kN) at the i+1 load step application

l_i = Load Line Displacement (mm) at the i step

l_{i+1} = Load Line Displacement (mm) at the i+1 step

Likewise, |m_75 | is the post-peak slope as shown in **Fig. 3,** which was calculated by using the following formula: -

$$|m_{75}| = \left|\frac{P_{85} - P_{65}}{l_{85} - l_{65}}\right| \quad (5)$$

And l_{75} was calculated by using a linear interpolation method.

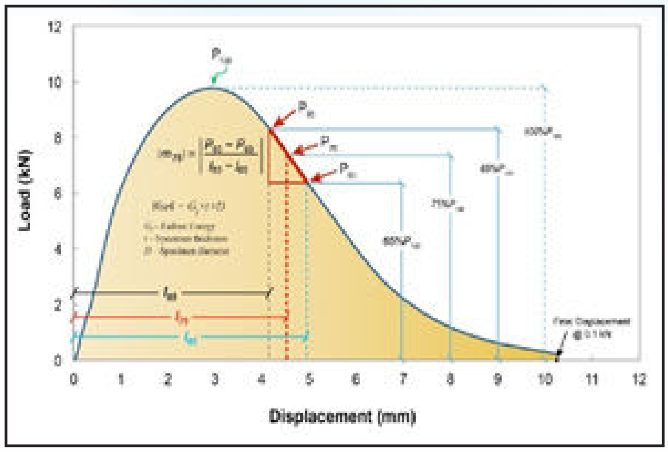

Fig.3 Load versus Load Line Displacement Curve

Fig.4 Ideal CT index Test Machine

4. DATA AND ANALYSIS

The Fineness modulus, or coarse ratio, shows the average size of the mix and was determined by using the formula in **Equation 4** to classify the asphalt mixture. The lower values show finer, and the higher values show coarser. As per **Table 7** below, the ARZ mixture is finer than the other mixtures, and BRZ indicates the coarser than the other mixtures.

$$Fineness\ Modulus = \frac{(n \times 100) - (a_1 + a_2 + a_3 + \cdots \ldots a_n)}{100}$$

(**Equation 4**)

Here,

n = Number of sieve sizes used

$a_1 a_2 a_3 \ldots an$= % Passing through the Sieve Size

Table 7. *Finess Modulus or Coarser Ratio of Asphalt Mixtures*

Gradation of Mix	Fineness Modulus or Coarse Ratio	
	Asphalt Mix	Fine Aggregate
ARZ	5.30	3.48
TRZ	5.42	3.76
BRZ	5.56	3.86

By the guidelines provided in the Handbook of asphalt pavement, Japan Road Association, the Optimum Asphalt Content for each zone was determined as shown in **Table 8,** and then the Marshall samples were prepared for different zone with the respective Optimum Asphalt Content (OAC). **Table 9** shows average parameters of the Marshall mix at OAC, which were obtained from laboratory experiments. Six Marshall samples were preprepared for each zone at OAC.

The Marshall stability, Flow Value, Residual Stability, Density, Air Voids, VMA, and VFA are the parameters of the Marshall mix design method. The coefficient of variation of each parameter of each mixture was less than 10%.

According to the fineness modulus value in **Table 7**, there seemed to be little change in the average size of the three kinds of asphalt mixtures. Therefore, Statistical Tool, one-way ANOVA test was used for comparing mean values of all three mixtures and Similarly, T-test was used for comparing mean values of the asphalt mixture in pairs at 90% confidence limit to verify the significance of the data.

For one-way ANOVA Statistical Analysis, it was assumed that the mean values of all parameters, as shown in **Table 9,** are similar for each type of mixture. There is no significant difference between the mean values of all parameters of the three mixtures at a 90% confidence limit, which is the null hypothesis.

$$\mu_{ARZ\ P} = \mu_{TRZ\ P} = \mu_{BRZ\ P} \qquad \text{(Null Hypothesis)}$$

$$\mu_{ARZ\ P} \neq \mu_{TRZ\ P} \neq \mu_{BRZ\ P} \qquad \text{(Alt. Hypothesis)}$$

Here,

μ= Mean Value

p = Parameters, i.e., Marshall stability, Flow Value, Residual Stability, Density, Air Voids, VMA, VFA

For a two-tailed t-test statistical analysis, it was assumed that the mean values of all parameters between the two types of mixtures, as shown in **Table 9,** are similar to each other. There is no significant difference between the mean values of all parameters of the three mixtures by comparing in pairs at a 90% confidence limit, which is the null hypothesis.

Null Hypothesis:

$$\mu_{ARZ\ P} = \mu_{TRZ\ P}$$
$$\mu_{ARZ\ P} = \mu_{BRZ\ P}$$
$$\mu_{TRZ\ P} = \mu_{BRZ\ P}$$

Table 8. *Values of Marshall Properties at the designed OAC*

Gradation	Bulk Density gm/cc	Air Voids %	VMA %	VFA%	Stability (KN)	Flow Value (mm)	Residual Stability (KN)	OAC
ARZ	2.418	3.77	16.26	76.7	10.19	3.48	8.91	5.19
TRZ	2.424	3.86	15.79	75.6	9.84	3.79	7.57	5.03
BRZ	2.399	4.37	18.06	75.6	7.97	3.49	8.03	5.89

Table 9. *Average Values of Marshall Properties at OAC*

Gradation	Bulk Density gm/cc	Air Voids %	VMA %	VFA%	Stability (KN)	Flow Value (mm)	Residual Stability (KN)	OAC
ARZ	2.434	3.75	15.49	79.63	10.36	3.2	8.91	5.19
TRZ	2.406	4.53	16.35	72.3	9.28	3.6	7.57	5.03
BRZ	2.401	3.5	17.31	79.76	9.16	3.3	8.02	5.89

Table 10. One-way ANOVA test results

Condition	Parameter	F Test Value	F critical Value	Null Hypothesis
ARZ=TRZ=BRZ	Stability	8.52	3.46	Reject
	Flow	13.9	3.46	Reject
	Residual Stability	5.55	3.46	Reject
	Density	52.36	2.69	Reject
	Air Voids	55	2.69	Reject
	VMA	119.15	2.69	Reject
	VFA	85.24	2.69	Reject

Alternative hypothesis

$$\mu_{ARZ\ P} \neq \mu_{TRZ\ P}$$
$$\mu_{ARZ\ P} \neq \mu_{BRZ\ P}$$
$$\mu_{TRZ\ P} \neq \mu_{BRZ\ P}$$

Here,

μ = Mean Value

p = Parameters, i.e., Marshall stability, Flow Value, Residual Stability, Density, Air Voids, VMA, VFA

Table 11. T-test Results

Mix Properties	Gradation Comparison	T-Stat	T Critical	Null Hypothesis
Stability	ARZ Vs TRZ	2.95	2.91	Reject
	ARZ Vs BRZ	2.62	2.91	Accept
	TRZ Vs BRZ	1.33	2.91	Accept
Flow	ARZ Vs TRZ	4.25	2.91	Reject
	ARZ Vs BRZ	4	2.91	Reject
	TRZ Vs BRZ	3.6	2.91	Reject
Density	ARZ Vs TRZ	11.37	2.01	Reject
	ARZ Vs BRZ	10.87	2.01	Reject
	TRZ Vs BRZ	1.18	2.01	Accept
Air Void	ARZ Vs TRZ	-14.06	2.01	Reject
	ARZ Vs BRZ	-3.01	2.01	Reject
	TRZ Vs BRZ	5.85	2.01	Reject
VMA	ARZ Vs TRZ	-10.18	2.01	Reject
	ARZ Vs BRZ	-17.96	2.01	Reject
	TRZ Vs BRZ	-6.37	2.01	Reject
VFA	ARZ Vs TRZ	16.09	2.01	Reject
	ARZ Vs BRZ	0.22	2.01	Accept
	TRZ Vs BRZ	-8.99	2.01	Reject

The Wheel Tracking Test Result data with Dynamic Stability Values are shown in **Table 12**. The data shows TRZ has higher Dynamic Stability and has higher rutting resistance than other mixtures. The **Fig. 3** shows that BRZ has a higher rutting depth as compared to other mixtures.

Table 12. Wheel Tracking Test results

Gradation	OBC	Dynamic Stability (times/mm)	Coefficient of Variance	No. of Samples
ARZ	5.19	530	13.4	3
TRZ	5.03	800	9.4	3
BRZ	5.89	430	15.1	3

Fig.5 Rutting Depth mm with Time

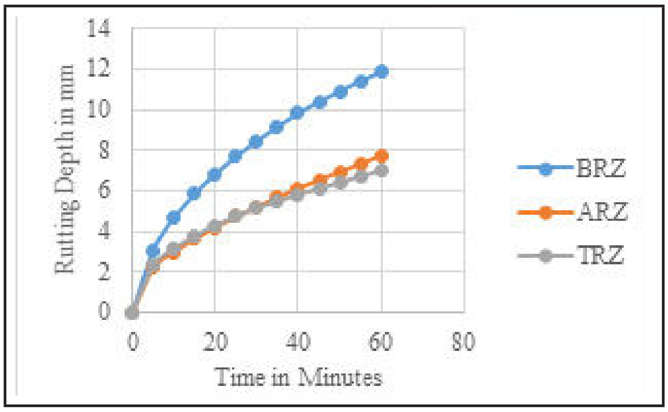

Ideal CT index Test Result data with Index Values are shown in **Table 13**. The data shows BRZ has a higher index value and has higher cracking resistance than other mixtures. **Figure 4** shows that BRZ has a higher load versus displacement area than other mixtures.

Table 13. Ideal CT index Test Results at 25 °C

Gradation	OAC	Ideal CT index Value	Coefficient of Variance	Number of Samples
ARZ	5.19	150	18.8	3
TRZ	5.03	166	16	3
BRZ	5.89	249	6.1	3

Fig.6 Load versus Displacement Graphs

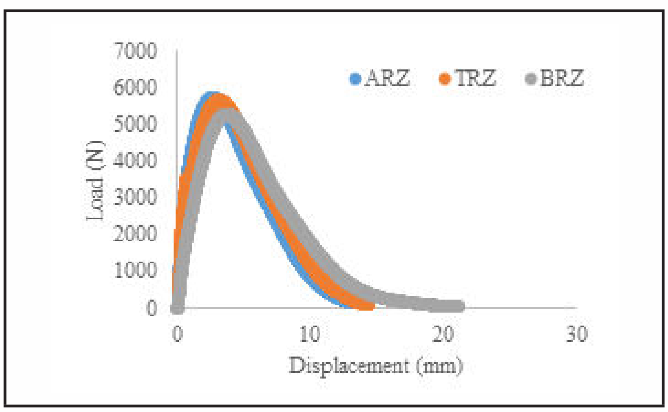

5. RESULT

Laboratory experiments were conducted to evaluate the Marshall parameters and the Performance Test of the Dense graded 13 mm nominal aggregate maximum size HMA, using different fine aggregate gradations that pass through, below, and above the restricted zone of the Superpave specified gradation. Based on the Analysis of data, the following results have been summarized: -

- All three kinds of mixture satisfied the Marshall Criteria mentioned in the standard.
- The mixture below the restricted zone demands a higher asphalt content as comparison to other mixtures.
- The statistical analysis at a 90% confidence limit showed that all three types of mixtures—above, though, and below the Restricted Zone—have significant differences in the average values of parameters.
- Between the above and below restricted zone, there is no significant difference in the Stability and the Void Filled with Asphalt at 90% confidence limit, and there is no significant difference in the Stability and Density between through and below restricted zone at 90% confidence limit.
- For the Wheel Tracking Rutting Test, gradation through the restricted zone shows more rutting resistance than other types of mixtures.
- The Ideal CT index Value shows that the gradation below the restricted zone has greater cracking resistance than other types of mixtures.

5. CONCLUSION

Based on the above literature review, data analysis, and results. The following conclusion can be made:-

1. The Superpave Restricted Zone did not influence the Marshall Criteria.
2. The results indicate that a small variation in gradation would significantly change in Hot Mix Asphalt properties.
3. For the coarser crushed fine aggregate in a mix of the same nominal aggregate maximum size, demands a higher asphalt content because of high Air Void, High Void in Mineral Aggregate.
4. For Rutting Test, through restricted zone mixture shows higher Resistance; however, the Dynamic Stability values are less than standard, and all mixtures have higher rutting depths.
5. Only fulfilment of the Marshall criteria is not sufficient for the better performance of asphalt.
6. Higher Asphalt Content creates higher Rutting Depth, but an increase in cracking resistance; therefore, Rutting Test Data and Ideal CT index data show mix design is required by considering the performance test of asphalt.

REFERENCES

1) Asphalt Institute. (2014). *MS-2 Asphalt Mix Design Methods (7 ed., Vol. Manual Series 2)*. Kentuky: Asphalt Institute. Retrieved 2014

2) Roberts, F., Kandhal, P., Brown, E., Lee, D., & Kennedy, T. (1996). *Hot Mix Asphalt Materials, Mixture Design and Construction. Lanham*, Maryland, USA: National Asphalt Pavement Association.

3) McGenis, R., Aderson, R., Kennedy, T., & Solaimanian, M. (1995). *Background of Superpave Asphalt Mixture Design and Analysis.* Verginia: Federal Highway Administration

4) Ahmed, M., & Attia, M. I. (2013). Impact of aggregate gradation and type on Hot Mix Asphalt Rutting in Egypt. International Journal of Engineering Research and Application.

5) Elliot R.P., F. M. (1991). Effect of aggregate gradation variation on asphalt concrete mix properties. *National Research Council*

6) TRL (2002). A Guide to the design of hot mix asphalt in tropical and sub-tropical countries (*Vol. Overseas Road Note 19*). Crownthrone House, Berkshire, UK: Transport Research Laboratory.

7) Chowdhury A., B. J. (2001). *Effect of superpave restricted zone on permanent deformation.* Texas, USA: Texas Transportation Institute.

8) ASTM. (2001). *Standard Specification for Hot-Mixed, Hot-laid Bituminous Paving Mixture*, Conshohocken, USA: American Society for Testing and Meterials.

9) Standard Specifications for Road and Bridge works. (2017). Kathmandu, Nepal: Department of Roads.

10) Japan Road Association. (2019). Manual for asphalt pavement (Vol. 3rd). Tokyo, Japan: Japan Road Association.

11) Chowdhury, A., Button, J., Kohale, V., & Jahn, D. (2001). Evaluation of Superpave Fine Aggregate Angularity Specification. Retrieved from https://repositories.lib.utexas.edu/items/d4c472f3-bc7e-4b37-8259-70a9316046f9

12) Gong, X., ,Dong, Z., Wang, H., Ma, X., Yu, H., & Hu, K. (2019). *Rheological characterization of asphalt fine aggregate matrix using dynamic shear rheometer. Polymers.* Retrieved from https://www.mdpi.com/2073-4360/11/8/1273

13) Ramli, I., Yaacob, H., Hassan, N., Ismail, C., & Hainind, M. (2013). *Fine aggregate angularity effects on rutting resistance of asphalt mixture.* Retrieved from https://journals.utm.my/jurnalteknologi/article/view/2154

14) Crawford, C. (1989). Tender mixes: probable causes, possible remedies. Maryland, USA: National Asphalt Pavement Association.

15) Chen, Y., Shibing, X., Tebaldi, G., & Romeo, E. (2022). Role of mineral filler in asphalt mixture. Road materials and pavement. Taylor &Francis, 247-286. Retrieved from https://doi.org/10.1080/14680629.2020.1826351

16) Choudhary, J., Kumar, B., & Gupta, A. (2020). Effect of filler on the bitumen-aggregate adhesion in asphalt mix. Taylor & Francis, 1482-1490. Retrieved from https://doi.org/10.1080/10298436.2018.1549325

17) Tarris, J., & Aderson, D. (1982). The Effects of Baghouse Fines on Mixture Design Properties. National Asphalt Pavement Association. Retrieved from https://trid.trb.org/View/380107

18) Hand,A.,&Martin,A.(2001).ImpactofGradation Relative to Superpave Restricted Zone on Hot-Mix Asphalt Performance. Transportation Research Board. doi:10.3141/1767-20

19) Hussain, A., Haq, F., Javaid, N., & Khurshid, M. (2019). Restricted zone of Superpave mix design and its impact on resilient modulus and permanent deformation. Stavebni Obzor. doi:10.14311/CEJ.2019.01.0003

20) JICA. (2020). Research on Improvement of Rut Resistance for Road Pavements in Developing Countries. Tokyo, Japan: Japan International Cooperation Agency.

21) Zhou, F. (2019). Development of an IDEAL Cracking Test for Asphalt Mix Design, Quality Control and Quality Assurance. Transportation Research Board

22) Zhou, F., Im, S., Sun, L., & Scullion, T. (2017). Development of an IDEAL cracking test for asphalt. Road Materials and Pavement Design

5.0 Possible Causes of Bridge Failures in Nepal

-Dr. Bijaya Jaishi, DG
DoR
Email: bijayadr@gmail.com

1. Background

Currently, there are approximately 2,350 bridges on strategic roads and around 1,000 bridges on local roads in Nepal. The earliest of these bridges were designed using foreign expertise and constructed by foreign companies with support from donor nations on major highways such as the East-West Highway, Tribhuvan Highway, Prithvi Highway, Kodari Highway, and Siddhartha Highway. Later, Nepali engineers began designing bridges and Nepali contractors started their construction. In the 1950s, only a few bridges were built annually, while in the 1960s, around 20 to 40 bridges were constructed each year. Currently, approximately 200 to 250 bridges are being completed annually.

Each year, as is the case of rest of the world, some bridges experience premature failure, especially during the monsoon season. In some cases, floods have washed away temporary supports during construction, causing damage to the bridges. Similarly, some steel truss bridges under construction have been damaged by strong winds. Some bridges, even after completion, experience foundation sinking leading to disruption in transportation. Additionally, unexpected floods and debris flow caused by landslides, in the upper regions of rivers, have led to significant damage to bridges in the lower areas. Similarly, on October 11 and 12, 2024, heavy rainfall, floods and landslides around the Sunkoshi River and other regions, including those directly impacting major highways such as the BP Highway, Prithvi Highway, and Mechi Highway, caused widespread damage to life and property. This event, in particular, also caused significant damage to bridges under construction or already completed in the Koshi Basin. This papers briefly presents key factors that contributes to Bridge failure in Nepal.

2. International scenario

According to a recent study conducted in China, a total of 418 bridges collapsed during the period from 2009 to 2019. The three main causes of these collapses were construction issues, flooding/ scouring, and collisions. Other causes are shown in the Figs. 1~2.

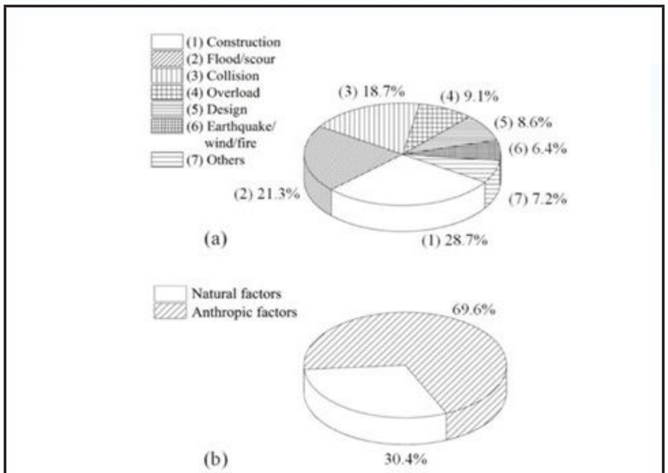

The distribution of bridge failure causes between 2009 and 2018.: (a) percentage of collapse reasons and (b) proportion of natural factors and anthropic factors leading to bridge failures.

Fig.1- The distribution of bridge failure causes between 2009 and 2018 in China [1]

The statistics of failures in bridges under construction and those that have been completed and are in service are shown in the diagram. The diagram also indicates that failures during the construction phase are significant.

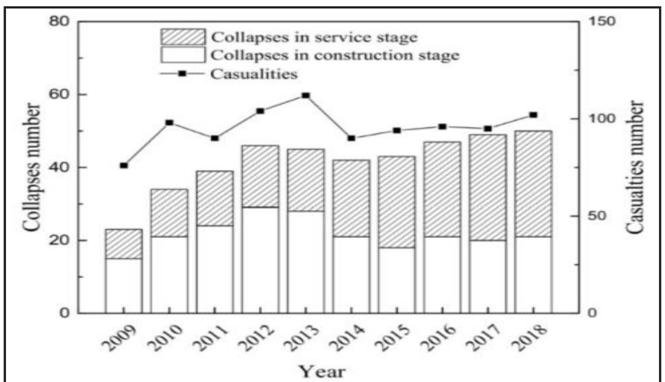

Number of bridge collapses and casualties between 2009 and 2018.

Fig.2- Number of bridge collapses and casualties between 2009 and 2018 in China [1]

The details of bridge collapses during their service life are shown in Fig. 3 According to the data, out of a total of 418 collapsed bridges, 30.3% collapsed within 0-10 years, and 33.8% collapsed within 10-20 years. In contrast, only 2.1% of bridges had a service life of more than 50 years.

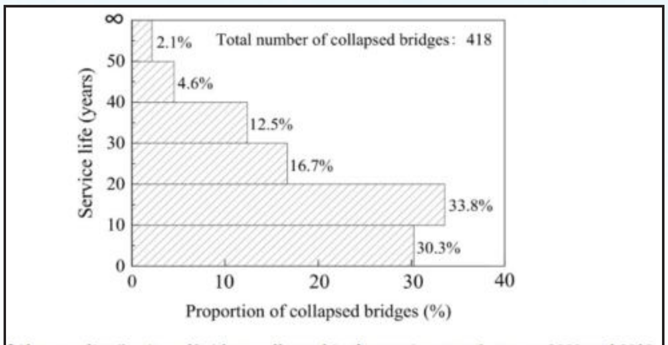

Life span distribution of bridges collapsed in the service stage between 2009 and 2018.

Fig.3- Life span distribution of bridges collapsed in the service stage between 2009 and 2018 in China [1]

A study conducted in the United States for the period 1980-2012 found that 47% of bridge collapses were caused by floods and scouring, 15% by collisions, 13% by overloading, and 7% by environmental degradation. Studies conducted in other countries also indicate similar major causes of bridge collapses. *[2]*

3. Bridge failure in Nepal

Observing the nature of bridge failures in Nepal, it appears that most collapses have occurred due to flood/scour affecting the foundation rather than issues with the superstructure. This pattern is consistent with international trends. In the past, several operational bridges, including the Ratu Khola Bridge, Bardibas; Bhapsi Khola Bridge; Charnawati Khola Bridge; Dudhaura Khola Bridge along E-W highway; Dholi Khola Bridg, Kamala Khola Bridge, and Triyuga Khola Bridge, collapsed due to foundation failure caused by excessive flooding/scouring. Among them, the Ratu Khola Bridge and the Dudhaura Khola Bridge were constructed with assistance from the Soviet Union government. Additionally, some bridges under construction collapsed when floods washed away their temporary supports. A recent study of bridge damages indicates the following major patterns of failure:

(a) Superstructure failure of Bridge during construction

Currently, bridge superstructures in Nepal are commonly constructed using the Cast-in-Situ method. In this process, steel staging/formwork is erected to support the superstructure during construction. This temporary structure bears the load of the superstructure until the concrete gains the required strength and is then removed afterward. Particularly in the case of Cast-in-Situ Prestressed Concrete Girders, staging/formwork cannot be removed until the first stage of prestressing is completed, which is generally done after 12 days.

Fig.4-(a) Jhimruk Khola Bridge along Dabra Majhidmar Road

Fig.4(b) Trishuli Bridge, Masstar that has been collapsed in 2021-04-17

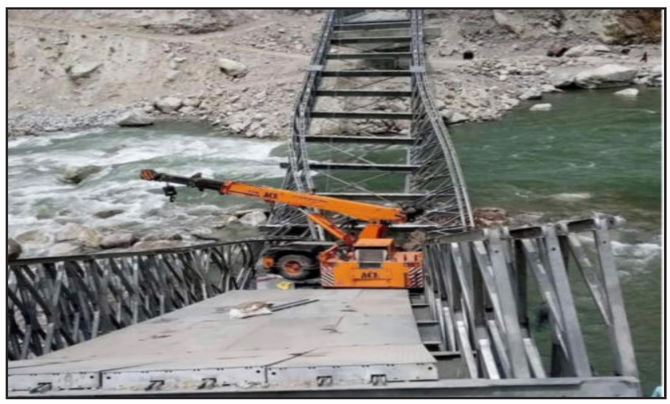

Fig 4(c). Bheri Bailey Bridge along Jajarkot-Dolpa collapse due to unbalanced crane in April 21,2003.

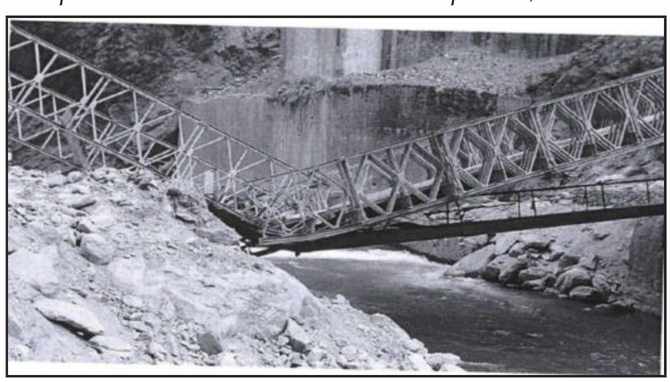

Fig.4(d). Larcha Bailey bridge failure during erection (in 2018-02-20)

Fig.4(e). Failure of Thimura Bridge during construction (in 2021-04-06)

Superstructure of many bridges, their names are listed in the subsequend parts of this paragraph, faced similar kinds of failure during the flood event of 2021 AD, where staging and formwork were damaged before the completion of first stage of prestressing. The examples are: Solabang Khola Bridge, Rapti Highway, Rukum; Jhimruk River Bridge, Dabra Majhidamar Road; Sunkoshi River Bridge – Nawalpurghat; Mahesh Khola Bridge – Dhading; Phuljor River Bridge – Lalbandi-Rampur Belbas Road, Sarlahi; Lugreli Gad Bridge. The photographs of Jhimruk Khola bridge that was damaged due to failure of staging is shown in Fig. 4(a). There is also failure of many bridges during construction due to high velocity wind load. For example, Sunkoshi Bridge, Ghumri; Trishuli Bridge Dashdhunga; Trishuli Bridge Masstar as shown in Fig. 4 (b). Similarly, there were several failure of Bailey bridge during erection due to ignorance or lack of understanding and technical capability of technicians. The examples are Larcha Bailey Bridge, Bheri Bailey Bridge Fig. 4 (c), 4(d) etc.

(b) Foundation failure in completed or under construction Bridges

Foundation failure has been observed in few bridges in Nepal. The examples of bridge failure in completed or under construction stage in 2021 AD due to foundation problem are:Triyuga River Bridge, Gaighat-Diktel Road (Under Construction); Kamala River Bridge, Hulaki Highway, Dhanusha (Under Construction); Ghodaha Bridge, East-West Highway, Rupandehi (Completed); Turiya Khola Bridge, East-West Highway, Rupandehi (Completed); Lodari Khola Bridge, Road from Parsa (Chitwan) to Chainpur (Completed); The photographs of Lodari Khola bridge that was damaged due to failure of foundation is shown in Fig.5 (d). The failure is mostly due to flow concentration in few substructures that increases scour depth, extraction of materials and bed degradation, sand boiling phenomenon etc.

Fig.5 (a): Lodari Khola along Parsa Chainpur road

Fig. 5 (b) Pier of Ratu Khola Bridge settled on 13 Aug, 2014

(c) Damage to Bridges in Lower Regions Due to Unexpected Floods and Landslide-Induced Debris Flow

In recent years, the destruction of bridges in lower river regions has become increasingly common due to sudden floods and debris flow caused by landslides blocking and then abruptly releasing river flow. This phenomenon, likely influenced by climate change, results in massive flooding and debris, leading to severe damage to downstream bridges. The following bridges were damaged due to this reason in 2021 AD. Timang Khola Bailey Bridge, Dumre-Besisahar-Chame-Manang Road; Melamchi Bazar Bridge, Melamchi-Nawalpur-Chautara Road; Fatte Khola Bridge, Melamchi-Fatte-Duvachaur Road; Nakatte Bridge, Constructed under the Melamchi Drinking Water Project; Timbu Bridge, Constructed under the Melamchi Drinking Water Project; Akase Bridge, Constructed under the Melamchi Drinking Water Project. The photographs of Melamchi Bridge that was washed away and devastating situation of Melachim bazzar area is shown in Fig.6 (a).

Fig. 6 (a) Washed bridges due to Melachi disaster (Aug 1, 2021), Melamchi Bridge, Sindupalchok

When designing bridges in Nepal, this scenario is generally not considered, as it is complex and could result in an uneconomical or unrealistic design. A sudden flood can increase the scour depth and apply additional hydraulic load to the bridge structure, weakening the foundation and causing the bridge to collapse. The impact of climate change has resulted in extreme precipitation events and flooding. In recent years, this factor has been considered in bridge design guidelines, but it was not included in earlier designs.

Fig.6 (b): Sadi Khola Bridge (washed on 2018/8/18)

(d) Excessive flooding occurred compared to the discharge calculated using the empirical formula in the hydrological analysis

In Nepal, hydrological analysis for bridges is primarily based on empirical formulas developed in foreign countries. The method for calculating scour depth is also empirical. The method for determining linear waterways has not been developed according to our terrain. As a result, the results vary significantly between different hydrologists. In flat Terai regions and complicated terrains, it is also difficult to accurately determine the catchment area. Due to the reliance on such empirical formulas, the foundation and height of bridges do not align with the actual conditions, leading to bridge failures. Mostly, in Koshi Basin, extreme flooding of 2024/9/27-2024/9/28 caused significant damage to bridges such as the Khaireini Bridge in Nepalthok, Khurkot Bridge, Foxingtar Bridge, and many Trail Suspension Bridges in Sunkoshi Basin. The water level exceeded the deck level of these bridges, which was not considered in the design. The water current hitting the deck level was not accounted for in the design code. The Photographs of various bridges before and after failure is shown in Fig. (7). Local road construction, land plotting, and crusher plants in river catchment areas have led to excessive sedimentation in the river, increasing the high flood level and causing damage: Design guidlines should be prepared to consider this phemena during the design phase, as it also contributes to bridge damage:

Before failure | After failure

Fig.7(a) Sunkoshi Bridge, Nepalthok

Fig.7(b) Sunkoshi Bridge, Nepalthok

Fig. 7(c) Sunkoshi Bridge, Khurkot

Fig.7 (d) Sunkoshi Bridge, Khurkot

Fig.7 (e) Sunkoshi Bridge, Foxingtar

Fig.7 (f) Sunkoshi Bridge, Foxingtar

Fig.7 Photographs of various bridges in Koshi Basin before and after failure that are collapsed due to record breaking extreme flooding of 2024/9/27-2024/9/28.

(e) Bridge Collapse Due to other reasons

Other important factors are overloading and unregulated traffic, inadequate maintenance and inspection poor construction practices, and design deficiencies. Larcha Arch bridge collapose due to sudden fall of rock from hill side is shown in Fig. 8(a). The failure of Binayi Khola due to possible overload of heavy loaded lorry is shown in Fig.8.

Fig.8-(a) Larcha Arch bridge collapose due to sudden fall of rock from hill side (2017-7)	*Fig.8(b) Failed Binayi Khola Bridge along E-W highway near Dumkibas (Jan 10, 2025)*

4.0 Conclusion

The main conclusions are summarized below:

- Increase the Freeboard of Bridges at Strategic Locations on the Gandaki, Koshi, Karnali, and their major tributaries. A recent damage study of bridges in the Koshi Basin suggests that maintaining a minimum freeboard of 3-5 meters would be appropriate.
- Prioritize the construction of long-span bridges at strategic locations on the Gandaki, Koshi, Karnali, and their major tributaries, rather than building multi-span bridges with piers in the middle of the river. The Department should take necessary steps to enhance the capacity of private sector engineers and those from the Department of Roads in long-span bridge design and construction. Sufficient attention should be given to climate-resilient bridge design and construction.
- Prevent debris siltation and concentrated flow near bridges: Debris accumulation, siltation, and boulders around bridges increase High Flood Level (HFL), leading to concentrated flow in some spans instead of distributing it evenly. This increases the risk of bridge damage during monsoon. The concerned authorities should implement preventive measures during winter through departmental circulars.
- Conduct studies on the impact of watershed encroachment and unplanned roads: Encroachment of watersheds and the construction of roads without proper study contribute to unexpected debris flow, which affects bridge design and construction. Hydrological analysis guidelines should be developed to include debris assessment. Research should also focus on the impact of climate change on bridge design and construction.
- Temporary staging must be mandatorily designed and approved to avoid failure of bridge during construction. Wind resistive scaffolding/support system and superstructure tie system should be implemented to avoid failure of truss bridges during construction.
- Since concentrating the river flow in only a few spans can cause excessive scour and severe damage to the foundation, debris should not be allowed to accumulate in river flow areas, ensuring water can flow through all spans of the bridge.

- Generally, prestressed and truss bridge work should not be carried out after the end of mid-May. If necessary, it should only be done based on the monsoon and flood projections from the Department of Hydrology and Meteorology to prevent damage.
- The practice of completely blocking the river with embankments for bridge construction should be immediately stopped.
- The effects of climate change on bridge design and construction should also be studied and researched.

References:

1 Ji-Shuang Tan, Khalid Elbaz,Zhi Feng Wang, Jack Shui Shen and Jun Chen, " Lessons learnt from Bridge collapse: A view of sustainable management" Sustainability 2020,12,1205;doi:10.3390/su12031205

2 Hersi, M.I. Analysis of bridge failures in the United States (2000–2008). Master's Thesis, Ohio State University, Columbus, OH, USA, 2009.

♦

6.0 Role of Capping Layer for Flexible Pavement Design and Construction over Weak Soil (CBR<5%)

- Er. Prabhat Kumar Jha,
Joint Secretary,
Ministry of Physical Infrastructure and Transport, Nepal

Q1: What is capping layer?

A **capping layer** is an engineered layer of material placed between the natural subgrade (existing soil) and the pavement structure (sub-base or base layers) in road construction. Its primary purpose is to **improve the load-bearing capacity** of weak or problematic subgrade soils, ensuring the pavement can withstand traffic loads without excessive deformation or failure. Skipping it may save initial costs but leads to catastrophic long-term failures and higher lifecycle expenses. Always assess subgrade conditions and design the pavement structure accordingly.

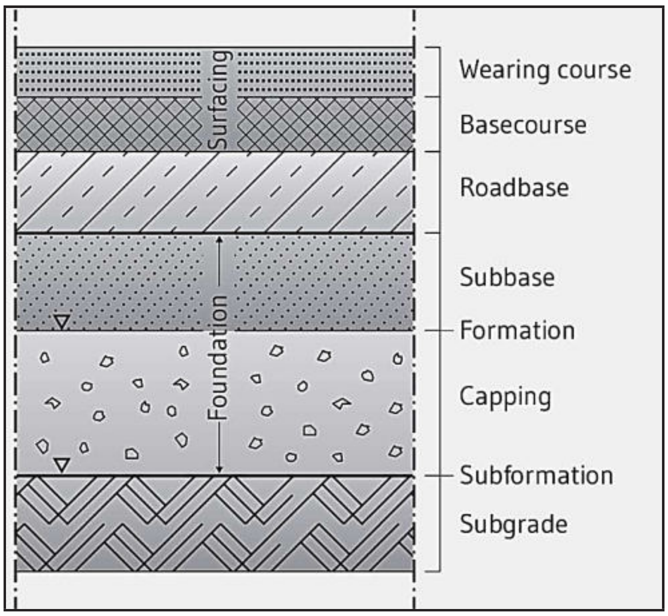

Figure 1: Typical Pavement with Capping layer

Q2: When the capping layer is provided for pavement design and construction?

Constructing a flexible pavement without a proper capping layer can lead to significant structural and functional issues. The capping layer is critical for distributing loads, stabilizing weak subgrades, and preventing moisture-related damage.

Required when:

- Weak Subgrade: If the subgrade's California Bearing Ratio (CBR) is < 5%, a capping layer is mandatory.
- Expansive Soils: To mitigate swelling/ shrinkage.
- High Water Table: To prevent capillary rise and saturation.

Standards & Guidelines

- AASHTO: Recommends capping layers for subgrades with CBR < 5%.
- IRC 37 (India): Specifies capping layers for weak subgrades in flexible pavement design.
- BS 5930: Highlights the need for subgrade improvement in problematic soils.

The key problems that may arise if capping layer is not provided to flexible pavement having CBR<5%:

1. Subgrade Failure

Issue: Weak or unstable subgrade (natural soil) may deform under traffic loads, leading to rutting, cracking, or uneven settlement.

Why? Without a capping layer, the subgrade bears direct stress from traffic, exceeding its bearing capacity if it is soft, expansive, or moisture-sensitive (e.g., clay soils).

2. Poor Load Distribution

- Issue: Excessive stress on the subgrade and sub-base layers, causing premature fatigue cracking and pavement failure.
- Why? The capping layer spreads loads over a wider area, reducing vertical stress on the subgrade. Without it, localized stress concentrations occur.

3. Moisture Damage

Issue: Water infiltration into the subgrade, leading to:

- Softening of subgrade soil (reduced strength).
- Swelling/shrinkage in expansive soils.
- Pumping (ejection of fines through cracks).

Why? A capping layer acts as a barrier to capillary rise and surface water ingress. Without it, the subgrade becomes vulnerable to moisture.

4. Construction Challenges

Issue: Difficulty in achieving proper compaction of upper layers (sub-base, base).

- Construction equipment may sink into weak subgrade, causing uneven layer thickness.
- Poor compaction leads to voids and weak spots in the pavement.

Why? A capping layer provides a stable platform for equipment and ensures uniform compaction.

5. Reduced Pavement Life

Issue: Accelerated deterioration due to:

- Rutting (permanent deformation in wheel paths).
- Alligator cracking (structural failure).
- Potholes (localized collapse).

Why? Weak subgrade support increases strain on the asphalt layers, shortening the pavement's service life.

6. Increased Maintenance Costs

Issue: Frequent repairs due to recurring subgrade-related failures.

Why? Without a capping layer, the root cause of failure (weak subgrade) remains unaddressed, leading to recurring issues.

Q3: What is the specification requirement?

The capping layers shall comply with the following requirements: -

(1) Material classification

Materials used for use in capping layers shall be selected among soils classified as GW, GP, GC, and SW in the General Classification of Soils, described in Clause 609.

(2) Material Requirements

Material for use in the capping layers shall not contain particles larger than 75 mm and their percentage passing by weight the 0.075 mm sieve shall be less than 15%. The material shall have a CBR of not less than 15% measured after a 4-day soak on a laboratory mix compacted to 95 % MDD (heavy compaction), a swell of less than 1%, a plasticity index of less than 12%.

(3) Laying and Compaction

The material shall be deposited in the layer of 150 mm compacted depth. Each layer shall extend over the full width of the embankments or cutting and shall be compacted in accordance with the requirements specified in Sub-clause 1003 (1) (a) to (d) of Standard Specification for Road and Bridge Works,2078.

Q4: Do we need Geotextile with capping layer?

The **use of geotextile with a capping layer** depends on the **subgrade condition and function of the capping layer**. When and why geotextile may or may not be required:

1 When Geotextile is Needed with a Capping Layer

✓ **Subgrade with CBR < 3% (Very Soft & Weak Soils)**

- Geotextile helps **separate** the capping layer from the weak subgrade, preventing intermixing.
- Improves **load distribution** and minimizes differential settlement.

✓ **High Moisture or Waterlogged Areas**

- Acts as a **drainage layer**, preventing water from rising into the capping layer.
- Reduces **pumping and erosion** of fine particles from the subgrade.

✓ **Clayey or Silty Subgrade (Highly Compressible & Expansive Soils)**

- Reduces **migration of fine soil particles** into the capping layer, maintaining long-term stability.

- Helps prevent **rutting and shear failure** in flexible pavements.

✓ **Use of Geogrid-Geotextile Combination**

- In extremely weak soils (CBR < 2%), a **geogrid+geotextile system** improves load distribution and prevents excessive deformation.

2. When Geotextile is NOT Needed with a Capping Layer

⊘ **If the subgrade has moderate strength (CBR > 3%) and is well-compacted**

- A properly designed capping layer (granular/stabilized material) is sufficient without geotextile.

⊘ **If the capping layer is made of well-graded granular material with a good filter layer**

- No risk of intermixing between layers.

⊘ **If subgrade drainage is well managed (e.g., subsurface drains are installed)**

- No need for geotextile as a drainage layer.

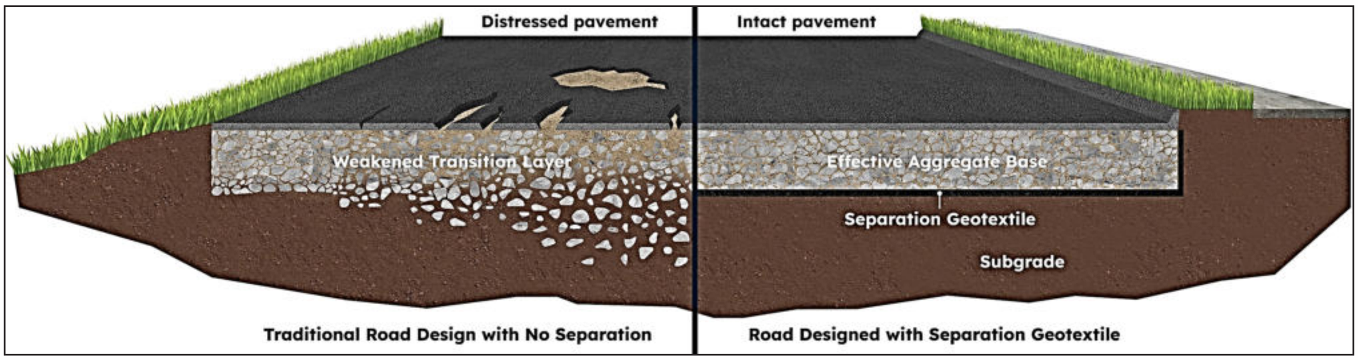

Figure 2: Typical elaboration of geotextile benefit as pavement element

Q5: How can we determine the effective CBR or working CBR?

In pavement design, **Effective CBR** (also called **Working CBR**) refers to the **equivalent California Bearing Ratio (CBR) value** used to represent the **improved strength of a weak subgrade** after the addition of a **capping layer** or other stabilization measures. It is a design parameter that accounts for the combined contribution of the natural subgrade and the overlying capping layer representing the improved subgrade CBR, enabling engineers to design the upper pavement layers (sub-base, base, and asphalt) appropriately.

The Japan Road Association (JRA, 1989) provides an equation to calculate the effective CBR for layered subgrade conditions. This method considers the influence of multiple soil layers on the overall subgrade strength. The formula given in equation provides a model that may be used to determine this equivalent subgrade design strength (CBRE) based on the strength of the supporting soil depth (Japan Road Association 1989).

$$CBR_E = \left[\frac{\sum_i (h_i CBR_i^{0.333})}{\sum_i h_i}\right]^3$$

where

CBR_E	=	equivalent subgrade design strength (%)
CBR_i		CBR value of layer i (%)
h_i	=	thickness of layer i (m)
$\sum h_i$	=	taken to a depth of 1.0 m

The following conditions apply to the use of equation

- ❑ Layers of thickness less than 200 mm must be combined with an adjacent layer.
- ❑ The lower CBR value must be adopted for the combined layer. It is assumed that higher CBR materials will be used in the upper layers.
- ❑ The formula is not applicable where weaker layers are located in the upper part of the subgrade.
- ❑ Filter layers must not be included in the calculation.
- ❑ The maximum equivalent subgrade CBR from the use of equation is 15%.

Q6: Can we use the Japan Road Association (JRA, 1989) to develop the Charts?

Yes.

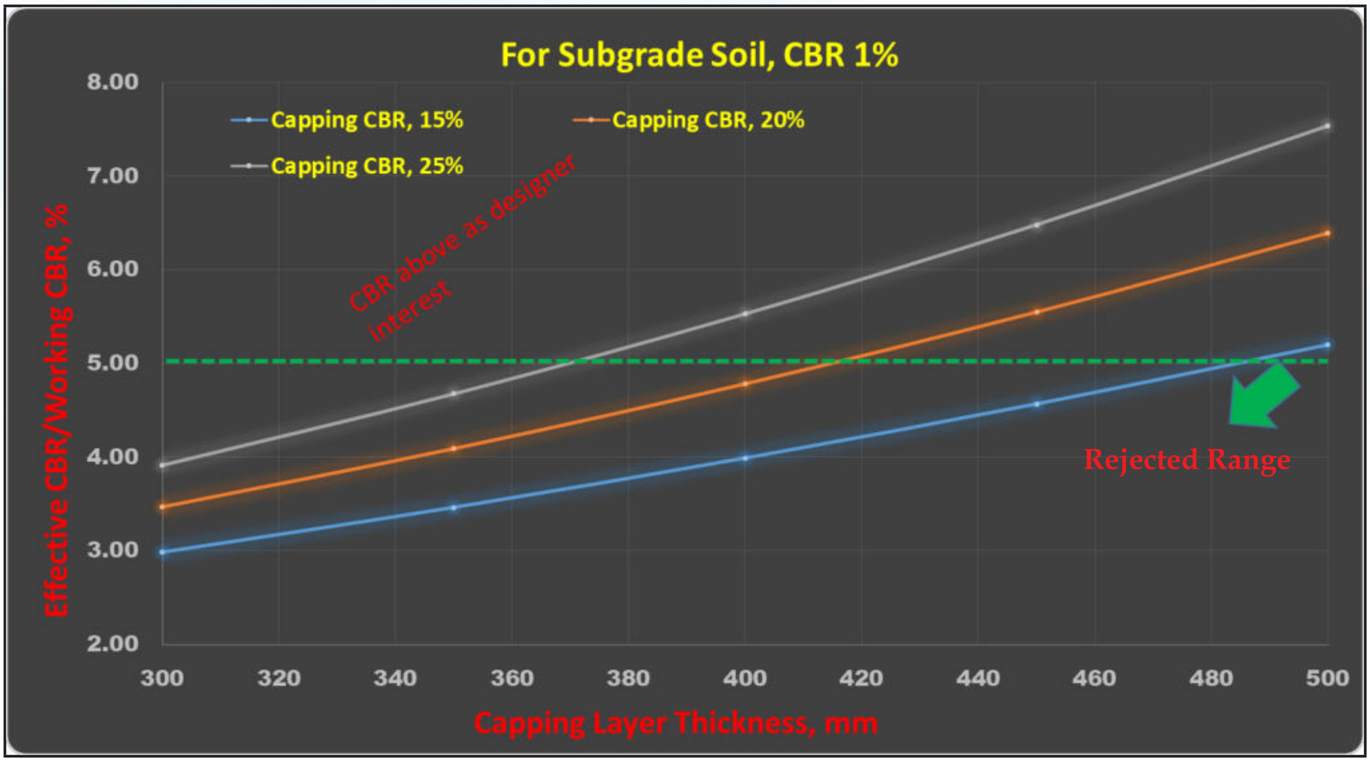

Figure 3: Effective CBR/Working CBR Chart for Subgrade Soil having CBR = 1%

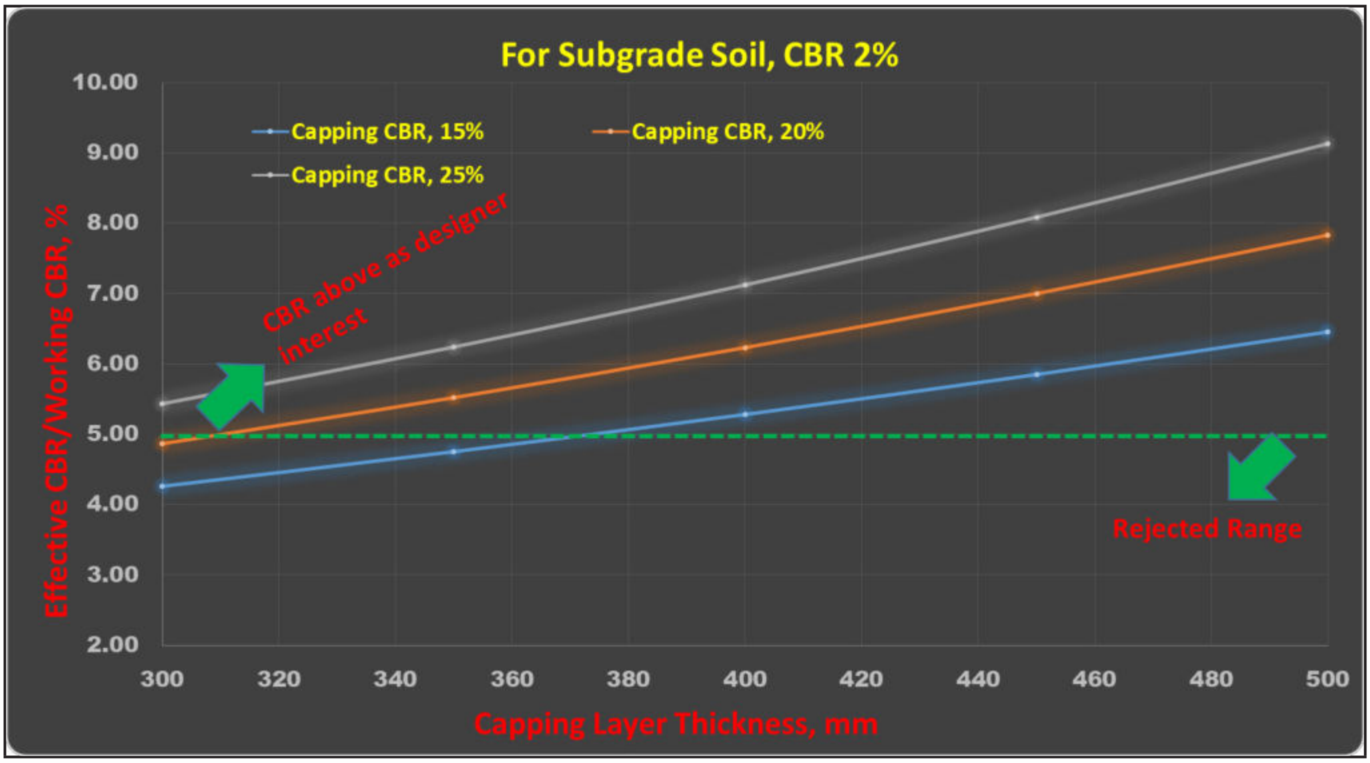

Figure 4: Effective CBR/Working CBR Chart for Subgrade Soil having CBR = 2%

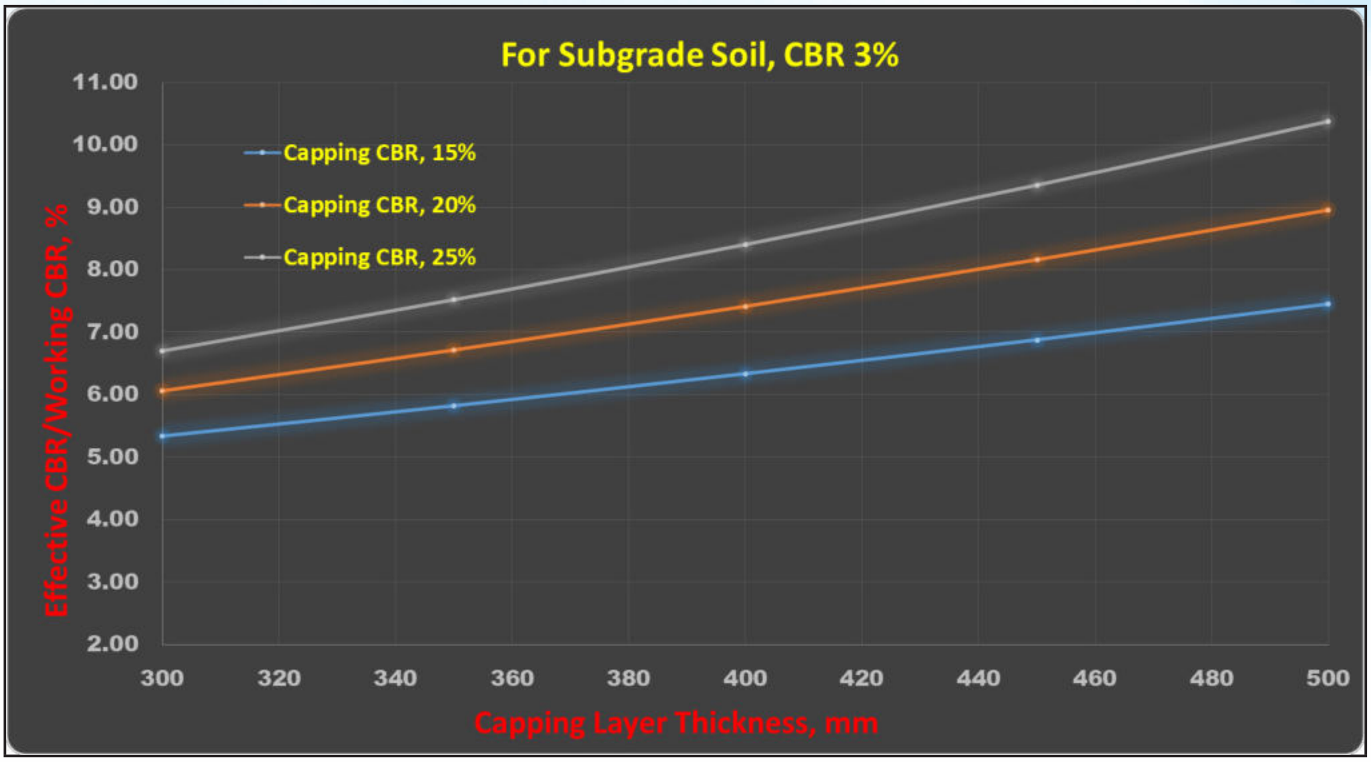

Figure 5: Effective CBR/Working CBR Chart for Subgrade Soil having CBR = 3%

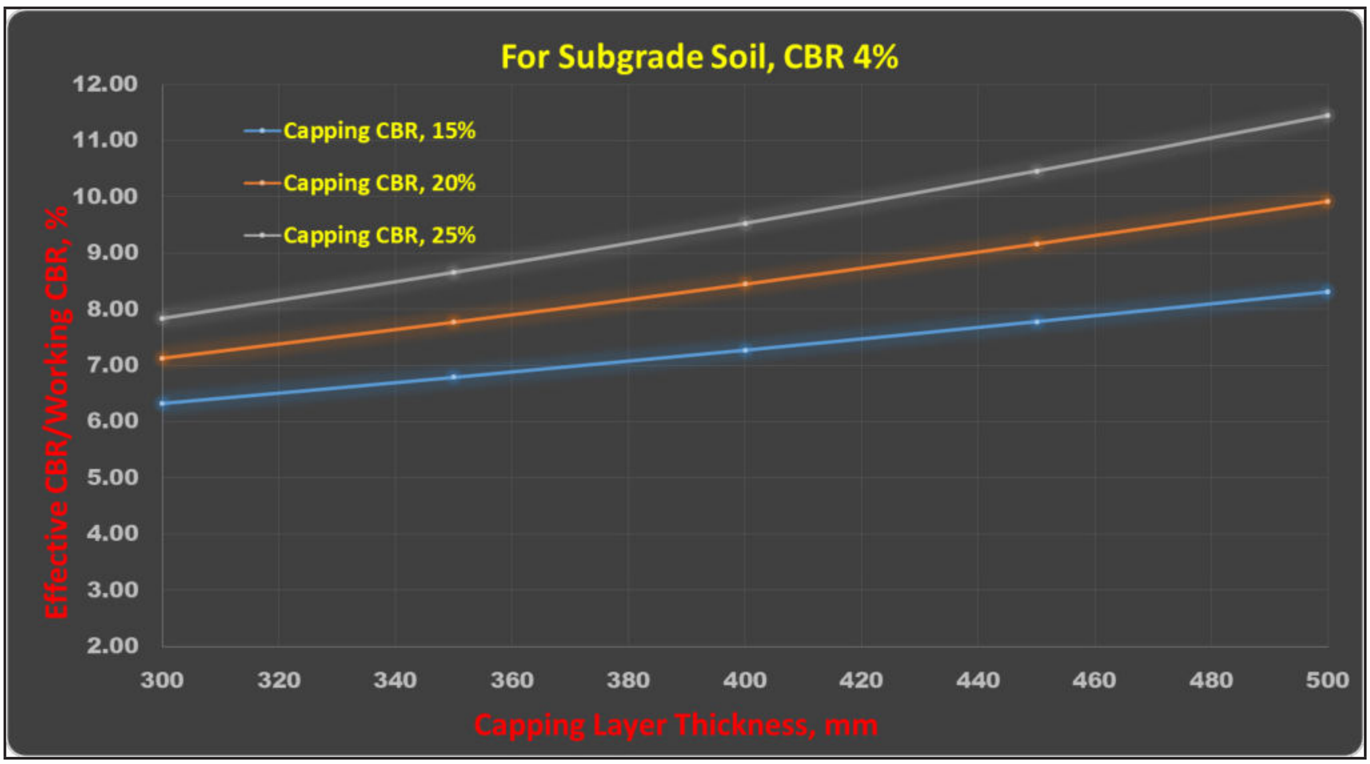

Figure 6: Effective CBR/Working CBR Chart for Subgrade Soil having CBR = 4%

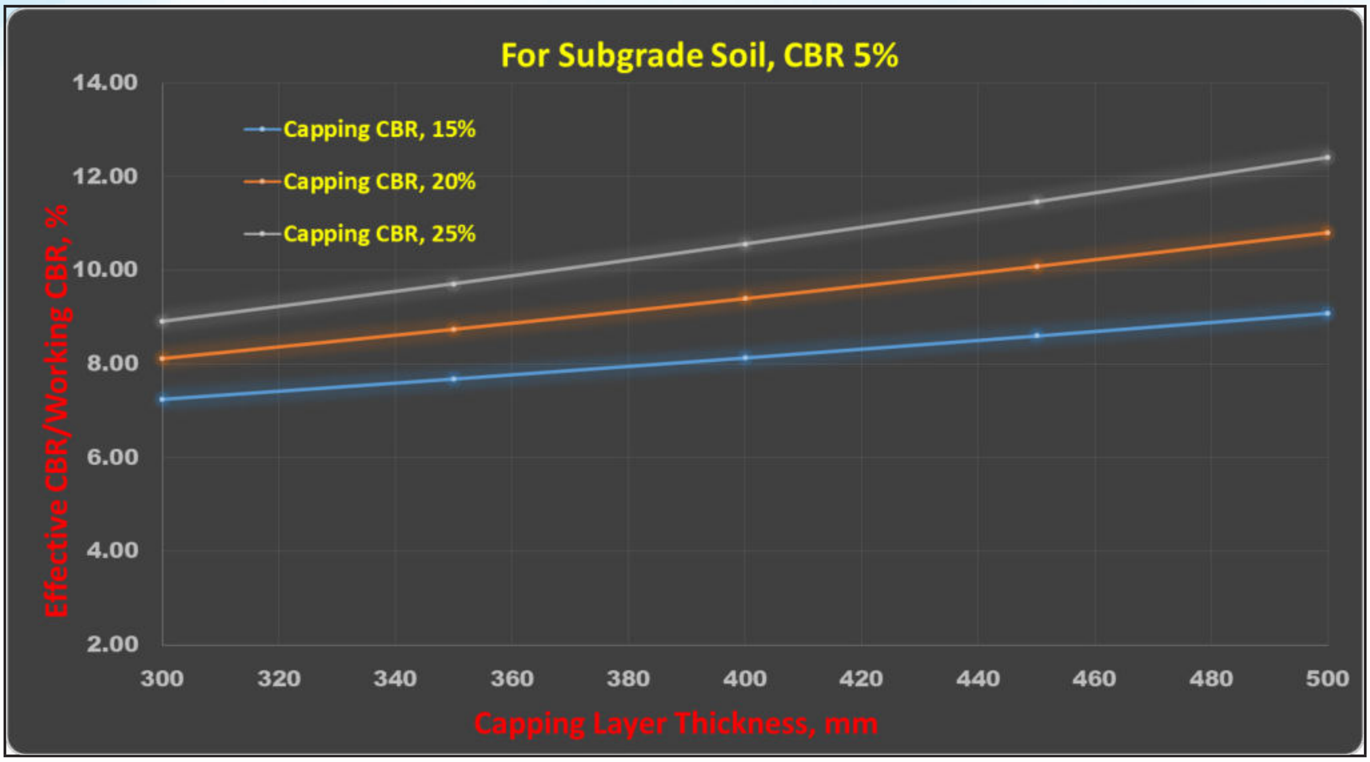

Figure 7: Effective CBR/Working CBR Chart for Subgrade Soil having CBR = 5%

7.0 Assessment of Damage and Loss by Extreme Rainfall Event (September 2024) in Nepal: A Case Study of Nagdhunga Naubise Mugling Road.

Ojha, Keshab Prasad
Senior Divisional Engineer
urkshab@gmail.com, kpojha@dor.gov.np

1. Background

Nepal faces high risks of adverse effects of climate change in different aspect including transport infrastructure due to its topographical diversity, fragile geological structure, varied climate and micro-climate zones [1]. It is also a part of Himalaya, Karakoram and Hindu Kush Mountain region of South Asia with altitude varying from 60m to highest peak of the world, this region stores more ice than any part of the world outside the poles. Rising temperatures pose additional risks through accelerated glacier melting, which can exacerbate flooding risks above and beyond those caused by variations in precipitation [2]. The recent record-breaking rainfall that occurred from September 26 to 28, 2024, which has caused devastating landslides and flooding across many districts of the country. This catastrophic event resulted in hundreds of fatalities and significant property damage nationwide, including extensive damage to the national highway and other road infrastructures. This article seeks to figure out the damage and losses occurred in Nagdhunga-Naubise - Mugling road during the recent extreme rainfall caused extreme climate events in many districts of middle and eastern part of the country.

2. Objective

This study aims to identify the impacts of rainfall-induced hazards on the Nagdhunga-Mugling Road by the extreme rainfall on September 26 to 28, 2024 and provide guidance for recovery planning. It assesses the damage, estimates losses, and evaluates financial needs for reconstruction and recovery of the Nagdhunga Mugling Road.

3. Study Area and Data Collection

3.1. Study Area

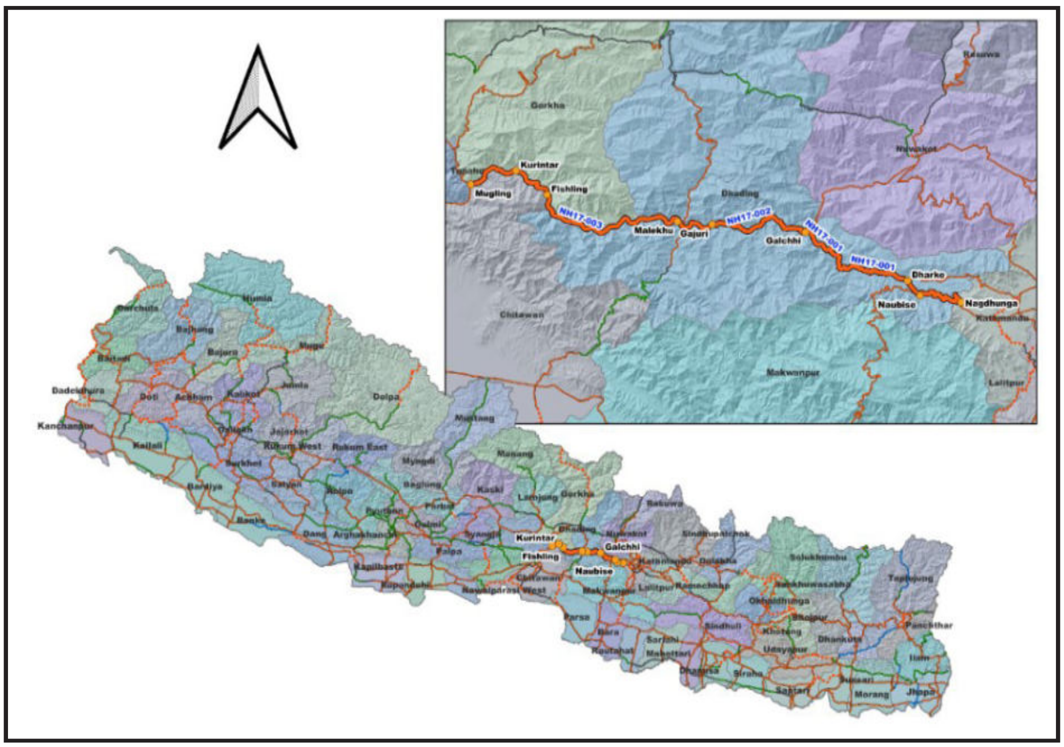

[Source: GIS Processing]

Figure 1: GIS map of Study area (Nagdhunga Mugling Road)

3.2. Baseline Information

About 390 Km long stretch of road from Kodari Kathmandu to Birgunj is part of Asian Highway (AH-42) and its Kathmandu Birgunj 275 km section is one of the most important trade corridor in Nepal. Naghdhunga Mugling Road, a part of this segment, is the one of the life line land routes to connect the Kathmandu with other district and Terai which supplies basic need commodities for the main part of the Bagmati province including Kathmandu Valley.

3.2.1. Road Length and Contract packages

The existing road, from Nagdhunga to Mugling (94.663 Km), consists of part lengths of two major highways of Nepal namely Tribhuvan Rajpath (TRP, NH41) and Prithvi Rajmarg (PRM, NH17) as listed below;

i. Nagdhunga to Naubise (12.260 Km, ICB 01) is a part of NH41 (Tribhuvan Rajpath, TRP).
ii. Naubise to Malekhu (43.542 Km, ICB 02) is a part of NH17 (Prithvi Rajmarg, PRM).
iii. Malekhu to Mugling (38.861 Km, ICB 03) is a part of NH17 (Prithvi Rajmarg, PRM).

This road section is generally having intermediate to two-lane with 6.0 m wide carriage way and 8.5 m wide formation width and currently being upgraded in standard double lane including the four to six lane in some settlement areas. There are 26 existing Bridges (length more than 6m) which comprises of 6 Major Bridges and 20 Minor Bridges including 462 cross-drainage (slab culverts and pipe culverts) structures. The overall road section is being implemented for the upgrading through three International Competitive Bidding (ICB) contracts on Nagdhunga to Naubise section through Contract No. (C.N.): SRCTIP-DoR-W-NNM-ICB-01 (Contractor: M/S Jaingsu - Sagun JV), Naubise to Malekhu section through C.N.: SRCTIP-DoR-W-NNM-ICB-02 (Contractor: M/S SHARMA-LAMA-ZICG JV) and Malekhu to Mugling section through C.N.: SRCTIP-DoR-W-NNM-ICB-03 (Contractor: M/S Sharma-ZICG JV) respectively.

3.2.2. Geological Data

The Nagdhunga-Mugling Road is situated in central Nepal's rocky terrain, crossing the Phulchowki and Bhimphedi Groups of the Kathmandu Complex and the Nawakot Groups of the Lesser Himalayas. The road passes through hilly areas with sharp curves and steep gradients. Several sections face challenges from high water tables, exposed springs, and streams, which increase moisture exposure to the infrastructure. A major landslide at Jyaple Khola in this area caused 35 casualties, highlighting the region's vulnerability.

The Tribhuvan Highway from Nagdhunga to Naubise traverses steep and fragile terrain, with the geology consisting of slightly metamorphosed to un-metamorphosed, deeply weathered, and highly fractured sedimentary rocks. From Naubise to Galchhi (Km 22+300), the road is challenging, following the left bank of the Mahesh Khola and its tributaries. However, from Galchhi (Km 22+300) to Bishaltar (Km 33+300), the road passes through market areas on alluvial terraces and steep hill slopes, where rock falls or landslides are potential risks. Section from Bishaltar (Km 33+300) to Hugdi Khola (Km 62+100) is more difficult, as it runs through steep terrain and weak geological formations of fractured black slate. This section includes the notorious Krishnabhir landslide area, where road widening or new construction will be challenging. The road section from Phisling Km 68+500 to Manakamana Cable Car Km 78+300 the road is proposed mainly along the alluvial or colluvial terraces above Trishuli River. The road section from Manakamana Cable Car Km 78+300 to the end of the road at Mugling Km 82+410 is anticipated to be among the most difficult section of road widening or construction. Steep topography, old landslide terrain and narrow river gorge at valley side will be quite challenging.

3.2.3. Meteorological and Hydrological Data

Table 1: Average monthly and annual rainfall near the road project corridor.

SN	Stations	Jan	Feb	Mar	Apr	May	Jun	Jul	Aug	Sep	Oct	Nov	Dec	Annual
1	Gorkha	20	19	35	75	161	325	428	358	195	51	9	12	1688
2	Dhading	22	24	42	72	166	352	525	515	295	60	8	10	2092
3	Thankot	18	28	37	69	142	284	476	416	258	65	9	15	1817
4	Dhunibesi	14	20	28	50	126	238	416	382	225	54	7	14	1574
	Average	**19**	**23**	**36**	**67**	**149**	**300**	**461**	**418**	**243**	**58**	**8**	**13**	**1793**

Table 2: Projected hourly and daily rainfall intensity for different return period project corridor.

SN	Station Name	Intensity	I_5-Yr	I_{10}-Yr	I_{25}-Yr	I_{50}-Yr	I_{100}-Yr
1	809 Gorkha	mm/day	129	150	175	195	214
		mm/hr	45	52	61	67	74
2	1005 Dhading	mm/day	145	177	216	246	275
		mm/hr	50	61	75	85	95
3	1015 Thankot	mm/day	134	160	193	218	242
		mm/hr	46	56	67	75	84
4	1038 Dhunibesi	mm/day	124	153	190	222	252
		mm/hr	43	54	66	78	88

Department of Hydrology and Meteorology (DHM) maintains a network of rain gauge stations throughout the country. Among those, four rainfall gauging stations Gorkha (809), Dhading (1005), Thankot (1015) and Dhunibesi (1038) are located within and in close proximity of the project area. The average annual rainfall details of the meteorological stations and projected hourly and daily rainfall intensity for different return period are provided in Table 1 and Table 2 respectively. Among the four station, significant variation on 24 hr. maximum rainfall can be seen from 28.1 mm on Dhunibeshi rainfall station for the year of 1974 A.D. to 300.1 mm in Thankot station for the year 2002 A.D. From the available rainfall data (1956 – 2014 AD), the average rainfall for the four station is shown on the following table with the value 1574 mm to 2092 mm with average to 1793 mm.

3.2.4. Traffic Data

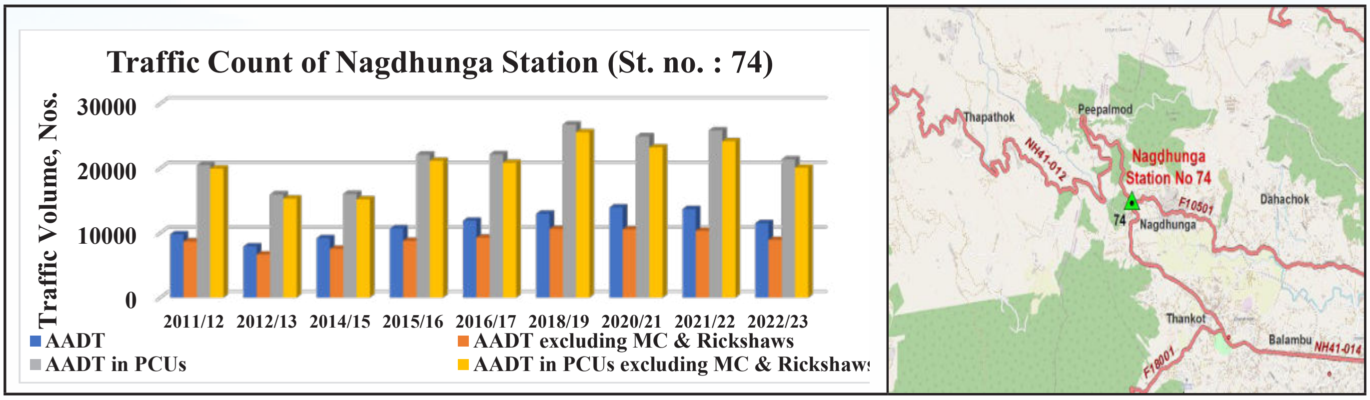

Figure 2: Comparison of the traffic volume at Nagdhunga Station (St. No.: 74).

Traffic count stations located at Naghdhunga (Start Point) having the more than twenty thousand AADT in PCU and Mugling station (End Point) having 4/5th of Naagdhunga. The past year traffic data for the Nagdhunga station (station no: 74) and Mugling East station (Station no. 51) from year 2011/12 to 2022/23 is shown in Figure 2 and Figure 3.

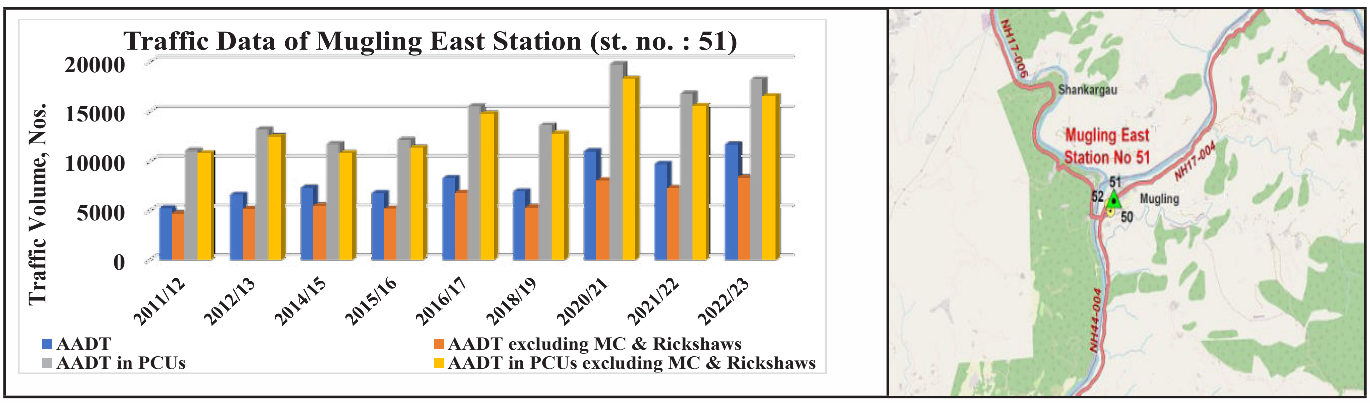

Figure 3: Comparison of the traffic volume at Mugling East Station (St. No. 51).

3.2.5. Landslide inventory Data:

The study area is located along the frequent recurring landslide area like Jhyple Khola, Parewa Bhir, Krishna Bhir, Jogimara, Mawa Khola etc. These site have experienced frequent landslides resulting in fatalities as well as road blockage for significant duration (sometimes: couple of days) during past year. This also cause the chocking of the longitudinal drain and cross drainage structures, damages on the road side retaining structure, deposition of debris on the road pavement causing damage on it, damage on the vehicles and properties, delay on travel time and additional economic burden for reconstruction and rehabilitation. Historical data regarding the road closure on the study area has been presented on Table 6, which shows that NNM road is potentially vulnerable to rainfall induced landslides.

4. Methodology

The Damage and Loss Assessment (DaLA) methodology is adopted for the study. The Damage and Loss Assessment (DaLA) methodology uses objective, quantitative information on the value of destroyed assets and temporary production losses to estimate, first, government interventions for the short term and, second, post-disaster financing needs. It avoids use of qualitative, subjective interpretations.

5. Reviewing the existing assessment reports

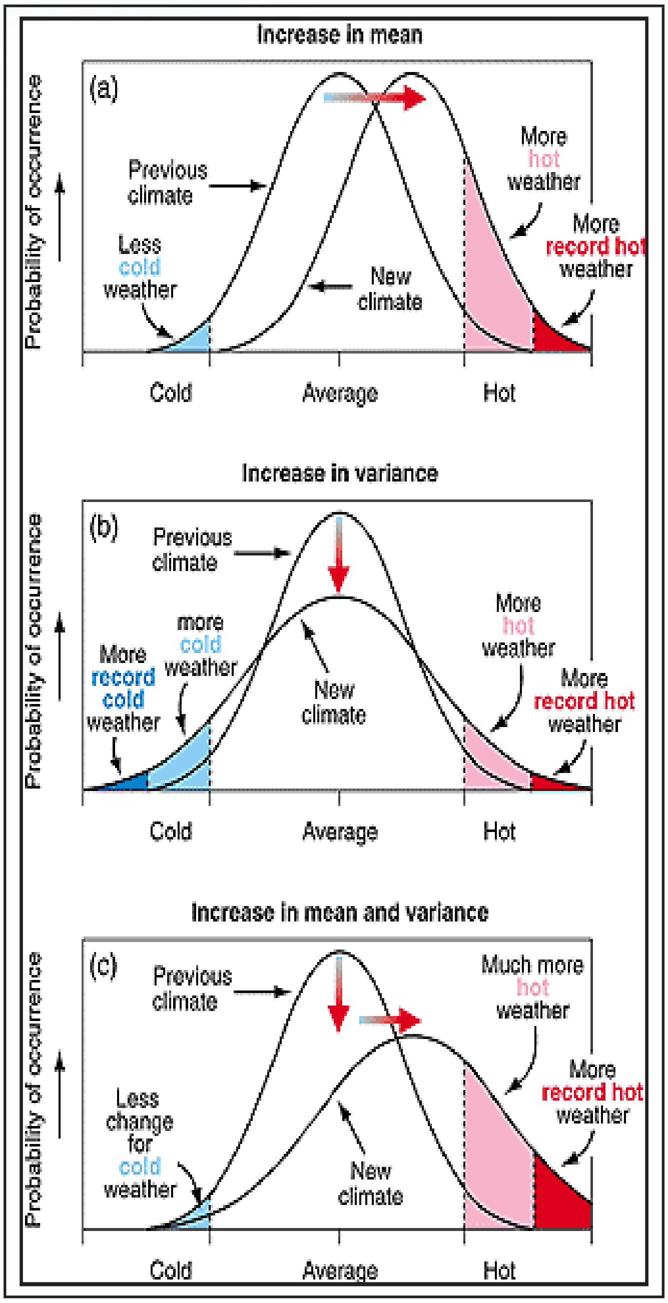

Figure 4: Shift of normal peak during extreme climate

Climate risk is identified as major risks that may adversely impact the road components of the project. Key risks include concentrated high rainfall, which could result in accelerated surface run-off from slopes of hilly terrain and increased flows in gullies, streams, drainage channels, and rivers. Other serious risks are the effects of climate change, which include flash floods, mudflows in rivers and streams, and increased incidence of landslides along the road alignment [3]. Annual precipitation is expected to increase in both the medium and long term by 2–6 % to 8–12 % with more precipitation expected in the higher regions. Winters are projected to be drier and monsoon summers wetter, with up to a threefold increase in rainfall [4]. A study on past trends in daily climatic extremes of temperature and precipitation in Nepal found that 73% of stations sampled exhibit an increase in the number of days with a rainfall level of 50 mm or more. About 65% of the stations showed an increase in the monthly maximum 1-day rainfall level. Overall, there is an increasing trend in total and heavy precipitation events [5].

Extreme Event: Climate as defined is associated with a certain probability distribution of weather events. Weather events with values far away from the mean (such as heat waves, droughts and flooding) are by definition less likely to occur. The least likely events in a statistical sense are called extreme events. Extreme weather in one region (e.g. a heat wave) may be normal in another [6] [7]. The project road is located within the high rainfall zone of 1,500 millimeters (mm) to 2,000 mm. The Department of Hydrology and Meteorology (DHM) of Nepal has defined rainfall threshold warning levels to assess the potential threat of rainfall-induced landslides in steep slopes and high flow in local areas. These thresholds help authorities and local communities anticipate and prepare for potential hazards due to extreme rainfall events. These thresholds, based on rainfall intensity (mm), are outlined in the Table 3. Similar threshold published by Government of India, Climate Research and Services, Pune regarding the rainfall event in Table 4 below [9].

Table 3: Rainfall threshold for potential threat of rainfall-induced landslides in steep slopes.

Duration	Threshold Rainfall	Duration	Threshold Rainfall
1 Hr.	60 mm	12 Hrs.	120 mm
3 Hrs.	80 mm	24 Hrs.	140 mm
6 Hrs.	100 mm	[Source: DHM, Nepal]	

Table 4: Threshold rainfall for classification of the climate event in India.

Description	Rainfall range in mm (24 hr.)
Heavy Rainfall	64.5- 115.5
Very Heavy Rainfall	115.6-204.4
Extremely Heavy rainfall	Greater or equal to 204.5

The EIA report of the project identified the active landslide area along the road corridor which have the high potential of landslide in future [10]. The locations are stated on Table 5 .

Table 5: high potential of landslide location along the road corridor.

S.N.	Location	Description	Length (m)	Remarks
1	0+100	Nagdhunga	150	Hillside, Active Landslide (L/S)
2	2+300	Jhakribas	150	"
3	2+800	Jhyplekhola	40	Valley Side
4	4+000	Khatri Pauwa	125	Hillside
5	4+150	Khatri Pauwa	50	Active L/S
6	4+500	West of "	250	Stabilized L/S
7	13+400	Koiralagaun	200	Potential L/S
8	16+750	Eklephant	300	Deep Rock cut
9	42+600	Malekhu	60	
10	57+500	Krishnabhir	1000	Stabilized L/S still potential
11	66+900	Jogimara	125	Potential rock fall zone
12	69+100	Fisling	200	Slow and active L/S
13	70+700	Mugling	500	

6. Observation of Meteorological and Hydrological Data

Network of the Meteorological station and Hydrological station maintained by the DHM observed the record-breaking observation on rainfall and flooding on river basin. These record-breaking observations are lies within the 10th or 90th percentile as well as crossed the threshold value of the DHM within last 70 years' time frame gives the clear evidence of extreme climate event of rainfall. Figure 5 shows the outbreak of the previous observed data and rainfall accumulation among the network of Meteorological station installed within the country. All four station near road corridor have crossed the 140 mm of threshold value for 24 hr. period which turns to rainfall induced landslides in steep slope and high flow in local areas.

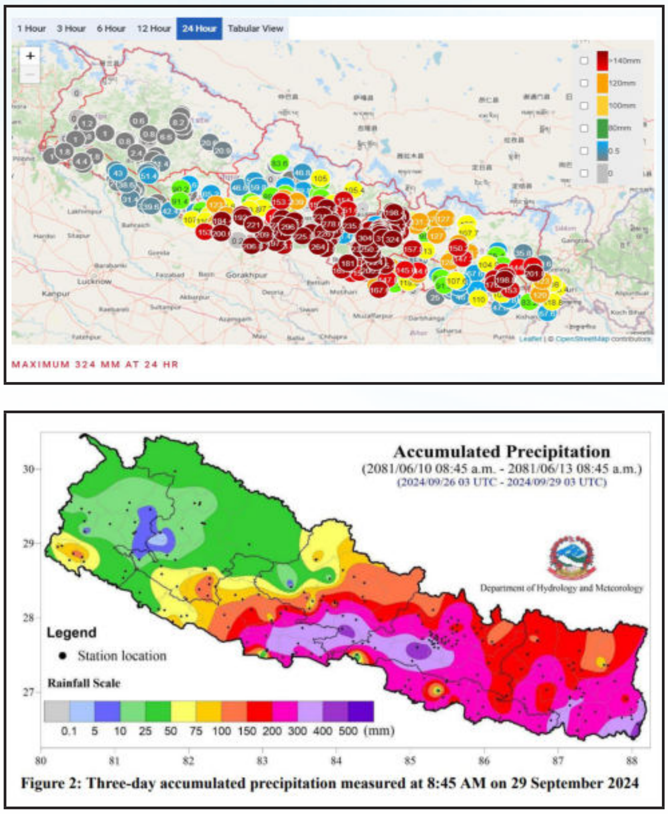

[Source: DHM, Nepal]

Figure 5: Distribution of Rainfall along the project area and three-day accumulated precipitation measured at 8:45 AM on 29 September, 2024.

Similarly, at least six river basins were observed record-breaking flood discharges since the start of flood discharge monitoring by the DHM. The data, presented in the Table 7 below, provides strong evidence that the road section from Nagdhunga to Mugling was severely impacted by the extreme climate event, and these rainfall and flood records substantiate the fact that the Nagdhunga-Mugling road section was heavily affected, leading to substantial damage and losses.

Table 6: Road Closure data before and after extreme rainfall

Highway Code	Road Link	Road Closure occurrence by landslide or flood			
		After Sept 26, 2024	2024	2023	2022
NH01 to NH80	All National Highway	181	817	299	231
NH41	Naghdhunga Naubise	2	4	0	0
NH17	Naubise Mauwa Khola	8	18	1	0
NH17	Mauwa Khola Mugling	5	10	0	13
-	**Total on study area**	**15**	**32**	**1**	**13**

Table 7: Comparison of historic maximum and observed gauge height of major rivers.

S.N.	Station Index	Station Name	Historic Extreme Date	Historic Gauge Height (m)	Observed Maximum Gauge Height on Sept 27 & 28, 2024 (m)
1	420	Kali Gandaki at Kota Gaun	7-Sep-1993	10.4	10.27
2	449.91	Trishuli River at Kali Khola	3-Jul-1999	13.1	14.97
3	450	Narayani River at Devghat	5-Aug-1974	10.1	13.62
4	550.05	Bagmati at Khokana	22-Jul-2002	6.0	6.16
5	589	Bagmati at Karmaiya (Padheradovan)	21-Jul-1993	20.0	10.86
6	681	Sunkoshi River at Hampachuwar	13-Jul-2019	14.3	14.5
7	695	Saptakoshi at Chatara	25-Jun-1980	11.5	11.83

[Source: DHM, Nepal]

7. Observation and Discussion

7.1. Immediate Action After the Event

i. Weather Advisory (September 25, 2024): On September 25, 2024, the Department of Hydrology and Meteorology (DHM), Government of Nepal (GoN), issued a weather advisory predicting a new spell of monsoon from September 26 to 29, 2024.The advisory warned of extreme climate-induced hazards due to moisture-laden winds from the Bay of Bengal and local weather systems, which could trigger flash floods, landslides, and river overflows across most provinces.

ii. Impact of the Weather Event (September 26-29, 2024): The forecasted extreme rainfall materialized, causing severe climate-induced disasters in Bagmati, Koshi, and Gandaki provinces, with moderate rainfall in other regions.

a. **Major Impacts:**

- Thousands of landslides, flash floods, and inundations, particularly in Kathmandu Valley, Roshi, Sunkoshi and other regions.
- Hundreds of lives lost, dozens missing, and widespread destruction of infrastructure, including roads, bridges, water supply system, school, electricity supply systems, and communication networks etc.
- Large landslides caused debris flows, subsiding road sections (for eg. TRP, Prithvi, BP highway etc.), washing away bridges (on Trishuli and Sunkishi river), blocking highways, and burying houses.

iii. Emergency Response and Rescue Operations (September 28-29, 2024): Immediate actions after the rainfall ceased, river water levels remained above dangerous levels, gradually falling.

- Rescue and evacuation efforts were launched by both the government and private sector, focusing on life-saving programs.
- A task center was set up with electricity, internet, and phone facilities to coordinate the response and allocate resources for rescue operations.

iv. Clearing of Road Debris on NNM road (September 28, 2024)

- As rainfall intensity decreased on the afternoon of September 28, the rescue operation intensified, focusing on clearing more than 113 debris spots along the road.
- Over two dozen heavy equipment were deployed to remove landslides and clear blocked roads, enabling traffic to resume by 17:00 hrs on September 28, except at Jhyaple Khola.
- By 16:00 hrs on September 28, it was reported that some vehicles might be buried under debris at Jhyaple Khola.

v. Recovery of Buried Vehicles and Casualties (September 28-29, 2024)

- The rescue team arrived at Jhyaple Khola, and by 23:00 hrs on September 28, 15 bodies were recovered from a buried public vehicle.
- The next morning, the rescue continued, and by 16:00 hrs on September 29, two more vehicles were found, and 19 additional victims were recovered, bringing the total death toll to 35.

vi. Passenger Evacuation and Restoration:

- On September 29, 2024, senior management decided to redirect passenger traffic through the under construction Nagdhunga Tunnel to alleviate congestion.

vii. Road Restoration:

- By 17:00 hrs on September 29, the road section from Nagdhunga to Mugling was opened for one-way traffic at slide-prone locations to allow for vehicle and passenger rescue.
- By September 30, after coordination with District Administration and security forces, a plan was implemented to open the road for two-way traffic, which was completed between 12:00 hrs. and 14:30 hrs. with the help of more than 50 pieces of available equipment.

This sequence of events demonstrates the immediate response, coordination, and significant efforts made by the authorities and rescue teams to mitigate the damage and loss caused by the extreme climate event.

7.2. Extensive field visit and Observation of Failure of the slope and Landslide

From the number of field visit of the Nagdhunga Naubise road under package ICB 01, it is found that more than thirty five location (shown in Figure 6) are triggered by the slope failure and flow of the debris resulting the washout of the road section, retaining structures, deposition of the stones, debris, mud and water resulting the thirty five death and several injuries, damage on about half dozen vehicle, pavement failure, subsidence and washout of the road section, closure of the road, delaying in travel time and loss of millions of the property.

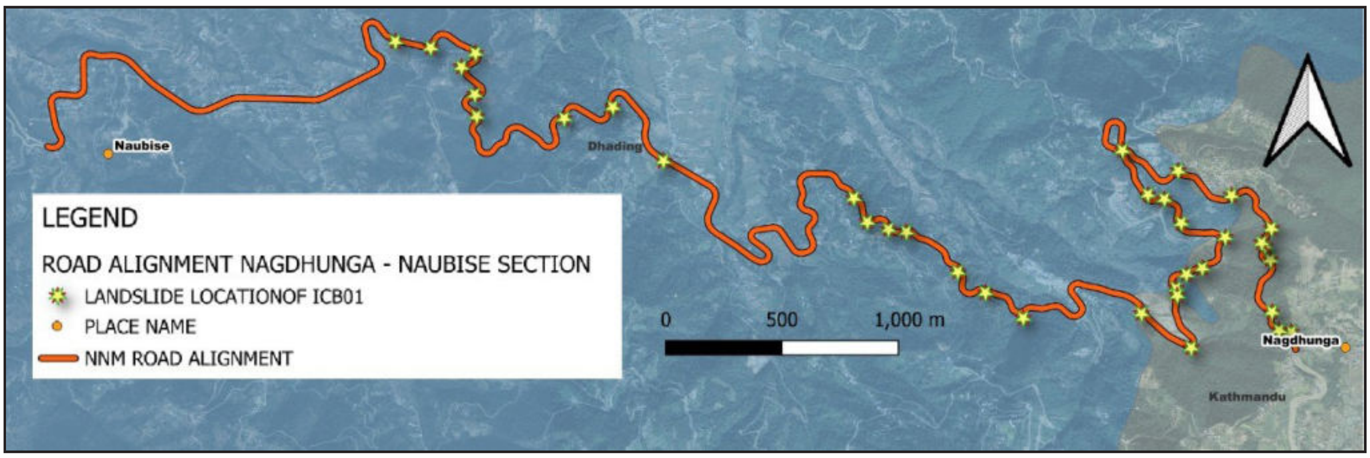

[Source: Field visit survey]

Figure 6: Observation of the slope failures and landslides on Nagdhunga Naubise road section.

[Source: Field visit survey]

Figure 7: Observation of the slope failures and landslides on Naubise Malekhu road section.

Similarly, the Naubise Malekhu road under package ICB 02, it is found that more than sixty-three locations ((shown in Figure 7))are triggered by the slope failure and flow of the debris resulting the washout of the road section, retaining structures, deposition of the stones, debris, mud and water resulting, existing pavement failure, subsidence and washout of the road section, closure of the road, delaying in travel time and loss of millions of the property.

In the same way, the Malekhu Mugling road under package ICB 03, it is found that more than thirteen locations (shown in Figure 8) are triggered by the slope failure and flow of the debris resulting the washout of the road section, retaining structures, deposition of the stones, debris, mud and water resulting, existing pavement failure, subsidence and washout of the road section, closure of the road, delaying in travel time and loss of millions of the property. During reporting, frequent slides within a short distance are counted as a single event, and minor slope failures and landslides are excluded.

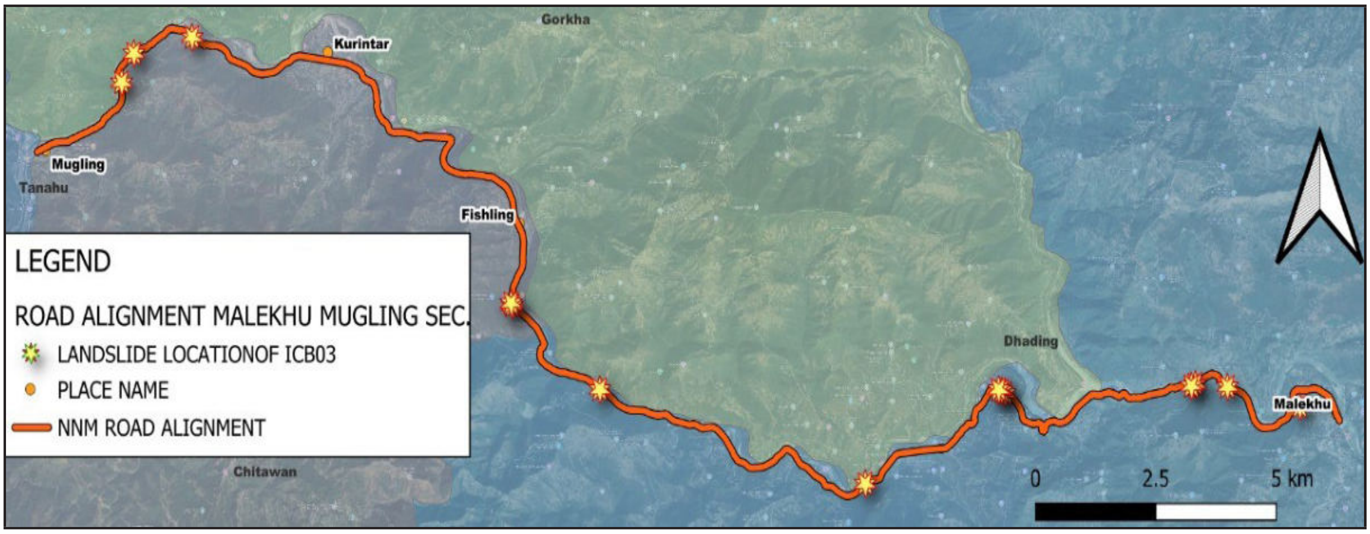

[Source: Field visit]

Figure 8: Observation of the slope failures and landslides on Malekhu Mugling road section.

7.3. Two notorious landslides, Jhyaple Khola and Krishna Bhir

a. **Jhyaple khola Incident**

Excessive rainfall triggered a slope failure near chainage 0+620, resulting in the collapse of a retaining wall panel and causing a debris flow downstream at Jhyaple Khola (chainage 2+800). This incident occurred around 4:30 AM on September 29, 2024, burying three vehicles and damaging four others. Vehicles buried included a Winger (Lu 1 Ja 4578), a Micro Bus (Ba 2 Kha 1345), and a Bus (Na 4 Kha 2270), all en route to Kathmandu. Additionally, a Micro Bus (Ba 2 Kha 1741), two cars (Ba 1 PA 1388 and Ba 1 Pa 8), and an Indian vehicle (HRAB 7070) sustained damage.

– At 0+620, the slope failure and retaining wall collapse may have been caused by diverted drainage water flowing along the road edge from blocked drains. This water, mixed with slope material, funneled through a steep gully, impacting Jhyaple Khola 150 meters below.

– The initial slide width was approximately 60 to 80 meters, including the existing retaining structures, but it narrowed as it descended, forming a narrow channel. The now-barren slope poses a significant risk to the remaining structures at 0+620.

– The mudflow filled a 10-meter space behind the gabion wall at 2+800, breaching it and possibly pushing parked vehicles.

– Due to heavy rainfall, extensive landslide deposits along the highway, and the delayed report of the buried passenger vehicles, excavators could not promptly access the site for timely rescue operations.

Chainage 0+620, Start point	gully formation and	clearance of debris on road surface

[Source: field visit survey]

Figure 9: Slope failure on Jhyaple Khola

b. Krishnabhir Landslide

A landslide and road pavement subsidence at Krishnabhir were observed due to toe failure at the slope base and a rise in the water table caused by soil infiltration and saturation within a fractured soil mass. The landslide was triggered by unexpectedly high-intensity and prolonged rainfall.

[Source: Field Visit Survey]

Figure 10: Failure of toe wall and restricted traffic flow at Krishnabhir area.

- Various structures, like the RCC toe wall, concrete wall, and launching apron, were damaged by river undercutting and scouring, leading to road pavement subsidence and mass movement downslope.
- The river's flood level surpassed the revetment wall, causing it to collapse and reactivate a previous mass slope failure.
- The gabion wall beneath the concrete revetment remains intact and still supports the riverbank.
- A steep slope failure on the valley side is ongoing, leading to road settlement and additional cracks and depressions along a 50-meter stretch.
- A previous mass from Krishnabhir was placed as a groin against the river and supported by the revetment.
- Shallow failures at the top of Krishnabhir require access and repair.
- The gabion screen wall, culverts, and roadside drain on the hillside are intact, though culvert outfalls were damaged. Water flow could damage the culverts further, as water enters through a boulder-filled bolster acting as a sub-surface drain.
- A temporary concrete hump directs water away from the slope, and polyethylene sheets cover the area to prevent rainwater infiltration into cracks.

- A gabion roadblock has been set up, with police directing one-way traffic on the hillside lane.
- A physical barrier and restricted traffic flow are in place to prevent water infiltration and ensure road safety.

8. Estimation of Damage and Loss

8.1. Estimation of Debris

Debris estimation was conducted through direct cross-sectional measurements. The total estimated quantity of debris is over 150,000 cubic meters. The breakdown of debris by contract package can be found in Figure11. The graph further states that quantity of the landslide to be removed from the road surface is about 71,000 m3, 50,000 m3 and 30,000 m3 in contract **Package I, II and II respectively**. Similarly, on average, **Nagdhunga Naubise section** has about 5,700 cubic meters of debris in a kilometer, the highest concentration among the packages. **Package II** has about one-fifth of this average, and **Package III** has about one-eighth. These measurements indicate that Package I is the most affected section in terms of quantity of debris, followed by Package II and Package III.

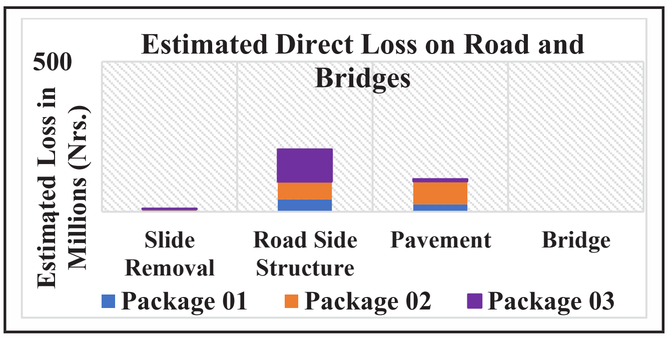

Figure11: Estimated quantity of debris of contract packages.

8.2. Estimation of Loss

a. Direct loss on the Road Section

The total direct loss from landslides, slope failures, and flooding along the Nagdhunga-Naubise Road section, including debris removal, road structure damage (such as retaining walls, breast walls, and drains), pavement damage, and bridge-related damages, is approximately NPR 330 million (illustrated by Figure 12). Of this, 63% is attributed to roadside structures, 33% to pavement damage, 3.3% to debris clearance, and less than 1% to bridge-related damages. In terms of geographic distribution:

- The Nagdhunga-Naubise section accounts for 22% of the total loss.
- The Naubise-Malekhu section contributes 43%.
- The remaining loss is attributed to the Malekhu-Mugling section.

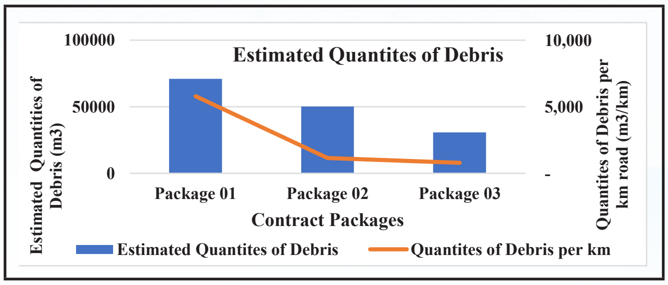

Figure 12: Estimated direct loss on all packages.

a. Estimated Total Loss

The severe rainfall event that took place in September has resulted in significant financial losses along the Nagdhunga-Mugling Road. The total damage is estimated at Nrs. 500 million and is distributed across various sectors as presented in Figure 13.

- **Road Structure Damage**: 66% of the total loss, highlighting the extent of damage to the road infrastructure.
- **Delay Costs**: 31% of the loss, reflecting the economic impact due to delays in transportation and traffic disruptions.
- **Vehicle Damage**: 3% of the total loss, accounting for the damage sustained by vehicles due to the adverse weather conditions.

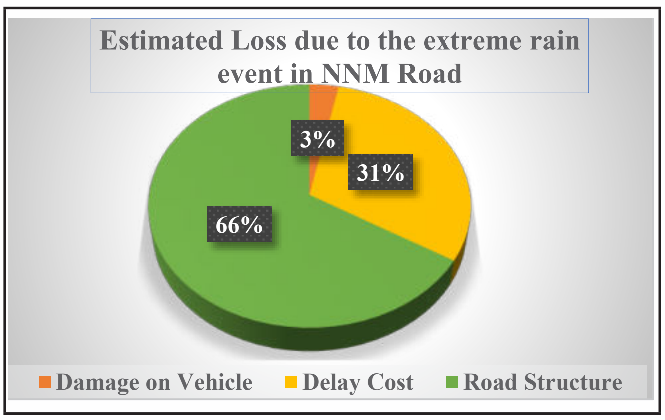

Figure 13: Overall loss by extreme rainfall event on Nagdhunga-Mugling Road.

This event underscores the vulnerability of critical transportation routes to extreme weather and the far-reaching effects on both infrastructure and the local economy.

9. Budget Estimation for Restoration of Road

Water management and slope stabilization are critical activities for this road section to address climate-induced hazards and other disaster-related challenges. Given these factors, slope stabilization works are primary activities for pre-identified landslide locations, including Jhyaple Khola, Khatripauwa, Mahesh Khola (3+800), Kamere Bhir, Chiraudi Bridge approach, Parewa Bhir, Krishnabhir, and many other locations. A preliminary budget of NPR 800 million has been estimated for slope stabilization in the mid-term plan on those locations. However, this estimate requires further detailed assessment, including necessary testing, design, and precise cost estimation. The goal is not only to restore the Nagdhunga-Mugling Road to its pre-event state but also to ensure that it is more resilient to future rainfall events and disasters. This approach aims to reduce the long-term economic and human costs associated with road failures, improve safety for travelers, and protect the broader environment along the route.

10. Conclusion

In conclusion, the Nagdhunga-Naubise-Mugling Road, situated in a geologically fragile and climate-sensitive zone, has faced severe impacts due to recent extreme rainfall. Over 113 locations along this route experienced landslides and debris flows, leading to significant loss of life and property. The tragic incident at Jhyaple Khola alone resulted in 35 fatalities, over 150,000 cubic meters of debris displacement, and damages to roads and bridges estimated at approximately NRs. 330 million. Including delays, the total losses are projected at NRs. 500 million. Rebuilding and strengthening this critical transport corridor will require a detailed assessment and design process, with an estimated future investment exceeding NRs. 800 million for the damaged sections alone. A thorough study is essential to refine the cost estimates and ensure the project's success.

References

[1] Government of Nepal (GoN), *National Climate Change Policy 2019*, 2019.

[2] Amadio, Mattia; Behrer, Patrick; Bosch, Lander; Kaila, Heidi; Krishnan, Nandini; Molinario, Giuseppe;, "Climate risks, exposure, vulnerability and resilience in Nepal," World Bank, 2022.

[3] Asian Development Bank, "CLIMATE CHANGE ASSESSMENT," Asian Development Bank, 2019.

[4] World Bank Group, Country Climate and Development Report : NEPAL, World Bank Group, 2022.

[5] S. K. Baidya et al., "Trends in Daily Climatic Extremes of Temperature and Precipitation in Nepal," *Journal of Hydrology and Meteorology*, vol. 5, no. 1, 2008.

[6] The Intergovernmental Panel on Climate Change (IPCC), "IPCC Reports on Working Group I: The Scientific Basis," IPCC.

[7] Intergovernmental Panel on Climate Change (IPCC), "Weather and Climate Extreme Events in a Changing Climate," 2021.

[8] Department of Hydrology and Meteorology (DHM), Nepal, "dhm.gov.np," [Online]. Available: https://www.dhm.gov.np/hydrology/rainfall-watch-map. [Accessed 06 11 2024].

[9] Government of India, India Meteorological Department, CLIMATE RESEARCH & SERVICES, PUNE, " CLIMATE RESEARCH & SERVICES, PUNE, INDIA," [Online]. Available: https://imdpune.gov.in/hazardatlas/extreme.pdf. [Accessed 06 11 2024].

[10] Development Cooperation Implementation Division (DCID), Department of Roads (DoR), "Environment and Social Impact Assessment for Improvement of Naghdhunga-Naubise-Mugling (NNM) Road," DoR, Kathmandu, 2020.

♦

8.0 MITIGATION OF A CHRONIC LANDSLIDE BY LOWERING GROUND WATER TABLE: A CASE STUDY FROM GORKHA-GHYAMPESAL ROAD

-Dr. Er. Madhu Sudan Acharya
Geotechnical Engineering Expert
e-mail: masuaa@yahoo.com

1. Background

This paper presents special road slope stabilization works implemented in Kokhe Aahale at Ch 11+000 of Gorkha-Ghyampesal Road. The problem of road subsidence due to rise in ground water table during monsoon season was already identified during the upgrading of this road under Decentralised Rural Infrastructures and Livelihood (DRIL) Project supported by Asian Development Bank in 2010. Although, the problems of this location were already identified during upgrading of earthen road to gravel standard under DRIL project implemented through DoLI (Department of Local Infrastructure), no appropriate mitigation measures were implemented by the project due to insufficient budget.

Previous site investigation conducted during upgrading under DRIL project revealed of potential threats to the road by two major landslides viz. Kokhe Aahale at Ch 11+000 and Khanchowk at Ch 21+820-22+240 where the road sections are damaged obstructing traffics. At that time, it was also suggested to consider these sites carefully. It was also suggested to design and implement appropriate mitigation measures in time, otherwise it may create problems in future. As the time passed by, not much care was given to mitigate the Kokhe Aahale landslide at Ch 11+000. Only typical retaining wall construction and embankment filling works to open the traffic were continued for several years by the road division office Damauli.

In the year 2022, this section of road at Kokhe Aahale was blocked several times during monsoon season, and it was very difficult to open the traffic timely. **Figure 1** shows the condition of roads in June 2022. When the road was blocked, division road office had always tried to open the traffic by putting gravel on the muddy road. As the gravel material subsides on the mud, the mobility along the section of road becomes impeded.

To solve this recurrent problem of this section, the division chief from division road office, Damauli, requested geotechnical engineering expert (GEE) from department of roads for a site visit. Then a site visit to this landslide area was carried out on 17th January 2023 by GEE, jointly with Regional Director of Federal Supervision and Monitoring Offices of the Department of Roads, Western Region, Division Chief, Damauli division and site Engineers. The detailed description on the site condition, the geotechnical investigation, geophysical survey, the design of mitigation measures, construction details, final slope condition and lesson learned are described in sub-sequent sections below.

Figure 1: *Existing condition of the slope at Km 11+000, near Aahale along Gorkha-Ghyampesal road, June 9, 2022.*

2. General features of landslide site

The **Figure 2** shows the existing condition of the landslide along Gorkha - Ghyampesal road at Km 11+000, near Kokhe Aahale during site visit in January 2023. The slope is south facing and relatively dry during winter which becomes fully saturated during monsoon and starts to move downwards from its own weight (See **Figure 1**). There is a natural forest with large trees on the uphill from where all the runoff and seepage water come into the landslide area.

The failed road slope has a gentle slope of about 45° on the uphill side and about 35°-40° on downhill side. There is cultivated field with scattered trees on the uphill side which continues to the margin of national forest with thick vegetations. The soil is gravel-mixed soil with substantial amount of silt. There was an existing gabion retaining structure on the roadside, which failed due to subsidence of road.

The failed slope is about 425m long and 70m wide and the elevation of the crown part is about 990 m, where some tension cracks are also visible. The toe part is only the transportation zone and there exists seepage water at an elevation of about 940m. Based on the information from the locals the section of road is sinking down 1-2 meter every monsoon. The landslide is deep seated, complex in nature and still active. From the site observation, it is evident that the prime factor of slope failure is ground water therefore the principal works required in this landslide is the management of sub surface water.

After the site visit by GEE, it was suggested to carry out topographical survey and ERT survey of this site. Both surveys were carried out by the Road Division Daumali, and there was not any large-scale geotechnical investigation required to be done.

Figure 2: *Existing condition of the slope at Km 11+000, near Aahale along Gorkha-Ghyampesal road, during site visit on January 17, 2023.*

3. Geophysical investigation of landslide site

As suggested by Geotechnical Engineering Expert, the Division Road Office hired a consultant to perform Electrical Resistivity Tomography (ERT) survey of the landslide area.

The ERT survey was aimed at delineating the subsurface geology and groundwater condition of the existing landslide area. Altogether 4 ERT profiles (as shown in Figure 3) each of different lengths were performed at the site to define the subsurface geology at different sections of the landslide. The details of the ERT profiles are given in Table 1.

The main objectives of 2D-Electrical Resistivity Tomography (2D-ERT) are.

- i To establish ground profile showing different layers of soil and rock,
- ii To find out depth to bedrock if any,
- iii To find out jointed, fractured and sheared zone (weakness zone) within the bedrock
- iv To find out plane of weakness for slope stability, deformed zones in bedrock, slopes and slides
- v To find out the groundwater table in landslide area.

Table 1: Locations of ERT surveys profiles, Kohke Ahale, Gorkha

ERT Lines	Northing	Easting	Surveyed Length (m)	Location
ERT 1	3101113.486	566105.916	450	Along the mid slope
	3100711.820	566137.034		
ERT2	3100949.440	566032.840	240	Across the landslide
	3100995.807	566247.315		
ERT 3	3101082.654	566073.772	230	Along the left margin side
	3100893.015	566126.281		
ERT 4	3101107.489	566142.925	240	Along the right margin side
	3100896.410	566147.912		

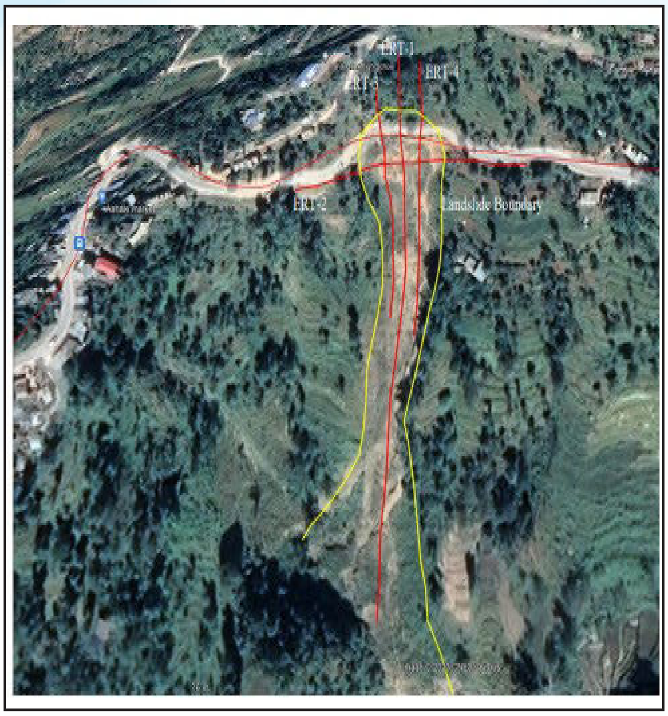

Figure 3: Location of project area and ERT survey lines

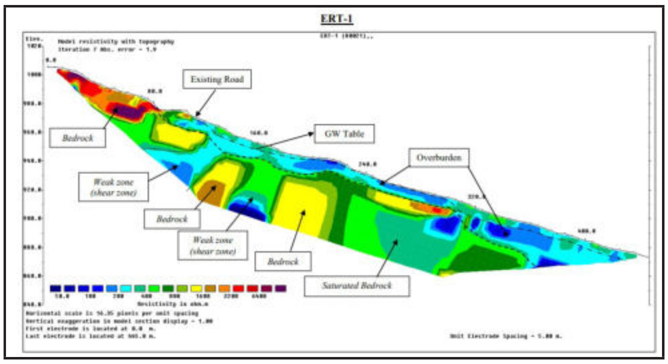

***Figure 4:** Interpretative tomogram for ERT-1 along the central part of landslide*

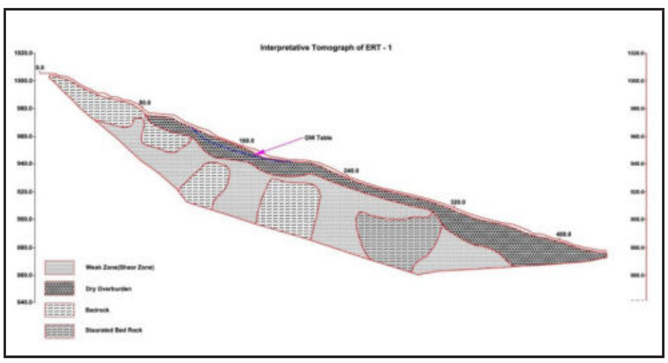

***Figure 5:** Interpretative soil model of ERT-1 along the middle part of the landslide*

Interpretative tomogram for ERT-1 and respective soil profile along the middle part of landslide is shown in Figure 4 and Figure 5 above. The slope length of this landslide has been completely mapped out by laying out the ERT-1 profile along the landslide's central margin and extending it for 450 meters downhill. This profile aims to outline the subsurface geology at the current landslide area and its upslope area.

The bedrock in this region is phyllite which is completely weathered, leaving behind residual soil. In addition, there is a fault gauge in this area close to the landslide and around the current road section. The existing road section is composed of a thick layer of sliding materials, as evidenced by ERT-1. This weathered residual soil material in this area has a thickness of 6 to 12.00 meters. At chainage 000+210 (ERT-1, along the slope), a thin layer of about 6.0 m overburden has been observed. At this chainage, a convex bedrock structure has also been observed in the ERT profile. The groundwater (GW) table is identified in the figure as a dashed line based on the apparent resistivity values and saturation state of the subsurface materials.

In contrast to the dry soil on the upper portion, on the lower section of this landslide, there is a presence of GW close to the surface. The GW table has been observed at a depth of about 3-5 meters from the surface. The lower layer, which serves as bedrock, has been distinguished from the upper layer by a remarkable change in apparent resistivity values and pattern within this tomogram, which has been delineated by a dashed line. The bedrock beneath this layer has also been divided into alternate layers of strong and weak bedrock. Those layers with apparent resistivity values in the range of 50-300 Ωm may be saturated, weak bedrock layers, occasionally even containing fault gauge. In contrast to this, the alternative layers with apparent resistivities of at least 1500 Ωm represent a moderately strong bedrock.

The soil profile from ERT-1 revealed that the current road surface is laying on a 12 m thick overburden soil layer made of residual soil. It seems that the movement of thick layer of soil mass is partially prevented by a convex shaped bedrock structure at chainage 000+210 which is located at about 3 m below the existing ground surface. The reduction in the shear strength of the loose overburden materials is mainly due to the presence of groundwater table near the road surface which was responsible for the retrogressive type of slope movement each year. Therefore, it is recommended to lower the existing GW table which will reduce the pore water pressure and increase the shear strength of soil which can significantly contribute to the stabilization of roadside slope at this location.

4. Detail design of mitigation measures

After analysing the ERT report, GEE prepared a detailed design of mitigation measures for this landslide area. As the surface and sub-surface water management is the main problem of this site, the mitigation measures mainly comprise of sub-surface drainages with gravel trench and horizontally drilled sub-surface drainage system.

As this slope is south facing it receives high amount of rainfall during monsoon, therefore, it is proposed to construct a large size side drain on the hill side to keep the road embankment dry also during monsoon. The proposed mitigation measure will help to manage the surface and sub-surface water and keep the ground water table as below as possible even during monsoon. From the soil profile It seems that it is required to carry out horizontal drilling for sub-surface drainages and horizontal drillings were planned accordingly.

As the existing slope on the right side of the road (valley side) is made of fill material from landslide debris, which are being damaged by the surface runoff and sub-surface water coming from the uphill and side drain, it is required to design an appropriate system of retaining wall to support the road embankment. As there is no presence of bed rock at shallow depth, the construction of retaining wall on loose material is not recommended. Similarly, construction of retaining wall or any rigid structure near road pavement is not recommended because of lack of appropriate foundation. Therefore, it is suggested to construct a gabion sleep wall (as shown in **Figure 6**) at an angle of ~33° starting from bottom of the failed slope which should be founded on original ground. The first layer of gabion should be secured against sliding by providing 25mm diameter, 1.5- 2.0 m long dowel bars hammered into the slope.

In addition, appropriate bioengineering measures are also implemented on the landslide area on uphill side and transportation zone of the landslide on the downhill side. After the construction of the roadside slope, the shoulder area on the right-hand side should be paved so that it should not allow to infiltrate water inside the backfill and prevent to flow the surface runoff directly on the failed slope area.

The proposed side drain is designed such that the surface water (runoff) from the road will be collected on the side drain and diverted through pipe culvert which finally flows through a suitable outlet (chute) from stable slope area. It is recommended to use semicircular side drain of corrugated PVC pipe and make a wider shoulder on the hill side and provide delineator posts or gabion barrier also on the side of the drain considering traffic safety. Alternatively, conventional side drains can also be constructed by using an impermeable liner at the bottom of the drain so that there will be no seepage of water into the road embankment. The proposed mitigation measures will help to manage the surface and sub-surface water and keep the ground water table as below as possible even during monsoon.

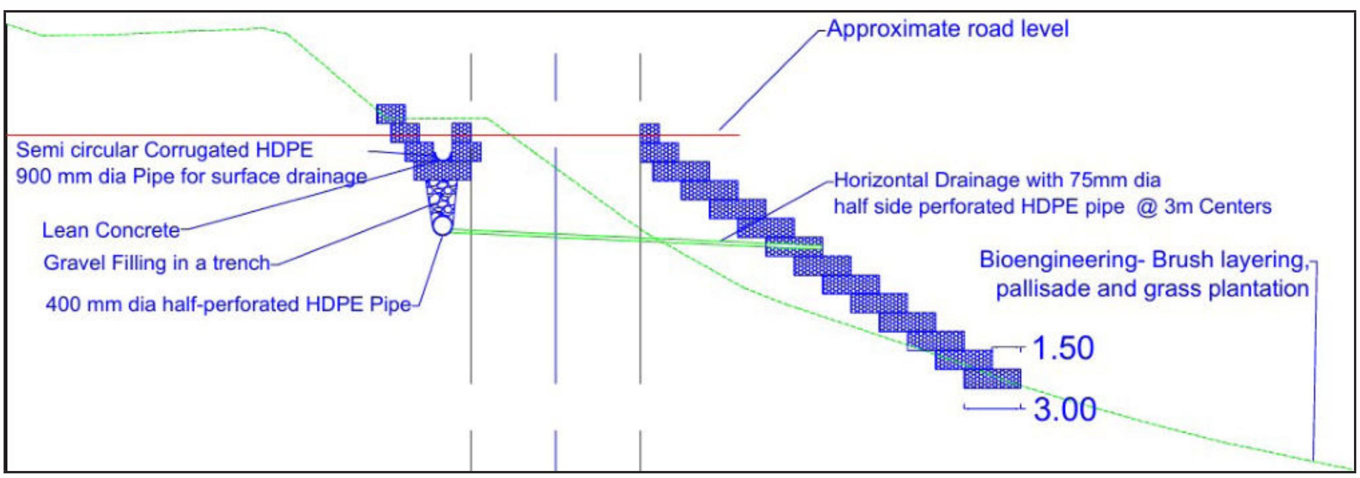

Figure 6: Suggested mitigation measures with gravel trench and perforated pipe below side drain, horizontal drainages 5-6 m below road surface and gabion sleep wall to protect the road embankment.

5. Construction Details

A. *Construction of sub-surface drainage*

The construction of sub-surface drainage has been carried out in two ways namely vertical gravel trench and use of perforated pipes on the sub-surface by horizontal drilling. Firstly, a vertical trench of 3 m wide and 2 m deep along the drain line has been dug out and then the middle portion of this trench is further excavated to a depth of about 2 m and then 40 cm diameter half side perforated corrugated polyethylene pipe wrapped with geotextile was laid and the trench is filled with gravel (free draining materials up to the base of gabion as shown in **Figure 7**. After construction of gravel trench (**Figure 8**), a layer of gabion is installed on the top of gravel trench and semi-circular section of corrugated pipe is laid on the top of gabion layer for surface drain as shown in **Figure 9**.

Figure 7: *Construction of gravel trench and perforated pipe below side drain and its outlet pipe across road*

Figure 8: *Corrugated half side perforated HDPE pipe on the bottom of gravel trench and gravel filling on the trench below the side drainage.*

Figure 9: *Semi-circular corrugated HDPE pipe on the top of gravel trench for surface drainage.*

Figure 10: *Perforated HDPE pipe and horizontal drainage in drilled hole for sub- surface drainage.*

After completion of cut off gravel trench and gabion work for surface and sub-surface drainage on the hill side, horizontal drilling work was conducted at about 5-6 m below the proposed road surface at an elevation of about 965.00 m above msl. For horizontal sub-surface drainages, first of all horizontal drilling of 100 mm dia. holes up to a depth of 30-35 m (as designed) were drilled and then 75 mm dia. half side perforated HDPE pipes were inserted into these drilled holes. These perforated pipes are wrapped with geotextile (see **Figure 10**) to prevent the clogging of perforation from soil material. The horizontal drilling works was done at an interval of 3 metres.

B. ***Construction of gabion sleep wall***

After construction of sub-surface drainage, the collected water is taken to the location of pipe culvert from where a sub-surface outlet is constructed. After completion of sub-surface drainage and culvert outlet the road embankment is secured by a gabion sleep wall at an angle of about 33° or 45° as shown in **Figure 6**. The purpose of this wall is to support the road embankment by providing a confined space for backfilling the slope. Bio-engineering works in the form of brush layering and palisades are implemented in the area below the gabion wall after slope trimming works. Similarly, bioengineering is also done on the barren and excavated area above the side drain. Photos of the horizontal drilling and gabion works are shown in **Figure 11**.

Figure 11: *Drilling works for horizontal drainage on left and gabion sleep wall construction on the right.*

6. Post Construction Scenario

After completion of construction works, there is no any obstruction on road traffic flow. The back filled road surface is left for consolidation for a year. After completion of major consolidation of road subgrade, appropriate pavement works will be carried out. The performance of sub-surface trench and horizontal drilling works is very good, a continuous flow of large amount of groundwater is observed. On the middle part of lowest level of gabion, there is still substantial amount of ground water coming out. Therefore, it is suggested to carry out additional horizontal drilling on this area and construction of appropriate surface drainage structure to manage the flow of ground water during monsoon. The **Figure 12** (left) shows the flow of ground water from subsurface drainage and the right photo shows the completed gabion structure and road surface. Similarly, the **Figure 13** shows the condition of road in June 2022 and May 2024.

Figure 12: *Functioning of sub-surface drainage outlets (left) and completed gabion structure, bioengineering works and drainage chute construction on the right.*

Figure 13: *Road condition at Kokhe Aahale in June 2022 (left) and road condition after application of mitigation measure in May 2024 (right).*

9.0 A Short Review on Gravel Loss Model for Unpaved Roads

- Thaneshwor Khatri, Prem Prakash Khatri, Sushil Babu Dhakal

Introduction

Prediction of deterioration of gravel roads is an important step for effective management of road network maintenance. Several models for such prediction of gravel loss in gravel roads are formulated in different countries including Nepal. In this review paper, reportedly most suitable models and a model formulated by Nepalese researchers are listed. Limitations for their use and hence further need of research and calibration are listed.

Reportedly Most Suitable Models

Robbie Uys in his paper recommends that "the TRH20 model or the HDM-4 model will be the most suitable to be calibrated or amended for future use, not only applicable to southern African conditions, but to be used worldwide" [1]. These models as described in the same paper [1] are reported as follows:

1. **HDM-4 model**

   "This model is the most widely used and most familiar deterioration model used internationally" [1]. The prediction of the annual quantity of material loss is:

MLA = Kgl*3.65(3.46 + 2.46* MMP*RF*10^{-4} + KT*AADT) …………………..Equation 1

Where,

MLA = the predicted annual material loss (mm/year),

RF = average rise and fall of the road (m/km),

MMP = mean monthly precipitation (mm/month),

AADT = annual average daily traffic (veh/day),

KT = the traffic-induced material whip-off coefficient,

Kgl = gravel material loss calibration factor.

The traffic-induced material whip-off coefficient is expressed as a function of rainfall, road geometry and material characteristics, as follows:

$$KT = Kkt * MAX\left\{0, \left[\begin{array}{l} 0.022 + \left(\frac{0.969 * C}{57300}\right) + 3.42 * MMP * P075j * 10^{-6} \\ -9.2 * MMP * PIj10^{-6} - 1.01 * MMP * 10^{-4} \end{array}\right]\right\}$$ ….Equation 2

Where,

C = average horizontal curvature of the road (deg/km),

PIj = the plasticity index of material j where:

j = g if a gravel road,

j = s if an earth road,

P075j = the amount of material passing the 0.075mm sieve,

Kkt = traffic-induced material loss calibration factor.

2. **TRH20 model**

The TRH20 manual was based on South African experience and research results. The traffic volumes, climatic conditions and material properties play a major role in the prediction of annual gravel loss. The annual gravel loss (AGL expressed in mm) can be predicted by the following:

AGL = 65.3 [ADT(.0 059 + .0 0027N − .0 0006P26) − .0 367N − .0 0014PF + .0 0474P26]………Equation 3

Where,

ADT = average daily traffic,

N = Weinert N-value,

P26 = percentage passing the 26.5mm sieve,

PF = product of plastic limit and percentage passing 0.075mm sieve.

Nepalese Model

Er. Prashant Kumar Yadav and Prof. Gautam Bir Singh Tamrakar have formulated a gravel loss model by monitoring seven number of roads for six months period in Nepal [2]. The formulated model is as follows:

GL=D (-34.061 + 0.044 ADT + 0.098MMP) -1.034 PI +1.698 G + 0.460 P20. …………Equation 4

Where:

GL = Gravel Loss,

ADT = Average Daily Traffic,

D = Observation days (days/100),

MMP = Mean Monthly Precipitation,

P20 = Percentage passing 20mm,

PI = Plasticity Index, and

G = Absolute Gradient.

Limitations and scope for further improvement of the gravel loss models

- The models reported here are not mechanics-based models; those are empirical models formulated by regression models with limited variables. There are several parameters of potential importance that are missed to be incorporated in the model. For example: hours of sunshine per day on the gravel road surface, road surface temperature, vehicle speed, road neighbors' behaviors, catchment characteristic, landslide and debris damage and road clearance activities, other routine and recurrent maintenance activities, etc.

- The Nepalese model is based on the gravel loss observation for only six months period predominantly in monsoon months (June to November) which might not be sufficient to capture the gravel loss pattern in other half of the year. At least few years of observation might be required for better modeling of the phenomena.

- Robbie Uys [1] also recommends that "either the HDM-4 or TRH20 models be re-evaluated to incorporate important factors that need to be included into these models that are currently omitted, such as the geometry (both vertical and horizontal), the influence of the percentage of heavy vehicles or an adjustment to the traffic volumes, to incorporate the effect of heavy vehicles on the performance and the influence of visual defects (riding quality) on gravel loss." He further recommends that "The effect of dry weather (high Weinert N-value) on the predicted annual gravel loss for the TRH20 model gives negative values and needs to be re-evaluated as well." Furthermore, he adds: The influence of the percentage of heavy vehicles, the inclusion of more extensive material properties such as the larger aggregate sizes or the bearing capacity as well as the adjustment of the influence or sensitivity of some of the parameters needs to be addressed."

- Local calibration of the models developed by observation of roads in other countries is a compulsory step before using the models. Moreover, several zonings of national territory depending on climate, topography, and other key features might be necessary for better accuracy of the models.

- The paper by Er. Prashanta et al. [2] also recommends following:

  » The model could not include traffic factors like vehicle speed, axle load, amount of dust created by vehicles; climatic factors like temperature; geometric factors like road width, cross-fall, horizontal curves and tangents. These variables can be included in further research.

  » It is difficult to do this type of research alone. It needs a group of technical persons in data collection procedure while road level survey, survey equipment manipulation and material testing.

  » More road sections for more data regression should be selected and duration of study for this type of research should have more than 18-24 months.

References

1. Robbie Uys. 2010. The Evaluation of Gravel Loss Deterioration Models: A Case Study.

2. Er. Prashant Kumar Yadav, Prof. Gautam Bir SinghTamrakar. 2018. Formulation of Gravel Loss Model for Unpaved Roads of Nepal.

3. Paterson, W. (1991). Deterioration and maintenance of unpaved roads: models of roughness and material loss. *Transportation research record*, *1291*, 143-156.

♦

10. Tunnel Displacement Measurement in Nagdhunga Road Tunnel

- *Govinda Dumaru*
Senior Divisional Engineer

1. Introduction

Tunnel construction involves excavating material underground, which disrupts the equilibrium state in the surrounding ground. This disturbance can lead to ground movements or a tendency for the reduction of the tunnel's excavated cross-sectional area until a new equilibrium state of stress distribution is established. Monitoring of these movements or displacements is crucial not only to assess the appropriateness of the tunnel construction methods but also ensure the safety of tunnel, tunnel construction, and integrity of the support structures and the ground area above the tunnel. It directly relates to the safety of construction workers and the overall stability of the tunnel. In tunnel construction, these displacements are known as tunnel convergence. Tunnel convergence refers to the inward movement or reduction in diameter of a tunnel over time, typically due to ground or soil/rock pressure. This phenomenon is a result of several factors, including the geological characteristics of the surrounding material, the construction method used, and the support systems in place. Tunnel convergence is one of the critical aspects of the New Austrian Tunnelling Method (NATM). The NATM was developed by the Austrians Ladislaus von Rabcewicz, Leopold Müller and Franz Pacher in the 1950s. The name was introduced in 1962 (Rabcewicz 1963) to distinguish it from the 'Austrian Tunnelling Method', today referred to as the 'Old Austrian Tunnelling Method'. They acknowledged that the ground is the main support of the tunnel not the lining.[3] They used strength of rock mass or ground to act as initial support system, that is the ground as supporting element rather than loading element and the use flexible or deformable support system as primary tunnel support system rather than stiff or rigid support system from the moment of excavation. Here the basic principle in the NATM is to take advantage of the load-bearing capacity of weak rocks. This principle is achieved practically by allowing the rock masses around the underground opening to deform in a controlled way providing flexible support system.[2] The extent of deformation shall be minimized to prevent excessive loss of the ground's initial stability while also to allow sufficiently large enough in order to activate the support of the ground as a closed arch and to optimize the usage of the support measures and the excavation.[3] Hence extensive deformation monitoring of the ground is the integral component of this method during construction in order to ensure that ground pressures are adequately controlled. Later, when the rate of displacement is less than a specified limit as described in section 8 below, the permanent support or lining is installed that may not be designed to withstand future loads. Nagdhunga Tunnel has been constructing by use of NATM.

2. Purpose of Observation and Measurement

Observation and measurement of tunnel behaviour during construction is an integral part of NATM. With the observation of the face of the tunnel, the geological state of the face during construction can be verified and the working procedures, thus can be optimised. It also helps to identify unexpected factors that could not be predicted at the design stage so that the design may be modified according to the actual site conditions. Continuous monitoring of tunnel convergence provides information about ground behaviour and early identifying potential stability issues during construction. This significantly enhance the safety of underground structures in the surroundings during construction. The adequacy of the installed support systems or the need of on additional system or shifting to new support pattern can also be confirmed. Thus, observation and measurement are important to construct safe tunnel at minimised cost. The results of observation and measurements can also serve as reference in performing the maintenance of the tunnel concerned after being put in service and in designing and construction of tunnels to be constructed under similar conditions. The purpose and roles of observation and measurement are shown in Fig. 1.[1]

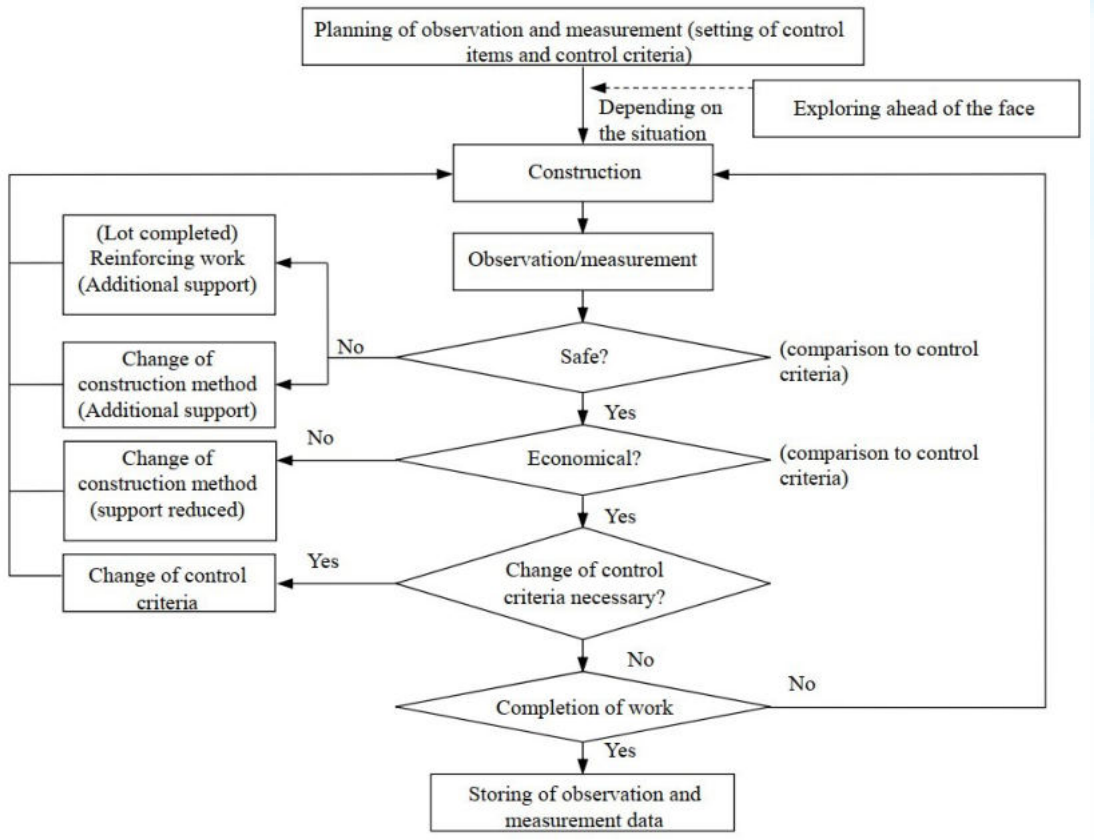

(Source: Standard Specifications for Tunneling-2016: Mountain Tunnels, Japan Society of Civil Engineers)

Figure 1: Purpose and role of observation and measurement [1]

3. Importance of Displacement Measurement

Importance of measurement of tunnel inner space can be summarized as follows:

i) Understanding the stability of the surrounding ground: The displacement measurement results reflect the structural deformation behaviour where the ground and support system are integrated. The convergence of displacement confirms the stability of the surrounding ground.

ii) Understanding the adequacy of supporting members: Depending on the magnitude of the displacement and the convergence state, it is possible to evaluate the excess or deficiency of the implemented support member.

iii) Judging the timing of lining construction: As a rule, lining is constructed after the displacement has subsided, so the results of displacement measurements are used when judging the timing of lining.

iv) Examination of invert closing time: In the sections where it is planned to construct invert, it is possible to examine early closure of invert based on the results of measurements such as the convergence of displacement, the magnitude and the amount of leg subsidence.

4. Method of Measuring In-Tunnel Displacement

Here the displacement and settlement measured by total station is discussed since this method is cheap and convenient method for tunnel convergence monitoring. Measurement point, reference point and total station are used for each measurement by total station. Measurement points are the target which are set to measure displacement/settlement. Measurement point shall have the structure that can be definitely fixed on rock in order to measure accurately. Reference point for measuring convergence/settlement by total station must be set up in the place where displacement does not occur for a long time. Bi-reflex or reflective sheet targets are used as measuring points. These points are fixed to the walls and crown by making a drill hole and inserting rod to the sufficient length.

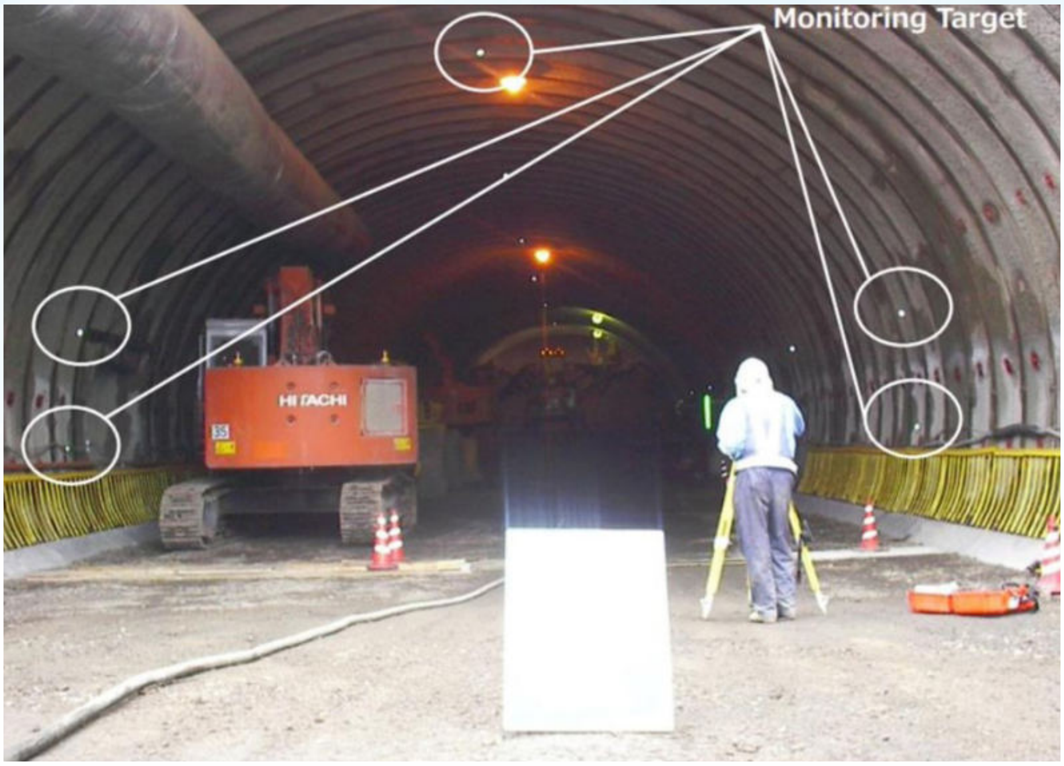

Figure 2: Convergence measurement

The distance of measuring line is obtained by the square root of the sum of the squares of the differences between corresponding three-dimensional coordinates of each measuring point and displacement is then calculated by the difference between the initial value and measuring value. Similarly, settlement of each measuring point is calculated by the difference of vertical level between the measuring value and initial value.

5. Positions of measurement and frequency of displacement measurement

As a general rule, the measurement positions for inner space displacement (ISD) and crest settlement measurement (CSM) shall be measured at the same cross section. The distance between measuring cross sections may vary depending on the specific properties of the ground surrounding the tunnel and the stage of construction. [1] At the initial stage of construction, the measurement interval is shortened in order to grasp the behavioural characteristics at an early stage. Table 1 shows the typical intervals of settlement measurement of a road tunnel. Measuring line layout shall be set out with consideration for the excavation method and foreseeable ground behaviour.[1] Figure 3 shows the examples for arrangement of measuring lines for roadway tunnel. Here A, B, C and D are displacement measurements and points 1, 2, 3, 4 and 5 are points for settlement measurements.

Table 1: Typical measurement intervals of crown settlement and convergence

Conditions / Class of Ground	Near the Portal	Earth covering 2D or less (D=tunnel excavation width)	Initial stage of Construction*	Steps after some advancement
A, B	10 m	10 m	20 m	To be Implemented as needed
CI, CII	10 m	10 m	20 m	30m
DI, DII	10 m	10 m	20 m	20 m
E	10 m	10 m	10 m	10 m

**Note) The initial stage of construction means an excavation distance progress of about 200 meters to which the tunnelling advances. (Source: Standard Specifications for Tunneling-2016: Mountain Tunnels, Japan Society of Civil Engineers)*

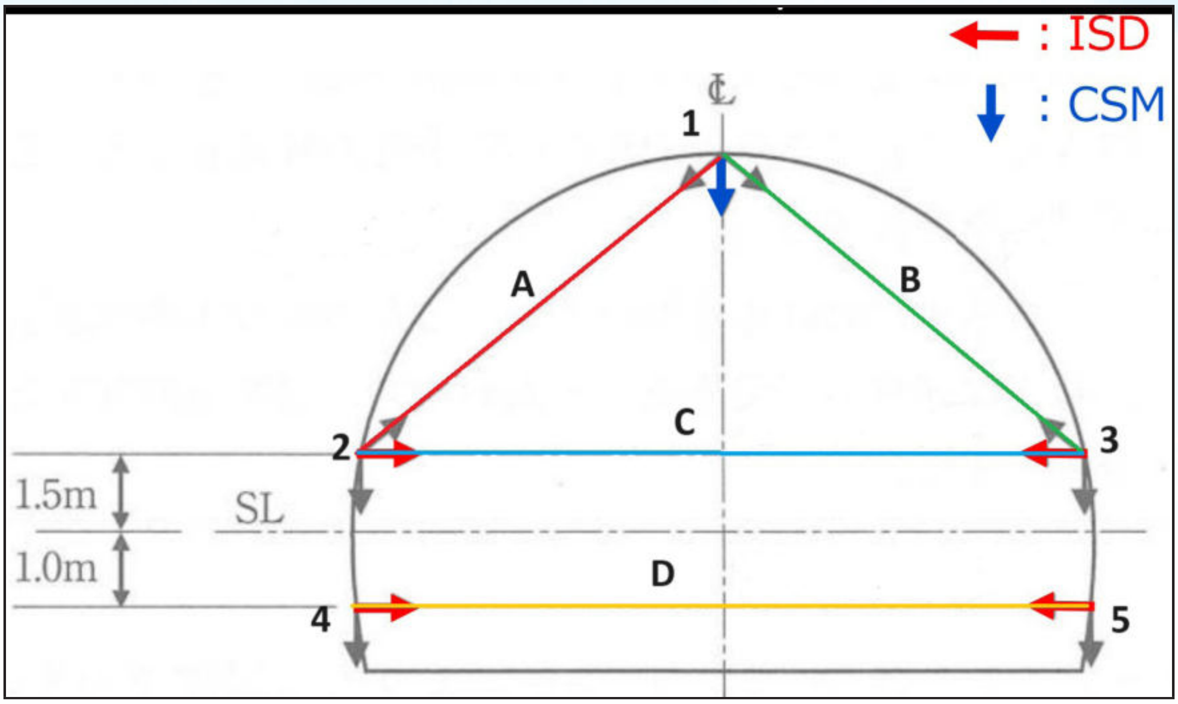

Figure 3: Examples of arrangement of settlement/convergence measuring lines

The frequency of measurement of displacement is determined on the basis of the distance from the face and rate of displacement. The selected measurement frequency should correspond to the higher value between the rate of displacement and the distance from the face.[1] Examples of measurement frequencies of convergence/ crown settlement of road tunnels are given in Table 2. Measurements must be taken until the displacements have become converged. An exactly defined period for measurements cannot be given because the time over which one has to measure is mainly dependent on the ground type and the deformation advance rate. Further, possible stoppages during excavation can increase the period of the measurements.[3]

Table 2: Examples of measurement frequency for convergence/crown settlement (road tunnel)

Frequency	Distance of measuring point from face	Rate of Displacement	Remarks
Twice/day	0 – 0.5D	10 mm or more/day	The measurement frequency to be selected is the frequency determined by the rate of displacement, or the frequency by the distance from the face, whichever is the higher.
Once/day	0.5D – 2D	5 – 10 mm/day	
Once/2 days	2D – 5D	1 – 5 mm/day	
Once/week	5D or more	Less than 1mm/day	

Note: D = tunnel excavation width (Source: Standard Specifications for Tunneling-2016: Mountain Tunnels, Japan Society of Civil Engineers) [1]

6. Understanding General Development of Displacements

The ground displacement at the specific point is influenced by the approaching tunnel excavation face. This influence of the tunnel excavation is such that the displacement slowly increases as the tunnel excavation approaches the monitoring point and slowly diminishes as the face moves forward. Typically, softer and weaker ground experiences displacement earlier and for a more extended duration. As a rule of thumb, the influence of the tunnelling excavation is about +-2D before and behind the monitoring cross section where D is the tunnel diameter. [3]. And this influence on the surrounding ground displacement is more pronounced within a range of approximately one tunnel diameter (±1D).[1] Ideal displacement curve of one monitoring point reacting to an approaching and leaving tunnel heading is shown in Fig. 3.

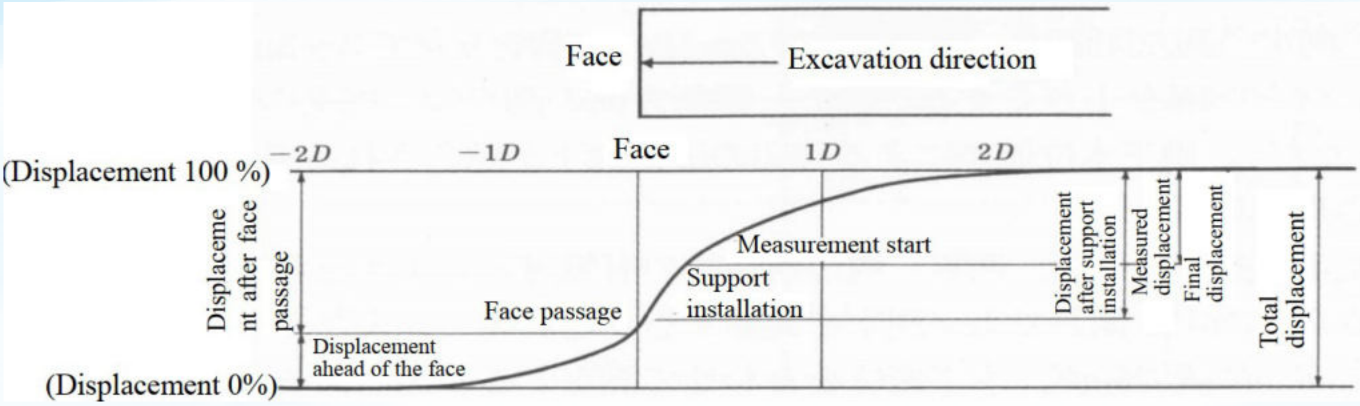

(Source: Standard Specifications for Tunneling-2016: Mountain Tunnels, Japan Society of Civil Engineers)

Figure 3. Typical relationship between face position and behaviour of surrounding ground

It is important to note that the monitoring devices cannot be installed until the tunnel support systems are fully installed at the planned locations. Consequently, the measurements taken from inside the tunnel can only capture a displacement value that is lesser than the total displacement actually occurring. These displacements load the support system and it is therefore important to consider these with respect to the stability of the tunnel. The monitoring cross-section is typically set up in the advancing face currently under construction, and the initial reading should be taken as soon as possible after the support members are installed.

7. Data Presentation and Interpretation

The results of displacement measurement are the data that demonstrate behaviours of surrounding grounds. Systematically organized data and presented in form of drawings, diagrams, etc., make the situation easier to understand. Fig. 4 shows the typical presentation of data for the crown settlement measurements. The graph shows settlement/displacement over time or displacement versus distance from the 'face – monitoring cross-section'. In general, the displacements increase quickly immediately after the base reading. The influence of the tunnel excavation then decreases and finally the displacements do not increase any further. A new stable equilibrium now has been established between the support and the ground and the displacements remain constant. This is very important with respect to settlement control and stability. The displacement graph is also important to identify adverse situations, for example when the displacements do not remain constant or increase again after a period of stability. Therefore, it is important that the measurements are not to be stopped too early as settlements/displacements of the measuring points can occur latter too. Possible adverse causes for increasing displacements are listed below:

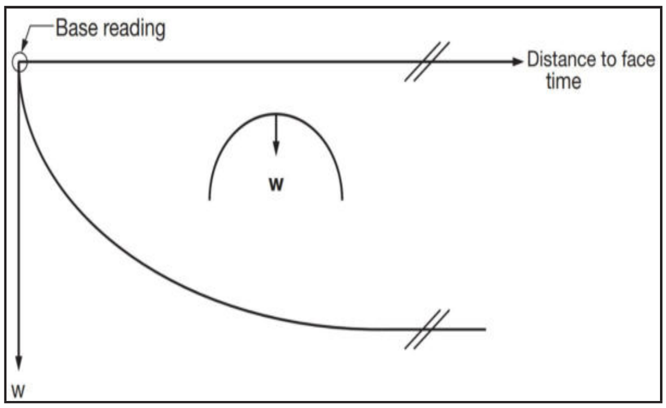

Fig. 4 Ideal Vertical Displacement at the Crown

- modification of ground behaviour due to ingress of water in joints, fissures.
- sudden failure of steel supports.
- effect of parallel tunnel or other structures under construction in the vicinity.

Others,

- In Fig. 5, black line denotes the distance of the excavation face from the measuring cross section. Here, settlements and displacements of measuring points are appeared to be converging but after the resumption of face excavation, those values again tend to increase. Further, displacement at bench section D continues to displace beyond the settlement criteria level II which means the tunnel is more squeezing below spring line.

- In Fig. 6, Horizontal displacement is large and predominant and the displacement at bench section D, is not converging even after the face progresses beyond 200 meters. Final displacement is increasing to about 210mm at the SL and 385mm at bench section. The displacement velocity is high up to a face distance of about 60 m or within 50 days of excavation and it is evident here that the initial displacement that occurs immediately after excavation is large. Further, rate of tunnel displacement has increased due to invert excavation.

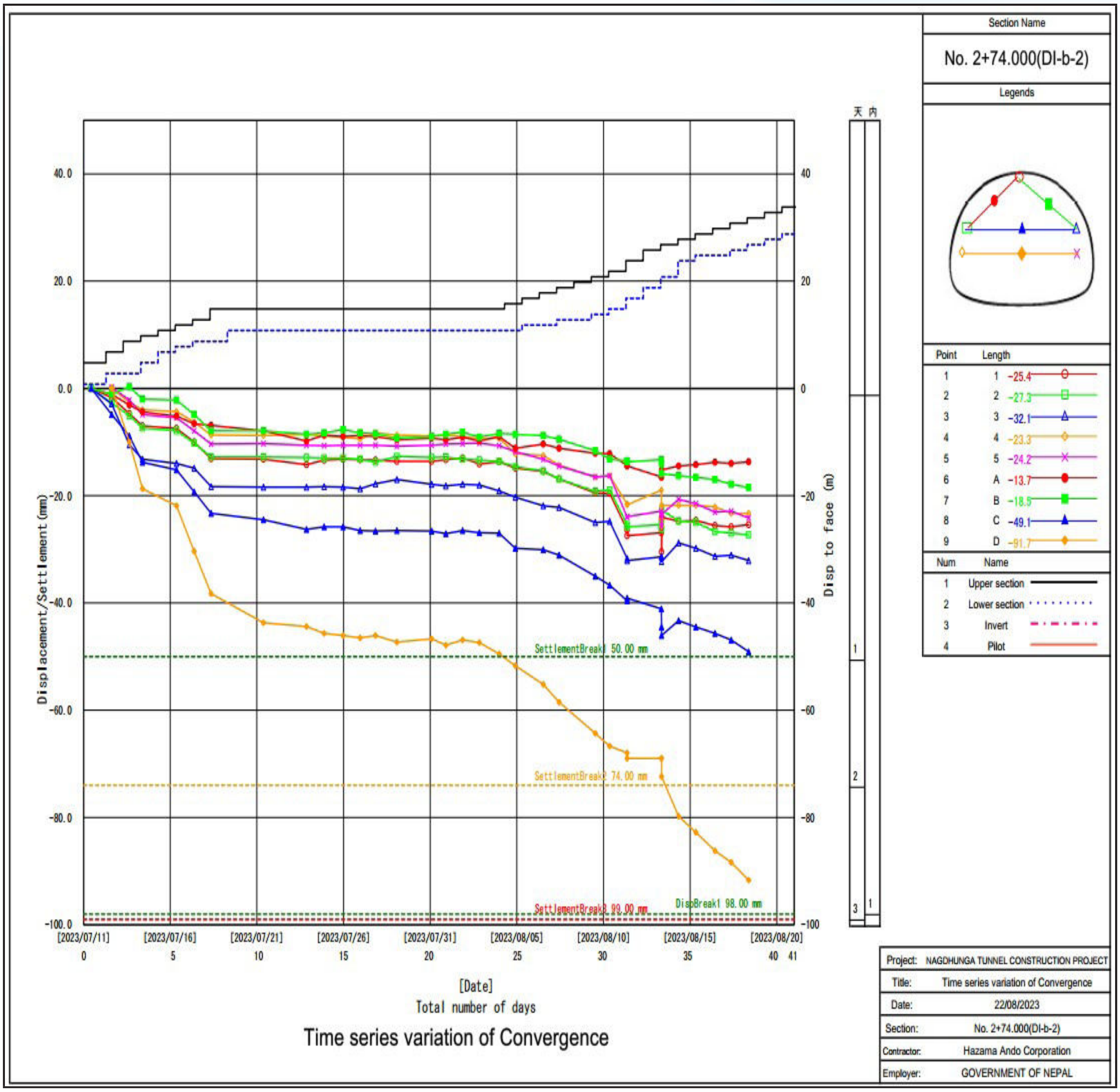

Fig. 5. Time Series Variation of Convergence. Effect of Tunnel Convergence after resuming the face excavation.

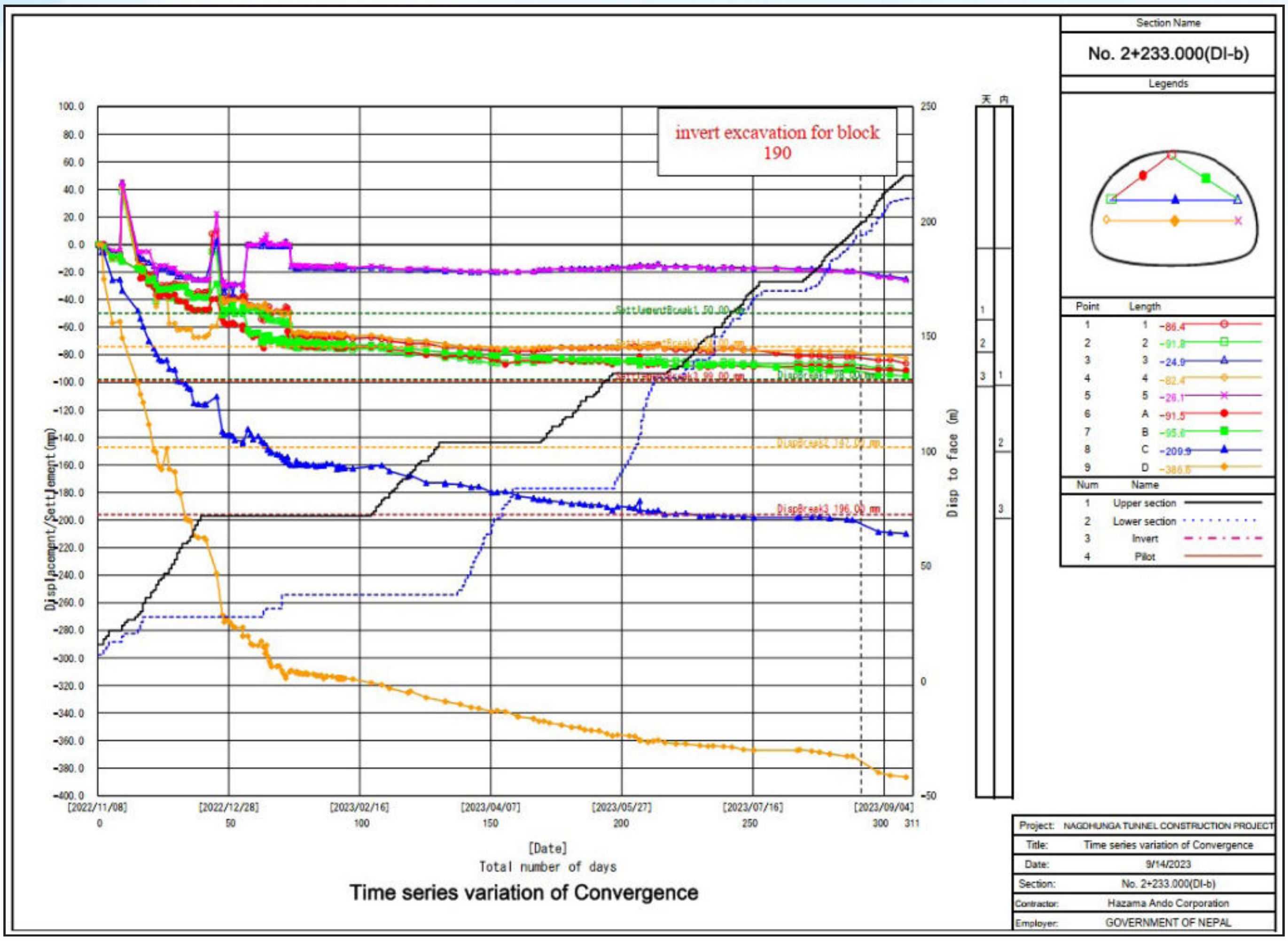

Fig. 6. Time Series Variation of Convergence. Effect on Tunnel Convergence due to invert construction.

However, interpretation of the measurements is not only to see whether a new stress or equilibrium state in the combined ground-support system has been established or not, but also to check the measured displacements against predefined control criteria or triggers for safety of construction, validity of design and impacts on the surrounding structures. [1]

8. Confirmation of Final Convergence

As mentioned earlier, measurements must be continued until displacements and settlement are converged. Here the term converged means that there is no or very less relative change in positions between measuring points According to JSCE's Mountain Tunnel Specification, displacement convergence is considered to be completed when displacement has been monitored at a rate of approximately 1 - 3 mm per month (or about 0.2 - 1 mm per week) for at least two consecutive weeks, at which point measurements may be concluded. [1] Nadhunga Tunnel Construction Project set the maximum convergence rate of 0.14 (1 mm per week) for two consecutive weeks for final convergence confirmation. Final convergence in sections where invert concrete is planned cannot be confirmed until the invert concrete has been constructed, as depicted in Figure 6. Also, final convergence in small parallel tunnel, e.g., evacuation tunnel cannot be confirmed until it may have effect from main tunnel or vice versa. That is, main tunnel face has yet remained to pass the measuring station of the evacuation tunnel.

9. Conclusion

Convergence is a critical factor in tunnel construction. Continuous monitoring of tunnel convergence, accompanied by clear data presentations, provides valuable insights into ground behaviour and potential instability risks during construction. This information may necessitate adjustments to support systems or remediation measures to ensure the tunnel's safety and integrity. Regular measurements of tunnel convergence enable engineers to evaluate the tunnel's performance over time and make informed decisions regarding construction methods and support strategies.

References:

1) Standard Specifications for Tunneling-2016: Mountain Tunnels, Japan Society of Civil Engineers
2) Sprayed Concrete: Properties, Design and Application, S.A Austin and P.J Robins, Whittles Publishing, 1995)
3) Introduction to Tunnel Construction by David Chapman, Nicole Metje and Alfred Stärk
4) Methods for Measuring Convergence and Crown Settlement on Rocks (JCJS 371 1-2001)
5) The New Austrian Tunneling Method (NATM) by Arild Palmström, dr. stipendiat, Norges Geotekniske Institutt, Oslo
6) Optimising convergence Measurement accuacy in Tunnel construction using total station. A case study o the Nagdhunga Tunnel Construction Project November, 2023

♦

Source: A Thesis for the Degree of Masters of Science in Construction Management, Pokhar University Nov, 2023)

11. OVERCOMING CHALLENGES IN THE BRIDGE CONSTRUCTION ACROSS TRISHULI RIVER ON DEVGHAT-THIMURA ROAD

- Er Sagar Karki Chhetri, Engineer, DOR
Email: Sagarkarki1991@gmail.com

1. Introduction

Figure 1: Trishuli River Bridge from the Right Bank Devghat Side

The bridge site is located over Trishuli River connecting Chitwan District of Bagmati Province at Thimura to Tanahu District of Gandaki Province at Devghat. The bridge lies about 3.0 kms upstream from confluence of Kaligandaki and Trishuli River. The Google Coordinates of Bridge site is 27°45'3.79"N, 84°26'37.35"E. The Bridge site is located about 2.6 km west by road distance of Narayanghat Mugling Highway (NH44) at Ramnagar. The contract for construction of this bridge was awarded to the Contractor Elite-Adventure-Indreni JV, Bharatpur. The bridge construction was completed on 2080/09/26 B.S. and Inauguration (figure:14 & 15) was done by Honorable President Mr. Ram Chandra Poudel on 2080/12/17 B.S.

2. Salient Feature

1 Name of the project: Trishuli River Bridge, Thimura.

2 Location: Connecting Province-3 & 4 Chitwan & Tanahun.

3 Classification:

- a. Classification: LRN
- b. Type of Bridge: Combination of Prestressed Concrete Bridge with Steel Truss
- c. Type of Foundation: Shallow Foundation at Abutment & Deep Foundation at Pier
- d. Type of Substructure: Two Abutment & Three Pier.
- e. No. of Foundation: Two Open & Three Pile

4 Length Of Bridge: 217.00 m

5 No. of Spans: 4

6 Span Length: Three Spans of PSC @40 m & One Span of Steel Truss@80 m

7 Geometrics Design.

- a. Total Width (m): 8.45
- b. Carriage Way Width (m): 6.00
- c. Footpath (m): 1.225 m Each Side

8 Type of Wearing Course: Premix Carpet

9 Contract Amount: NRs. 215,013,746.89 Including VAT & PS (Revised)

10 Date of Agreement: 2071/07/20

11 Original Date of Completion: 2074/07/19

12 Revised Date of Completion: 2080/09/29

3. **Construction**

Construction Sequence

	F/Y	Activities
1	071/72	a. Foundation Stone laying Program on B.S. 2071/10/03. b. Confirmatory Bore hole and Soil Investigation is Done.
2	072/73	a. Approval of Revised Design and Drawing. b. Chitwan Side Abutment Foundation and Substructure. c. Chitwan Side Pier 1 Foundation. d. Chitwan Side Pier 2 Foundation.
3	073/74	a. Chitwan Side Abutment Substructure Completed. b. Chitwan Side Pier 1 Foundation and Substructure Completed. c. Chitwan Side Pier 2 Foundation and Pier Stem Completed
4	074/75	a. Chitwan Pier 2 Pier Cap Completed. b. Tanahau Side Pier Foundation and Pier Stem Completed. c. Tanahau Side Abutment Foundation and Substructure Completed.
5	075/76	a. Tanahau Side Pier Cap Completed.
6	076/77	a. Chitwan Side PSC Span 1 Completed. b. Tanahau Side PSC Span 3 Completed.
7	077/78	a. Chitwan Side PSC Span 2 Collapse before prestressing during Construction. b. Chitwan Side PSC Span 1 Collapse. c. Steel Truss span Collapsed during Construction.
8	078/79	a. Chitwan Side PSC Span 2 Completed. b. During Construction of Steel Truss span disassemble of all Truss and False work is done after Yielding of Arch Falsework.
9	079/80	a. Chitwan Side PSC Span 1 Completed. b. Steel Truss span Completed.
10	080/81	a. Approach Road/ Footpath/Railing/ Wearing Course Work Completed. b. Bridge Load Test and Other Necessary test were Completed for both PSC and Steel Span. c. Inauguration

Major Problem and Challenges Faced during Construction

1. The soil investigation Report is prepared after Confirmatory Bore hole before the beginning of construction work by the contractor resulting in Revised Design Drawing with Change in the Pile length for two pier, open foundation to pile foundation for one pier, change in Substructure, Superstructure, Approach Road and Protection work.
2. Earthquake, Border Blockage, Corona Pandemic, Local, Province and Federal Elections, Unseasonal Rainfall, Crusher band, Lack of Sufficient Budget etc. caused the project delay.
3. The Collapse of two PSC Superstructure of Chitwan Side in 2077/12/24 B.S. and Steel truss span in 2078/01/12 B.S.
4. The Sag seen on the bottom chord of truss during erection caused by hitting of 5 Mt Top Chord Member which get detached from one side and hit the bottom chord from height of 10m in 2079/01/30 B.S. causing yielding of arch falsework and results in complete disassemble of Truss erection Works.

Facing the Problems

1. The compaction of embankment for the falsework is done and MS Pipe Falsework system is designed(figure:5) for the PSC Span using the SAP2000.

2. The Design of Foundation, Members, connections and bracing of Arch Falsework (figure:3 & 4) for the Steel Truss System Considering the Load from the Structure.

3. Horizontal Bracing and 2 no of Longitudinal Cable for each arch with Dia 40 mm was provided to Support the Twin Arch Falsework.

4. Two Cable of Size 26 mm Dia each on one side connected between two Iron Tower is used for carrying the Truss member from the End Point.

4. **Discussion and Conclusion**

1. Any change in the subsoil behavior must be taken in consideration during the time of construction and to take necessary decisions.

2. Rigorous planning and Monitoring should be followed at each stage during the time of Construction

3. Regular monitoring on daily basis and emergency response plan for the unforeseen emergency conditions.

4. Follow the Standard Specifications provisions for Temporary Works/ False Works/Erection Method during the construction of Prestressed Concrete Bridge and Steel Truss Bridge.

5. The special type of design and appropriate type of Construction method must be implemented for Bridge Construction over river like Trishuli.

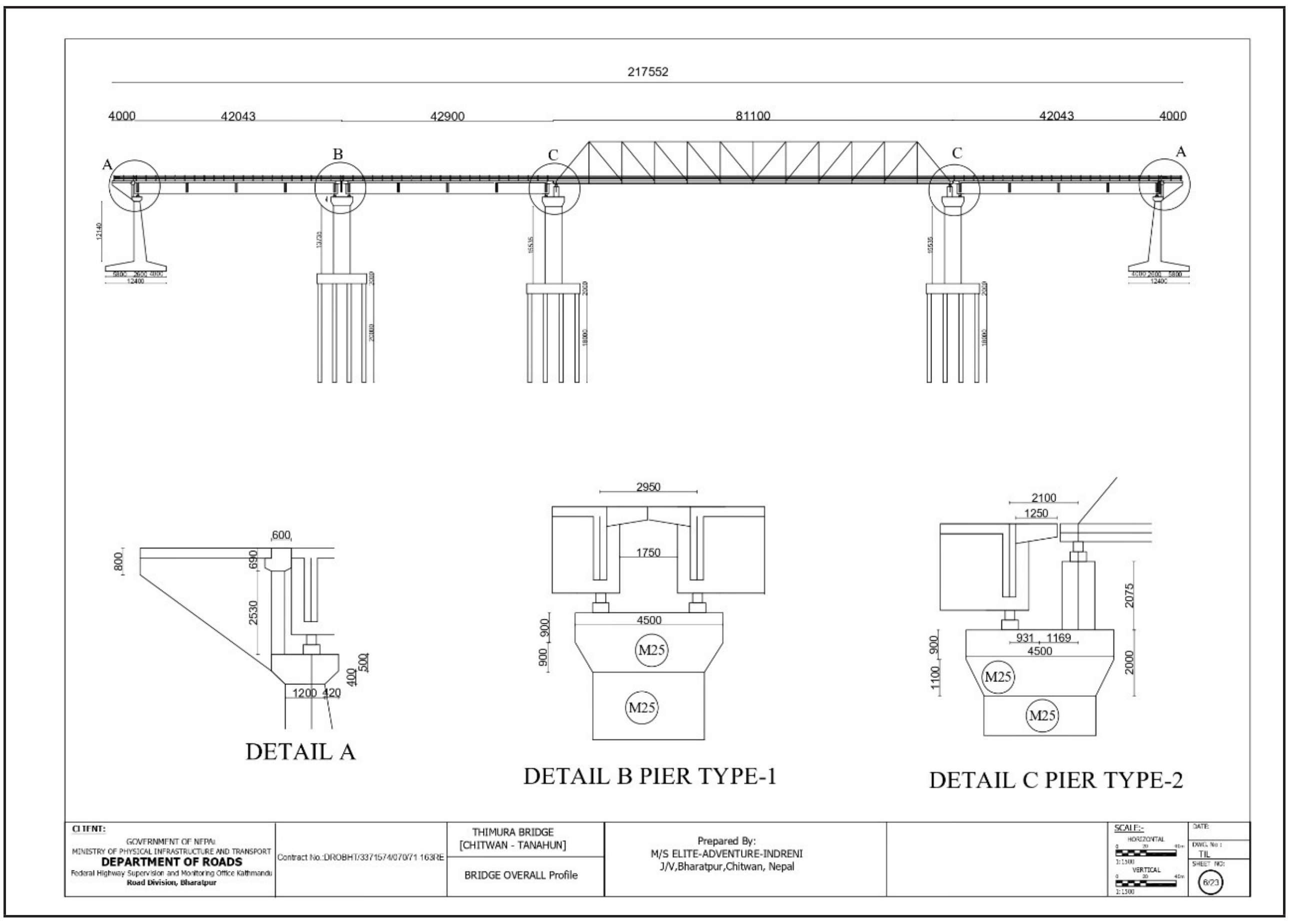

Figure 2: General Arrangement of Trishuli River Bridge

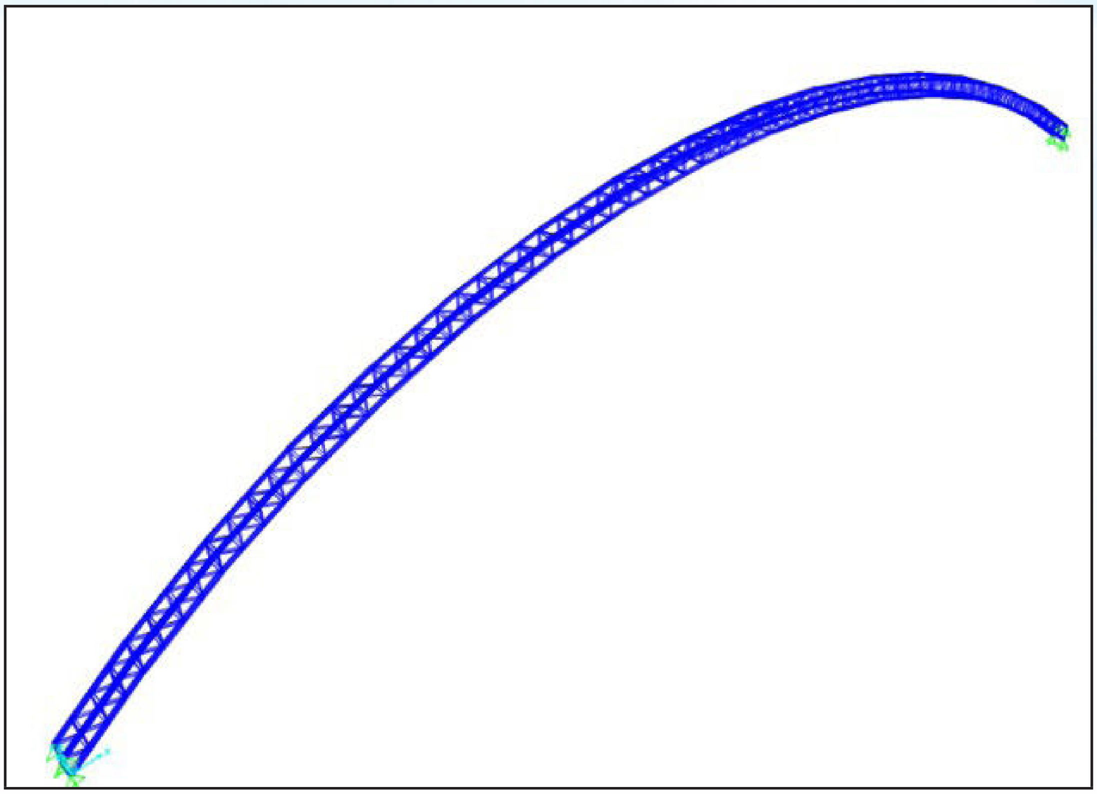

Figure 3: Foundation and Substructure Works

Figure 4: Construction work of PSC and Truss Span

Figure 5: Bridge Load Test on PSC Span and Truss Span

12. Notice and its importance in Construction Contract Management

- *Er. Vijay Kumar Mahto,*
Senior Divisional Engineer, DOR

Background

Notice clauses are found in Standard Condition of Contract and are of great importance. These clauses provide notifications from the parties to the contracts to each other in the event of certain circumstances to make them aware of any problems that may arise. Notice clauses are essential because they give the employer an opportunity to look into the issue at hand and give them more time in order to determine the cause of the problem and whether or not the contractor is entitled to additional time or money as a result. Notice requirements are particularly common in construction contracts, and often stipulate when claims for litigation or alternate dispute resolution (ADR) procedures can be launched and when a contract can be suspended or terminated. Some type of contractual notices in law are "Condition Precedent" which means that if the notice is not given, the remedy or relief will not apply. These can be hard to spot and have a draconian effect. The contractor's failure to follow the contract upon giving notice results in him not being entitled to claim anything.

Introduction

In the commercial activities of today's highly complex society, standard forms of contract have become an essential part of the day-to-day transactions of most agreements. The majority of standard forms have been developed by commercial organizations for the purpose of efficiency, to build on the experience gained from the repeated use of these forms, but most of all for the optimum protection of one or both parties' interests. Standard forms of contract developed for construction activities, however, have mostly been drawn up by independent professional organizations, rather than by one or other of the parties to the contract, in order to establish or to consolidate a fair and just contract.

The Standard Conditions of Contract is drafted on the basis of sharing of risks between the employer and the contractor. The genesis and development of the standard form of construction contract was and remains based on the need to redefine and reapportion the risk ascribed to the respective parties by the applicable law. The construction contract is unique in that it seeks to provide for a specific remedy in the event of any breach of the terms and conditions within its framework and/or for a contractual entitlement in respect of specified events. By including a mechanism to give one party a certain remedy if a specified event arises, the risk of that event, which would otherwise remain with that party, is transferred to the other party. However, whether the remedy sought is in respect of a breach of the contract terms and conditions or for the occurrence of a specified event, all construction contracts place an obligation on the party who wishes to avail themself of that remedy to follow a set procedure, which is referred to as 'the claims procedure. In all construction contracts, claims and the right to claim play a significant role in the contractual relationship between the employer and the contractor.

Contractual notices in construction contracts serve a wide range of functions. For example, claim notification provisions in construction contracts almost always in practice, cover contractual entitlement to time and money. Events and circumstances giving rise to such entitlements include force majeure change in law, unforeseen physical conditions, variations and a range of other compensable matters. The giving of notices is invariably related to matters of importance which need to be formally recorded, not only so that there is a record of giving and receipt of the notice, but also so there is a record of the events giving rise to the notice for future reference. Notices generally fall into the following categories:

- Notice that an action required under the contract needs to be taken.
- Notice that an action required or permitted under the contract has been, or will be, taken.
- Notice that an event has occurred which could cause, or is causing, delay.

- Notice that an event has occurred which would cause, or is causing, the occurrence of additional cost.

- Notice that the Contractor considers that the contractor is entitled to an extension of time (EOT).

- Notice that either party considers that the party is entitled to additional payment from the other party.

- Notice of instructions by the Engineer of the Employer.

- Notice of an error of default by one of the parties.

- Notice of agreement or determination.

- Notice of disagreement or dissatisfaction.

FIDIC Condition of Contract (Red Book)

In FIDIC 1999 Red Book, there are almost 58 situation or places where notices could be issued by the parties out of which Contractor could issue at 33 circumstances, Engineer or Employer could at 19 places and either party could issue at 6 places.

FIDIC 1999 Edition has the following provisions regarding the notices:

Sub-Clause 1.3- approvals, certifications, consents, determinations, **notices,** and requests required to be communicated.

Sub-Clause 1.4- provides the language for communication.

Sub-Clause 1.2(d)- defines the written communication.

Sub-Clause 4.21 (Progress Report)- should be included all the list of notices given under Sub-Clause 2.5 (Employer's claim) and Sub-Clause 20.1 (Contractor's claim).

Many of the clauses which require notice in the FIDIC 1999 Contracts stipulate time frames which must be complied with. FIDIC uses various phrases such as:

- Promptly.

- As soon as practicable.

- Not less than (a stipulated number of) days.

- Not later than (a stipulated number of) days after the contractor became aware or should have become aware, of the event or circumstance.

In FIDIC 1999 notices are generally issued in three stages for events or circumstances.

<u>Notice-1</u>: *Notice that action is require*

For example, Sub-Clause 1.9 (Delayed Drawings or Instructions) deals with the circumstances whereby the contractor requires information drawings or instructions to be able to maintain progress and states that: "The Contractor shall give Notice to the Engineer whenever the works are likely to be delayed or disrupted if any necessary drawing or instruction is not issued to the Contractor within a particular time which shall be reasonable. The Notice shall include details of the necessary drawing or instruction details of why and by when it should be issued, and details of the nature and amount of the delay or disruption likely to be suffered if it is late."

<u>Notice-2:</u> *Notice of Delay and/or the incurrence of cost*

<u>Sub-Clause 1.9:</u> "If the contractor suffers delay and/or incurs cost as a result of a failure of the Engineer to issue the notified drawing or instruction within a time which is reasonable and is specified in the notice with supporting details, the contractor shall give a further Notice to the Engineer and shall be entitled subject to Sub-Clause 20.1 to:

a. An extension of time for any such delay, if completion is or will be delayed, under sub-clause 8.4, and

b. Payment of any such cost plus reasonable profit, which shall be included in the contract price."

<u>Notice-3</u>: *Notice of Entitlement*

S.C. 20.1 (contractor's claim) provides that: 'If the contractor considers himself to be entitled to any extension of the Time for Completion and/or any additional payment, under any clause of these connection with the contract, <u>the contractor shall give notice</u> to the Engineer, describing the event or circumstance giving rise to the claim. The notice shall be given as soon as practicable and not later than 28 days after the contractor became aware, or should have become aware of the event or circumstance.'

FIDIC 2017 has given more importance compared to FIDIC 1999 by providing the Notice as defined word which means notice is written with first letter as capital as Notice, however FIDIC 1999 has used word "notice" which means notice is defined as per condition or situation. Party to the contract has to issue the notices many more situation or places (more than 58) in FIDIC 2017 compared to FIDIC 1999.

Standard Bidding Document for National Competitive Bidding.

Public Procurement Monitoring Office (PPMO) has published Standard Bidding Document (SBD) for national competitive bidding of construction works, however PPMO has recommended FIDIC Condition of Contract for international competitive bidding of construction works. The notices provisioned in PPMO, SBD may be condition precedent or just for notification to other party. If the notice provisioned in the clause of Condition of Contract is of condition precedent then the remedy or relief sought by the party will not be applied when the notice is not issued in stipulated time period. For example, Sub-Clause 35.2 "if the contractor has failed to give early warning of a delay or has failed to cooperate in dealing with a delay, the delay by this failure shall not be considered in assessing the new intended completion date. Contractor shall submit full detail documents entitled to extension of time (EOT) within 21 days prior to the intended completion date."

The following Sub-Clauses of the condition of contract of the SBD, PPMO has provisioned of contractual notices-
Sub-Clause 12 has stipulated that the notice shall be effective only when it is delivered to other party.
Sub-Clause 42.1 - Project Manager shall give notice to the Contractor of any defect before the completion of defect liability period of the contract.
Sub-Clause 35.2 - Contractor shall give notice of early warning of delay.
Sub-Clause 39.1 – Contractor shall warn the Project Manager future events or circumstances that may adversely affect the quality of the work, increase the contract price or delay the execution of the works.
Sub-Clause 46.5 – Contractor shall not be entitled to additional payment for costs that could have been avoided by giving early warning.
Sub-Clause 62.1 – The notice shall be given within 14 days after the party became aware, or should have become aware, of the relevant event or circumstance constituting force majeure.
Sub-Clause 63.2 – Party shall give notice to other party when it ceases to be affected by the force majeure.
Sub-Clause 66, 72, 73 – Party shall give notice to other party before termination of the contract.

Conclusion

In conclusion notices are placed such important places due to the following reasons:

1. To make the Employer and the Engineer aware that:
    - An action that could affect the project is required from them.
    - An event which could affect the project has happened.
    - The Contractor is suffering delay.
    - The Contractor is suffering cost.
    - The Contractor intends to make a claim.
2. Timely issue of notices allows the Employer and/or Engineer to mitigate the circumstances
3. If mitigation is not possible, the Employer and/or Engineer may make provisions for additional time and/or cost.
4. If a notice is not submitted, then the Contractor may have prevented the Employer and/or Engineer from taking such actions and the Contractor would be regarded as having caused damage to the Employer.

Good practice of the notice dictates the following:

- Submitted in the format of a letter or other formal document.
- Clearly state that the communication is notice.
- Contain reference to the contractual clause or clauses under which the notice is submitted.
- Clearly describe the events or circumstances giving rise to the notice.

- Record the dates of the relevant events or circumstances where appropriate.
- Avoid going into details of delays and/or payment. Because the place to do this is in a fully detailed claim.
- Avoid blame allocation and "figure pointing".
- Compose the notice so that it may be clearly understood if relied upon in a claim or furing dispute processing by someone with no prior knowledge of the events or circumstances.
- Be signed by a person authorized by the party issuing the notice to do so.

Finally, in our present situation, Contractors has gradually aware of their contractual rights however, Employer are declining of their right and duty and even if the employer are aware, they are reluctant to issue notice or response to the notice in stipulated time period mentioned in the exclusionary clauses of the condition of contract. This ultimately causes the Employer, Department of Road (DOR) to lose in contractual disputes awarded by the Arbitral tribunal.

References:

1. Conditions of Contract for Construction for Building and Engineering Works Designed by the Employer, First Edition 1999 Published by FIDIC.
2. Axel-Volkmar Jaeger and Go¨tz-Sebastian Ho¨k, FIDIC-A Guide for Practitioners, Springer-Verlag Berlin Heidelberg 2010.
3. Nael G. Bunni, The FIDIC Forms of Contract, 3rd Edition 2005, Blackwell Publishing Ltd., 9600 Garsington Road, Oxford OX4 2DQ, UK.
4. Geoff Smith, Practical Use of the FIDIC Conditions of Contracts, 2012.
5. The FIDIC Contracts Guide, First Edition 2000, ISBN 2-88432-022-9.

♦

13. Assessing the transferability of the Highway Safety Manual crash prediction model in the context of the mountainous rural two-lane highway of Nepal

- *Nitesh Acharya, Department of Roads, Nepal; Email: acharyanites@gmail.com*
Michael Henry, Shibaura Institute of Technology, Japan; Email: mwhenry@shibaura-it.ac.jp

Adapted from the Springer Publication: 17th WCEAM Proceedings, Sustainable Management of Engineered Assets in a Post-Covid 19 World: Industry 4.0, Digital Transformation, Society 5.0 and Beyond, 2024 (https://doi.org/10.1007/978-3-031-59042-9; Print ISBN: 978-3-031-59041-2). Copyright by International Society of Engineering Asset Management 2024.

1. Introduction

1.1 Background

Every year, approximately 1.3 million people die because of road traffic crashes, and it is one of the leading causes of the death among age group 15-29. The losses due to road traffic crashes contribute to around 3% of their gross domestic product and could be even higher in the case of low-and-middle income countries where 93% of the world's total crashes occur (WHO, 2022). For Nepal, a landlocked and mountainous country, road or surface transportation is the primary mode of transport and is extremely important for economic activities. However, road crash statistics show that the status of road traffic safety is not improving, as every year the number of road crashes and fatalities are rising significantly.

A mountainous, rural two-lane two directional roadway named Dhulikhel-Sindhuli-Bardibas (H13) highway of Nepal is considered for this study. The 160-kilometer highway connects the capital Kathmandu to the flat eastern region of the country and thus has huge socio-economic importance. Geographically, the highway passes through rolling, mountainous and steep terrains, and follows both river and hilly routes. Other salient features of the highway include steep gradients, narrow carriageways, and shoulders accompanied by multiple horizontal curves. These characteristics make road traffic safety very challenging, and crashes are rife. From the crash records maintained by Nepal police, it was found that after the formal opening to traffic in the year 2015, an annual average of 95 road crashes and 39 fatalities were recorded. This accounts for 0.243 fatality/km, which is far above the national average of 0.115 fatality/km and therefore it can be noted that crashes are very frequent on this highway and have become a major concern for road authorities. This has also led to emphasizing and enhancing road safety on this highway by adopting a road safety management plan. In this context, a crash prediction model for this highway is developed using the guidelines provided in the Highway Safety Manual (HSM) of the American Association of State Highway and Transportation Officials (AASHTO). However, since this prediction model is developed for the highways in the USA, the estimation of crashes using this model may result in erroneous crash frequencies and hence its adaptability needs to be assessed before application in Nepal.

1.2 Overview of the HSM and related literature

HSM is a guidance manual developed by AASHTO in 2010 that provides overall guidance for quantitative safety analysis during highway safety management. It aids in decision-making at four major stages: network screening, site assessment, project prioritization, and safety effectiveness evaluation (AASHTO, 2010). The manual also provides predictive methods for road infrastructure improvement projects by using safety performance functions (SPFs) for crash prediction by severity, specific facility types, and base conditions. SPFs are statistical models used to estimate average crash numbers for a specific road type and base conditions based on traffic volume and roadway segment length. They are developed through regression modeling of the available historical crash data. The HSM also provides calibration techniques to make the model applicable to conditions different from the ones in which they were developed. The estimated crashes are then subjected to crash modification factors (CMFs) and calibration factors to calculate predicted crashes for each segment of the roadway. Furthermore, HSM provides a clear methodology to combine the predicted crashes with observed crashes to obtain a more reliable estimate of expected crash frequency by using the Empirical Bayes (EB) method. Therefore, because of its simplicity, flexibility, and robustness, the HSM crash prediction model is the most used model among road management authorities.

As described in the HSM, it is always recommended to develop the SPFs using the crash database of the target jurisdiction so that the developed model can precisely estimate the crashes. However, the development of individual SPFs can be a very difficult task because it requires extensive crash data and other resources. Thus, it may be rational to use the SPFs provided by HSM, but they should be used along with calibration factors and CMFs. Calibration factors are used to incorporate geographical changes from one location to another because it affects the estimated crash frequency. As mentioned in the HSM itself, the changes include climatic conditions, road crash reporting thresholds, reporting systems, and populations of drivers and animals. Similarly, CMFs are required to adjust the crash frequency predicted using the SPF for a site using base conditions to the predicted crash frequency for the specific condition of the selected site. In other words, CMFs are applied to account for the geographical and geometric difference between the base conditions of the developed SPF and the local conditions of the site under consideration.

The relation provided by the HSM for predicting crash frequencies using the developed SPF is as follows.

$$N_{predicted} = N_{spf} \times (CMF_{1X} \times CMF_{2X} \times \ldots \times CMF_{YX}) \times C_X \quad \textit{Equation 1}$$

Where,

$N_{predicted}$ = predicted average crash frequency for a specific year for site type x

N_{spf} = predicted average crash frequency determined for base conditions of the SPF developed for site type x

CMF_{yx} = CMFs specific to site type x and specific geometric design and traffic control features y

C_x = Calibration factor to adjust SPF for local conditions for site type x

The SPF for rural two-lane two-way site type is given through the following function.

$$N_{spf} = (AADT) \times (L) \times (365) \times 10^{(-6)} \times e^{(-0.312)} \quad \textit{Equation 1}$$

Where,

N_{spf} = predicted average crash frequency estimated for base conditions using a statistical regression model

AADT = annual average daily traffic volume (vehicles/day) on a roadway segment

L = length of roadway segment (miles)

Also, the calibration factor is calculated using Equation 3

$$C_X = \frac{\sum_{all\ sites} Observed\ crashes}{\sum_{all\ sites} Predicted\ crashes} \quad \textit{Equation 3}$$

Many researchers have studied the transferability of the HSM crash model in the past relating to their own country and driving conditions. The results of these studies have mixed outcomes as some research shows that the HSM predictive model could be successfully implemented to predict crashes with high accuracy, whereas other research exhibited poor performance when adopted in their respective countries.

A study conducted in Iran for the calibration of the HSM predictive method for a rural two-lane two-way road showed that the model could be successfully transferred to a developing country. The results show that the performance of the HSM-based SPF model was better than the local SPF model developed under different research (M. Haghani et al., 2021). Similarly, a study was performed to develop SPF and predict crash frequency for horizontal curves in Thailand. Different types of statistical models and HSM-based models were used for different curve types and the results showed that the calibrated HSM model had even better results than the locally developed SPF (N. Kronprasert et al. 2021).

However, a study carried out in the Arezzo province of Italy to calibrate HSM's prediction model revealed practical application problems of the HSM in the context of the Italian secondary road network. The issues were mainly related to road segmentation and overestimation of crash frequency due to road curvatures (F. Martinelli et al., 2009). Another study in Italy that assessed the transferability of the HSM crash prediction model for freeways found that the local SPF development approach yielded better goodness-of-fit than the HSM predictive model (Torre, et al., 2022).

2. Methodology

2.1 Data Collection

Most of the data on the road geometry and features were extracted from the design and as-built drawings of the highway. Road properties such as lane width, shoulder width and type, longitudinal gradient, length and radius of curve, super-elevation, and presence of spiral curves were obtained from the drawings, whereas information about the presence of rumble strips, median, presence of lighting, information on roadside hazards, number of driveways, presence of passing lanes and two-way turn lanes, and auto speed enforcement were gathered during a field survey conducted in July 2022. Seven-year crash data from 2015 to 2021 were obtained from the records maintained by the Nepal police. Data regarding traffic volume (AADT) were obtained from the annual survey conducted by the Department of Roads, Nepal, and the project office for the construction, operation, and maintenance of the study highway.

2.2 Road segmentation

HSM recommends the formation of homogenous roadway segments before the application of the SPF-based HSM predictive models. This segmentation process results in the formation of a set of homogenous segments with varying lengths and homogeneity concerning road characteristics like traffic volume, road design, geometric properties, and traffic control features maintained within each segment. Hence, a new homogenous segment is formed when there are changes in any of the major road features like traffic volume, lane width, shoulder width and type, driveway density, condition of roadside, and presence of safety measures like centerline rumble strip, lighting, and automated speed enforcement. In addition to the above, HSM also recommends the formation of a new segment if any of the following conditions exist:

- At the center of each intersection
- At the beginning and end of the horizontal curves
- At the point of vertical intersection of the vertical curves, i.e., change in the gradient.

In the context of this study roadway, which is a mountainous highway, there are frequent changes in road characteristics over short intervals, particularly in the presence of horizontal curves. Due to this reason, there were chances of formation of very short road segments which makes analysis cumbersome and impractical. Also, such a segmentation approach would lead to the formation of numerous short sections with zero crashes recorded in the last three years, which is a minimum requirement of crash data required for calibration while predicting crashes using the HSM model. This is the first issue encountered while assessing the transferability of the HSM predictive model.

The effect of segmentation on the transferability of the SPF-based prediction model was studied by a group of researchers in Egypt. Four segmentation methods were used for multilane roads: 1) fixed length at one-kilometer segments; 2) homogeneous segment approach; 3) variable segments with respect to the presence of curvatures; and 4) variable segments with respect to the presence of both curvatures and U-turns. For each segmentation type, different SPF transfer methods were also applied. These methods include 1) the use of the HSM default CMFs; 2) locally developed CMFs; and 3) the recalibration of the constant term of the transferred model. The results showed that the segmentation approach has a very big influence on the transferability of the models and the best approach for the prediction is to recalibrate the constants of the adopted or transferred model (Elagamy et al., 2020). A similar study on an Italian rural motorway used four segmentation approaches: 1) homogeneous segments with respect to AADT and curvature; 2) segments each containing two curves and two tangents; 3) fixed length segments of 650 meters; and 4) completely homogenous segments. The results showed that the segments with two curves and two tangents and the fixed length segmentation yielded the best results (Cafiso et al., 2018)

Based upon the ideas from those studies, a mixed approach for segmentation was adopted in this study where fixed length segmentation (250 meters) was used for straight road sections, and variable length segmentation was applied to the base 250-meter segments considering the series of curves. It is believed that the segments of 250 meters can satisfactorily reflect the road characteristics and considering larger segments would lead to a loss in homogeneity. However, two major recommendations from the HSM were considered: 1) the lengths of the segments preferably be longer than 0.1 miles (160 meters); and 2) while calculating the CMF for the presence of a horizontal curve, the entire curve should be considered as a length of a curve. Considering the above criteria, the base length of 250 meters, and the inclusion of an entire horizontal curve within a single segment, 638 segments were formed with an average length of 250.518 meters. Hence, the segments formed using this approach could be either a combination of tangent portions (straight road section) and curves (single or multiple curves with different radii), straight sections, or single, compound or reverse curves.

2.3 Data analysis

The descriptive statistics of the road segments and their road features are shown in Table 1. Next, CMFs were calculated for each of the twelve road features listed in Exhibit 10-13 of HSM for rural two-lane two-way roadways. The base condition for each road condition is described in the HSM and, whenever there are any changes in the features of the road segment being assessed other than the base conditions, the CMF is calculated. The CMF value for any road feature greater than 1.00 indicates higher crash frequency and less than 1.00 represents lower crash frequency than the base condition. The CMFs associated with rural two-lane two-way highways were calculated using Exhibits 10-14 to 10-23 of the HSM. Four road features (centerline rumble strips, passing lane, two-way left turn lane, and automated speed enforcement) were not found in the entire roadway, so a CMF value of 1.00 was adopted in accordance with the HSM's base conditions.

Table 8: Descriptive statistics of road segment and features

Road features	Max	Min	Mean	S.D.
No. of road segments (n)	638			
Length of Segment (L), m	348.05	162.48	250.52	24.72
AADT (veh/day)				
Year 2015	5457.00	1058.00	2611.92	1201.14
Year 2016	7118.00	1798.00	3457.29	1409.88
Year 2017	8778.00	2538.00	4302.15	1646.11
Year 2018	10044.00	2866.00	4930.76	1772.55
Year 2019	11309.00	3180.00	5558.87	1928.61
Lane width (m)	4.95	2.26	2.63	0.27
Shoulder width (m)_LEFT	2.00	0.00	0.47	0.43
Shoulder width (m)_RIGHT	1.90	0.00	0.62	0.35
Length of horizontal curve (m)	337.06	7.80	135.61	58.41
Radius of curvature (m)	1025.00	15.00	129.18	128.64
Grade (%)	10.00	0.00	3.83	2.30
Driveway density (driveway/mile)	25.75	0.00	1.20	3.33
Roadside hazard rating (1-7 scale)	7.00	3.00	4.72	0.75

The next major problem encountered while executing the HSM predictive model was the calculation of CMF values for horizontal curves. The formula to calculate CMF for horizontal curves is given in Equation 4.

$$CMF_{HC} = \frac{(1.55 \times L_c) + \left(\frac{80.2}{R}\right) - (0.012 \times S)}{(1.55 \times L_c)} \quad \textit{Equation 4}$$

Where,

CMF_{HC} = Crash Modification Factor for the effect of horizontal alignment on total accidents

L_c = length of horizontal curve (miles) including spiral transition

R = radius of curvature (feet)

S = 1 if spiral transition curve is present; 0 if absent and 0.5 if spiral transition curve is present at only one end of the horizontal curve

As discussed previously, since a mixed approach for segmentation was adopted, hence each segment can contain several horizontal curves and straight sections (tangents) between them. The HSM also recommends the calculation of CMF values separately for each curve and, since it has not envisaged multiple curves within a single segment, there is no guidance regarding how to utilize the individual CMF values of curves so that they can represent the whole segment considered. However, in the case of compound curves or reverse curves, where the curves are adjoining to each other, the

HSM recommends that while calculating the CMF using Equation 5 the length of the curve (Lc) should be considered as the length of the entire curve set. Nonetheless, the above recommendation is only valid in the case of curve sets consisting of a compound and reverse curve, and it is unclear how to address road sections containing consecutive curves with short curve lengths and tangents.

The resulting CMFs for most of the curves were found to be very high because the length of the radius of curvature and curve length were very small. The presence of such multiple curves contributed to the calculation of CMFs with high values, and it was likely that the prediction of crashes using these CMFs would lead to an overestimation of crashes. To cope with this issue, this research proposes to include the tangent lengths between the curves as part of the curve length based on the hypothesis that this would increase the curve length and result in decreased CMF values. The reason for including the tangents within the curve was that the average length of the tangents between the curves was found to be 31.70 meters. The design speed of the highway varied between 20 kmph to 40 kmph and the results of the spot speed study showed that the average speed of the vehicles on the highway was 39.35 kmph. This means the average time required to travel the tangent portions was approximately 4 seconds, which is a very limited time for the driver to relax. Hence, such short straight stretches (tangents) can also be considered as a part of the curve while calculating the CMF for horizontal curves.

The descriptive statistics of the CMF values calculated before and after considering tangent lengths within curve lengths are shown in Table 2. It can be noted that the average CMF values have significantly reduced after considering the tangent lengths within the length of a curve (L_c), and hence it was decided to proceed using this approach.

In this analysis, the average CMF value of individual curves within a segment was considered and used to predict crashes within that segment. Although the crash data was available for the seven years between the period 2015 to 2021, the crashes for the years 2020 and 2021 could not be predicted because the traffic count survey was not carried out in those years due to the COVID-19 pandemic. In addition, the traffic flow during that period was reduced because of lockdowns imposed by the Government of Nepal.

Table 2: Descriptive results of CMF values under two approaches

Parameters	Not including tangent length	Including tangent length
No. of curves	1994	1994
Max	28.32	19.63
Min	1.00	1.00
Mean	13.65	3.165
SD	9.29	1.95

3. Results and discussion

Annual crash frequency was estimated for the year 2015 to 2019. It was calculated according to Equations 1 and 2 using all twelve CMFs for all 638 road segments. The predicted crashes in each segment were summed up to calculate the total crashes predicted to occur along the entire highway. The calibration factor was then calculated using Equation 3 for each year, with the obtained results shown in Table 3.

The resulting average calibration factor of 0.126 means the observed crashes are much less than the predicted crashes. In other words, the HSM predictive model is overestimating the crash frequency. The probable reasons for this could be either underreporting of the crashes or some error in the prediction model itself. The estimated crashes are a function of traffic volume, segment length, CMFs, and calibration factor and, since information on traffic volume and segment length is reliable, there likely exists some problem in the calculation of CMFs.

Table 3: Calibration factor for each year

Year	Total observed crashes	Total predicted crashes	Calibration factor
2015	60	414	0.14
2016	33	551	0.06
2017	87	687	0.13
2018	139	790	0.18
2019	104	893	0.12
	Average calibration factor		0.126

The descriptive statistics of the resultant CMF values are shown in Table 4. Among the twelve CMFs, CMF values for the horizontal curves were found to be significantly higher than others, thus leading to overestimation. This suggests that the nature of the horizontal curves of the roads in the USA was different than that of the mountainous road of Nepal. From the above analysis, it was found that the CMF values for the curves with smaller radii were higher. Also, the CMF values were very large when the segment contained curves with shorter curve lengths. The results make sense practically because maneuvering a curve after driving continuously in a long stretch of a straight portion makes the driver more prone to make mistakes, potentially resulting in a crash. The same phenomenon may not come into effect while driving on a road with a series of curves because the driver is cautious and alert of the next curve ahead, thus reducing the chances of a crash occurring.

Table 4: Descriptive statistics of resultant CMFs

Road Features	Max	Min	Mean	S.D.
Lane Width	1.325	1.000	1.313	0.054
Shoulder width and Type	1.325	0.984	1.221	0.047
Horizontal curves	19.630	1.000	3.165	1.950
Superelevation	1.000	1.000	1.000	0.000
Grades	1.160	1.000	1.072	0.063
Driveway Density	1.317	1.000	1.008	0.030
Centerline Rumble Strips	1.000	1.000	1.000	0.000
Passing Lane	1.000	1.000	1.000	0.000
Two-way Right Turn Lane	1.000	1.000	1.000	0.000
Roadside design	1.306	1.000	1.123	0.057
Lighting	1.000	0.922	0.998	0.012
Automated Speed Enforcement	1.000	1.000	1.000	0.000

Another factor that may be playing an integral role is vehicle speed. Usually, the average speed of vehicles on rural roads in the USA is above 80 kmph (NHTSA, 2018), whereas the average speed of vehicles on the roadway in this study was around 40 kmph. Mountainous highways are usually winding roads with sharp turns and steep gradients, which forces drivers to limit their speed, and the lower speed may aid in reducing the occurrence of crashes.

In this analysis, a new technique of segmentation was used in which the segments in the straight sections were first formed at lengths of 250 meters and segments having horizontal curves were formed including the tangents between the curves, resulting in segments slightly more or less 250 meters. While the crash prediction using this technique was still overpredicting the crashes, the use of entirely homogenous segments or homogenous horizontal curve segments would have led to even more overprediction. Therefore, further research should be carried out using other segmentation approaches to develop more accurate prediction models.

4. Conclusions

The HSM prediction model is very popular and well-recognized because of its simplicity and robustness. It recommends using the calibration factor to predict crash frequency when the model is used for a jurisdiction other than the one for which it was developed. In this study, the objective was to calculate the calibration factor of the HSM model for predicting crash frequency for a rural two-lane two-way highway in Nepal and to assess the transferability of the HSM model in the context of mountainous roads.

While adopting the HSM predictive model two major issues were identified. The first is the segmentation of the highway considering homogeneity in various road features. The use of this approach led to the formation of very small segments because there were numerous horizontal curves with short lengths. It would be difficult to use and predict crashes in such small segments because many segments would have zero crashes and it would be impractical to consider this approach. Hence, a hybrid approach beginning with fixed length segments of 250 meters and adjusting based on the tangent length within the curve length was considered for this analysis, however, even this approach is overpredicting the crash frequencies. It is well known that segmentation plays a significant role in the outcomes of the prediction models, therefore, a better segmentation approach for the curvy mountainous roads should be identified. Another issue identified was regarding the CMF for horizontal curves. The relation specified in the HSM resulted in very large modification factors in the presence of horizontal curves, thus overestimating the crashes. As a result, the average calibration factor was very low.

The results of the study suggest that the current HSM model may not precisely predict crash frequency in mountainous roads unless there are some considerations and additional guidance for such roads. The same issue of overprediction may arise if the model is used in other countries with similar terrain and road features and hence its transferability to mountainous roads must be reconsidered. However, the two issues identified through this study could be essential for further modifications in the HSM predictive model and would also be helpful to other researchers working on the development of similar crash prediction models. For future works, different road segmentation approaches in the case of mountainous roads could be studied, and using a rich crash database, different CMF relations can be developed for such roads.

Acknowledgment

This research was supported by a scholarship for road asset management from the Japan International Cooperation Agency (JICA). The authors are also thankful to the Department of Roads, Nepal, for providing the necessary design and drawings of the study highway.

References

National Highway Traffic Safety Administration (NHTSA), 2018. *National Traffic Speeds Survey III: 2015, Report No. DOT HS 812 485,* s.l.: U.S. Department of Transport.

American Association of State Highway and Transportation Officials (AASHTO), 2010. *Highway Safety Manual (HSM),* s.l.: s.n.

Cafiso, S., D'Agostino, C. & Persaud, B., 2018. Investigating the influence of segmentation in estimating safety performance functions for roadway sections. *Journal of Traffic and Transportation Engineering; 5(2),* pp. 129-136.

Elagamy, S. R. et al., 2020. Segmentation Effect on the Transferability of International Safety Performance Functions for Rural Roads in Egypt. *Safety 2020, 6, 43.*

Haghani, M., Jalalkamali, R. & Haghani, H., 2021. Calibration of Highway Safety Manual's Crash Prediction Model for Rural Two-Lane Two-Way Roads in a Developing Country: A Case Study. *Computational Research Progress in Applied Science & Engineering, CRPASE: Transactions of Civil and Environmental Engineering 7,* pp. 1-9, Article ID:2311.

Kronprasert, N., Boontan, K. & Kanha, P., 2021. Crash Prediction Models for Horizontal Curve Segments on Two-Lane Rural Roads in Thailand. *Sustainability 2021,13, 9011.*

Martinelli, F., Torre, F. F. & Vadi, P., 2009. Calibration of the Highway Safety Manual's Accident Prediction Model for Italian Secondary Road Network. *Transport Research Record: Journal of the Transportation Research Board, No 2103,* pp. 1-9.

Torre, F. L. et al., 2022. Transferability of the highway safety manual freeway model to EU countries. *Accident Analysis and Prevention 178 (2022) 106852.*

World Health Organization, 2022. *Road Traffic Injuries-Key Facts.* [Online] Available at: https://www.who.int/news-room/fact-sheets/detail/road-traffic-injuries

♦